Antiviral Function of Mx Proteins - Role of Cellular Factors and Subcellular Localization

Dissertation

zur

Erlangung der naturwissenschaftlichen Doktorwürde
(Dr. sc. nat.)

vorgelegt der

Mathematisch-naturwissenschaftlichen Fakultät

der

Universität Zürich

von

Fiona Steiner

von

Freienbach (SZ)

Promotionskommission

Prof. Dr. Alexandra Trkola (Vorsitz)
PD Dr. Jovan Pavlovic (Leitung der Dissertation)
Prof. Dr. Cornel Fraefel
Prof. Dr. Peter Stäheli
Prof. Dr. Silke Stertz

Zürich, 2018

1 Table of Contents

Summary

Viruses and their hosts co-evolve and both sides constantly adapt to develop more refined methods to gain the upper hand in this arms race. In an infected cell viral components activate the innate immune system of the cell, which leads to the production of interferons. This in turn triggers the expression of numerous antiviral proteins in the infected as well as neighboring cells. We focused on one group of those interferon-induced proteins: the Mx proteins. These are dynamin-like GTPases, which exert antiviral activities against a wide range of viruses. Different Mx proteins localize to different subcellular compartments and also vary in their antiviral specificity. Human MxA has been studied extensively in its antiviral function against many negative-stranded RNA viruses, among them influenza A virus (IAV). However, despite intense efforts the antiviral mechanism is still not resolved yet. Human IAV strains seem to have adapted to MxA, since they are generally more resistant to MxA as opposed to avian IAV strains. It is clear that the nucleoprotein (NP) of IAV represents the target of MxA, not only because it shows binding to MxA but also because a small number of mutations in NP alter the sensitivity of those virus strains to MxA dramatically. The closely related human MxB protein, on the other hand, has only recently been associated with antiviral functions and has been shown to inhibit lentiviruses and herpesviruses.

In this thesis we investigated the potential of MxB to inhibit IAV. We showed that by artificially changing the localization of MxB to the nucleus, MxB potently inhibits IAV primary transcription like MxA, which is re-localized to the nucleus and the mouse homolog Mx1, which naturally resides in the nucleus. The finding, that nuclear MxB harbors the potential to restrict IAV suggests the existence of a universal antiviral mechanism of Mx proteins. We further aimed at gaining a more insights into the molecular processes of IAV restriction by MxA. MxA and viral NP both associate with UAP56, a cellular RNA helicase involved in mRNA nuclear export. It also acts as a chaperone on newly synthesized viral NP to deliver it safely to viral RNA in the nucleus. We showed that MxA does not inhibit the shuttling of newly translated NP, chaperoned by UAP56, from the cytoplasm to the nucleus. Also, the sensitivity of different IAV strains to MxA does not positively correlate with the capacity of NPs of those viral strains to bind to MxA. Stable binding of MxA to NP is only observed with dimeric MxA mutants and independent of its activity. We further showed that two residues in NP, which are associated with NP oligomerization, are crucial for its binding to MxA and UAP56, since binding to both proteins is abrogated when those two residues are mutated. We thus suggest that MxA induces post-translational modifications on NP and/or UAP56 by recruitment of additional factors, which abrogates the functional integrity of the NP-UAP56 complex.

Zusammenfassung

Viren und ihre Wirtsorganismen passen sich laufend einander an. Das Virus entwickelt Strategien um das Immunsystem der Zelle zu umgehen und die Zelle wiederum entwickelt immer komplexere Systeme für eine erfolgreiche Bekämpfung von Pathogenen. Virale Moleküle werden in einer infizierten Zelle von speziellen Rezeptoren des angeborenen Immunsystems erkannt und als Reaktion darauf werden Proteine, sogenannte Interferone, produziert. Diese Interferone induzieren die Expression zahlreicher antiviraler Proteine sowohl in der infizierten Zelle, als auch in den Nachbarzellen. In dieser Dissertation fokussierten wir uns auf eine Familie solcher antiviraler Proteine, die sogenannten Mx Proteine. Diese Dynamin-ähnlichen GTPasen weisen eine hohe antivirale Aktivität gegen eine Vielzahl unterschiedlicher Viren auf, unterscheiden sich jedoch in ihrer antiviralen Spezifität und ihrer subzellulären Lokalisation. Humanes MxA Protein inhibiert DNA- und RNA-Viren, primär jedoch letztere, zu denen unter anderem Influenzaviren gehören. Trotz großer Bemühungen konnte der antivirale Mechanismus von MxA bis heute noch nicht gelöst werden. Es wurde jedoch gezeigt, dass sich die humanen influenza A virus (IAV) Stämme besser an MxA adaptiert haben als die aviären Stämme, welche generell sensitiver gegen die antivirale Aktivität von MxA sind. Zudem wurde gezeigt, dass das Angriffsziel von MxA das virale Nukleoprotein (NP) ist, da MxA und NP zum einen interagieren und zum anderen nur wenige Mutationen im NP die Sensitivität für MxA dramatisch verändern.

Dem eng verwandten humanen MxB Protein sind im Gegensatz zu MxA erst kürzlich antivirale Funktionen zugeschrieben worden. Es wurde gezeigt, dass MxB die Replikation von Lentiviren und Herpesviren inhibiert.

In dieser Dissertation haben wir MxB zu dessen Potential untersucht IAV zu hemmen. Wir konnten zeigen, dass MxB, welches artifiziell in den Zellkern verschoben wurde (TMxB), die Primärtranskription von IAV stark inhibiert. Dieser Mechanismus scheint der gleiche zu sein wie der von Mx1, dem MxA Homolog in Mäusen, welches sich im Kern befindet, und von nukleärem MxA, welches artifiziell in den Zellkern verschoben wurde. TMxB bindet zudem an NP, was auch für MxA und MxB gezeigt wurde. Diese Befunde deuten auf einen universellen antiviralen Mechanismus von Mx Proteinen hin.

Das Ziel dieser Arbeit war einen tieferen Einblick in die molekularen Prozesse der IAV Restriktion durch MxA zu gewinnen. MxA und das virale NP assoziieren mit UAP56, einer zellulären RNA Helikase, welche in den mRNA Transport involviert ist. Darüber hinaus spielt UAP56 eine wichtige Rolle im Zusammenhang mit IAV, da es als Chaperon fungiert um frisch synthetisiertes NP sicher zur viralen RNA im Zellkern zu transportieren. Wir zeigten, dass MxA den Transport des UAP56-NP Komplexes in den Kern nicht beeinflusst. Des

Weiteren konnten wir beobachten, dass die Sensitivität von verschiedenen IAV Stämmen für MxA nicht positiv mit der MxA-Bindungskapazität der NPs dieser Stämme korreliert. Eine stabile Bindung zwischen MxA und NP konnten wir mit der dimerischen Form von MxA sehen und diese Bindung ist interessanterweise unabhängig von der Aktivität von MxA. Wir konnten zudem zeigen, dass zwei bestimmte Aminosäurereste im NP, welche mit dessen Oligomerisierung assoziiert sind, für die Aufrechterhaltung des Bindungspotentials zu MxA und UAP56 entscheidend sind. Diese Bindung wurde zerstört, wenn diese zwei Aminosäuren zu Alanin mutiert wurden. Wir schlagen deshalb vor, dass MxA mit der Hilfe zusätzlicher Faktoren posttranslationale Modifikationen in NP und/oder UAP56 hinzufügt. Diese Modifikationen wiederum setzen die Funktion des NP-UAP56 Komplexes außer Kraft.

1 Background

1.1 Influenza A virus

Influenza A viruses (IAVs) are the causing agents of the illness commonly known as the flu. For a healthy individual an IAV infection is generally non-fatal and cleared after 7 to 10 days. Phenotypic manifestations include fever, muscle and joint pain, fatigue and milder symptoms such as a runny nose or a headache. Nevertheless, IAV infection is particularly dangerous to children, elderly people and immunocompromised individuals and an infection can lead to the death of those patients. IAV infections are especially evident in the annual flu epidemics and thus pose a recurrent health threat. These epidemics result in high economic losses (3 to 5 million cases of severe illness) as well as many deaths (290'000 - 650'000) (WHO, February 2018). There have also been a number of pandemics, worldwide Influenza outbreaks, first and foremost the so-called Spanish flu in 1918-20, infecting over 500 million people and 50-100 million deaths (3-5% of the world's population)[1]. Besides humans, IAV also infects other mammals as well as birds, where aquatic birds represent the natural reservoir[2].

IAV normally infects epithelial cells of the upper and lower respiratory tracts in humans with virus predominantly replicating in the upper airways and trachea. In fatal cases high virus loads can also be found in the lower respiratory tract[3]. In birds, on the other hand, the primary site of IAV replication is the gastrointestinal tract[4]. Independent of IAVs host tropism it binds to the same receptor, which is sialic acid on glycosylated host cell proteins.

IAV is a rapidly mutating virus, which enables fast evasion from the host antibody response, a phenomenon also called antigenic drift[5], leading to the occurrence of seasonal influenza epidemics. The rapid generation of virions harboring adaptive mutations is also the reason for the need to annually produce new vaccines. Antigenic shift on the other hand is a process, where a virus of a new subtype is introduced into the human population potentially leading to pandemic outbreaks. This antigenic change can occur through reassortment, which is the swapping of gene segments between at least two different viruses[6]. Antigenic shift, however, occurs much less frequently than antigenic drift. Since the early 20th century four IAV pandemics have occurred: the 'Spanish flu' (H1N1) in 1918, the Asian pandemic (H2N2) in 1957, the Hong Kong pandemic (H3N2) in 1968 and the 'swine flu' (H1N1) in 2009[7]. Nevertheless, infections with viruses originating in various animal species are generally not transmitted from human to human and the pandemic potential is thus relatively low[7].

1.1.1 IAV virion structure

IAV belongs to the orthomyxovirus family and is an enveloped, single-stranded RNA virus with a segmented genome of negative polarity[2,8]. Typically, virions are spherical particles of approximately 100 nm in diameter but also rod-shaped up to 300 nm long virions are observed. The viral genome is segmented and consists of 8 strands, each associated with numerous copies of the nucleoprotein (NP) and one single RNA-dependent RNA polymerase (RdRp) complex composed of the three proteins polymerase basic protein 1 (PB1), polymerase basic protein 2 (PB2) and polymerase acidic protein (PA). The resulting so-called viral ribonucleoprotein complexes (vRNPs) are bound through NP to the matrix protein M1. The virus displays two glycoproteins on its surface; hemagglutinin (HA), important for binding to the influenza receptor sialic acid on the host cell surface, and neuraminidase (NA), responsible for the release of the virions after budding by hydrolyzing glycosylic linkages on cell surface glycoproteins. These two types of viral glycoproteins are embedded in the viral envelope, a lipid bilayer derived from the host cell plasma membrane.

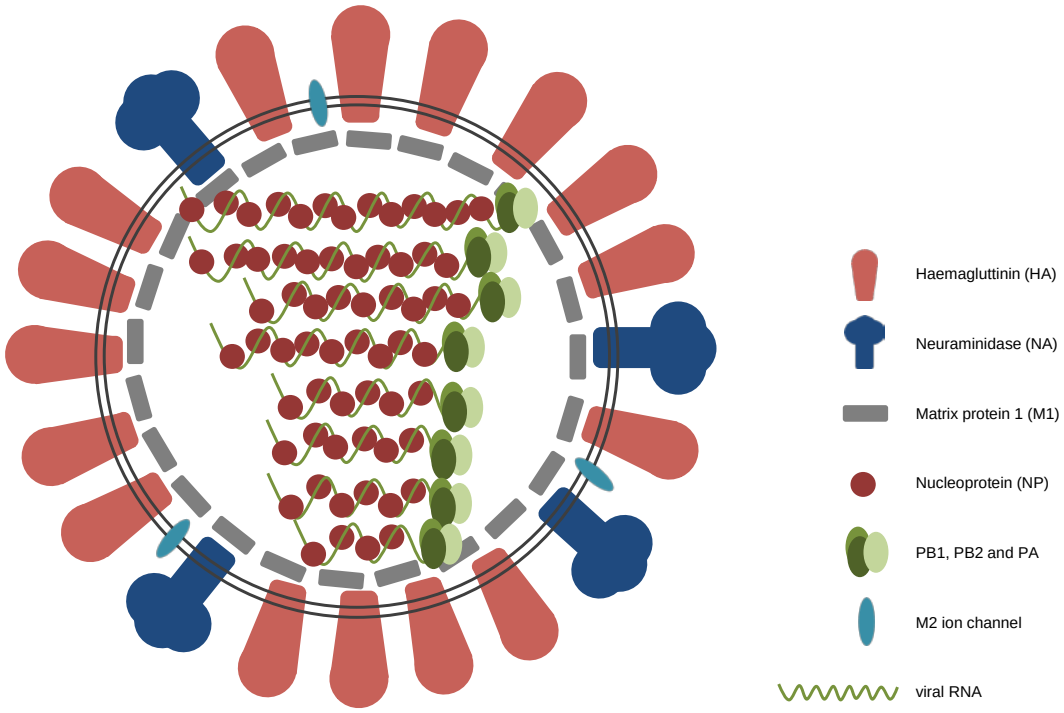

Fig. 1.1. Structure of influenza A virus. The 8 genomic viral RNA (vRNA) segments are encapsidated in numerous copies of the nucleoprotein (NP). Each segment is further associated with one polymerase complex comprising the proteins polymerase basic protein 1 and 2 (PB1 and PB2) and polymerase acidic protein (PA). vRNA plus NP and the polymerase is called a viral ribonucleoprotein (vRNP) complex. These complexes are associated with the matrix protein 1 (M1), which is situated right underneath the viral host-derived envelope. The envelope is studded with the

two viral surface glycoproteins hemagglutinin (HA) and neuraminidase (NA). The M2 ion channel also resides in the viral envelope.

There are 16 different HA and 9 different NA protein subtypes, classified according to their sequence similarities. This is also how the names of different IAV strains are derived from. The H and N in a given virus strain (eg. H5N1) stand for the subtypes of HA and NA proteins (HA protein of subtype 5 and NA protein of subtype 1 in this example). Two other influenza-like viruses have recently been discovered in bats: H17N10 and H18N11[9,10]. They are classified as 'influenza-like' viruses, since the HA and NA proteins have some unusual features unseen in influenza A viruses. These include the missing sialidase function of the NA protein and the inability of HA to bind to sialic acid.

Additionally to the two surface glycoproteins, an ion channel (M2) is located in the viral envelope[8]. The eight viral genome segments encode for 14 proteins in total[11,12], each segment encodes at least one protein. Besides PB2, PB1, PA, HA, NP, NA, M1 and M2 these segments further encode for several non-structural proteins: NS1, NS2/NEP, PB1-F2, PB1-N40, PB2-S1[13], PA-X, PA-N155[12], PA-N182[12] and M42[11]. NS1 is a multifunctional protein with a major role in antagonizing the host innate immune response[14]. It does so by interacting with and inhibiting retinoic-acid inducible gene 1 (RIG-I) downstream signaling but also shielding viral dsRNA from recognition by its receptor. NS1 also inhibits cellular pre-mRNA maturation and nuclear export[15,16] and it is involved in viral mRNA translation regulation[17]. On the same segment as NS1 the nuclear export protein NEP (also known as NS2) is encoded, which plays a crucial role as vRNP exporter into the cytoplasm after vRNP assembly[18]. PB1-F2 is associated with initiation of apoptosis, increasing sensitivity to secondary bacterial infections and the regulation of polymerase activity[19]. The functions of PB1-N40, PB2-S1, PA-X, PA-N155, PA-N182 and M42 are less thoroughly investigated. It is thought that PB1-N40, an N-terminally truncated PB1 version, regulates transcription and replication[20]. PB2-S1 is translated from an alternative splice variant of the PB2 mRNA. Functionally it has been shown that it can inhibit RIG-I-dependent interferon signaling as well as viral polymerase activity but its relevance for viral replication and pathogenicity is questionable[13]. PA-X harbors the same N-terminus as PA but its C-terminus is truncated and different in sequence as a result of ribosomal frameshifting[21]. It was shown to induce the degradation of host mRNAs and its loss leads to increased inflammation, apoptosis and induction of the adaptive immune system[22,23]. PA-N155 and PA-N182 are translated from alternative AUG codons from the PA mRNA at the 11th or 13th in-frame position after the PA start codon[12]. A specific function has not been assigned to those two proteins yet. It has been shown, however, that they do not harbor polymerase function in combination with PB1

and PB2. M42, a splice variant of M2, has been proposed to also have an ion-channel function similar to M2 and to be able to replace the function of M2 *in vitro* and *in vivo*[11].

1.1.2 IAV replication cycle

One of the first hurdles a virus needs to overcome is the entry into the host cell. IAV initializes this entry process by binding to the host cell surface via its receptor sialic acid. Depending on how these sialic acid residues are linked to other sugar moieties, they are more strongly bound by human or bird influenza viruses. Human viruses preferentially bind to α2,6-linked sialic acids, which are found in the upper respiratory tract, whereas bird influenza viruses favor α2,3-linkages[24,25] present on intestinal epithelial cells[26]. The virus subsequently gets internalized mainly via clathrin-mediated endocytosis and travels along the endocytic route to late endosomes[27]. The drop in pH leads to the ion channel M2 pumping protons into the virion and the lower pH triggers the release of the vRNPs from the matrix protein M1. Following the cleavage of the HA precursor protein HA0 to HA1 and HA2 by cellular proteases, which exposes IAVs fusion peptide, acidification in the late endosomes further leads to a conformational change in HA and subsequently fusion of the viral with the cellular endosomal membrane[28]. The vRNPs are imported into the nucleus, where primary transcription takes place and viral mRNA transcripts are generated through a cap-snatching mechanism. Thereby the virus cleaves of the 5'-cap on cellular mRNAs and uses them for the production of viral mRNA molecules, thus disguising its own transcribed RNAs as cellular mRNAs. These viral RNA transcripts are exported into the cytoplasm and translation by the host cell machinery is initiated. Newly synthesized NP as well as the viral polymerase translocate to the nucleus, where they drive viral genome replication. NP thereby binds co-replicationally to the nascent viral genomes[29]. NA and HA proteins, which are translated at the endoplasmic reticulum (ER), travel to the plasma membrane via the trans-Golgi network (TGN), where they are associated with lipid raft domains[30].

Newly assembled vRNPs exit the nucleus and are transported to the plasma membrane most likely via Rab11-positive endosomes[31]. Influenza virions assemble and bud from the plasma membrane and NA subsequently cleaves sialic acid to release the virions from the host cell.

There are basically two steps, at which IAV can be currently inhibited by antiviral drugs. Firstly, the acidification of endosomes can be inhibited by targeting the ion channel M2 so that the virus is unable to perform uncoating and the vRNPs cannot be released into the cytoplasm. These drugs are called adamantane (eg. Amantadine, Rimantadine). The other group of drugs inhibits the sialidase function of NA so that the progeny virus is not released from the plasma membrane. Zanamivir and Oseltamivir (commonly known as Tamiflu)

belong to this category of neuraminidase inhibitors[32]. Due to the IAVs high mutation rate and the high selection pressure for drug evasion many circulating virus strains are already resistant to both classes of anti-IAV drugs[33], thus, there is urgent need to develop new antivirals or a universal vaccine.

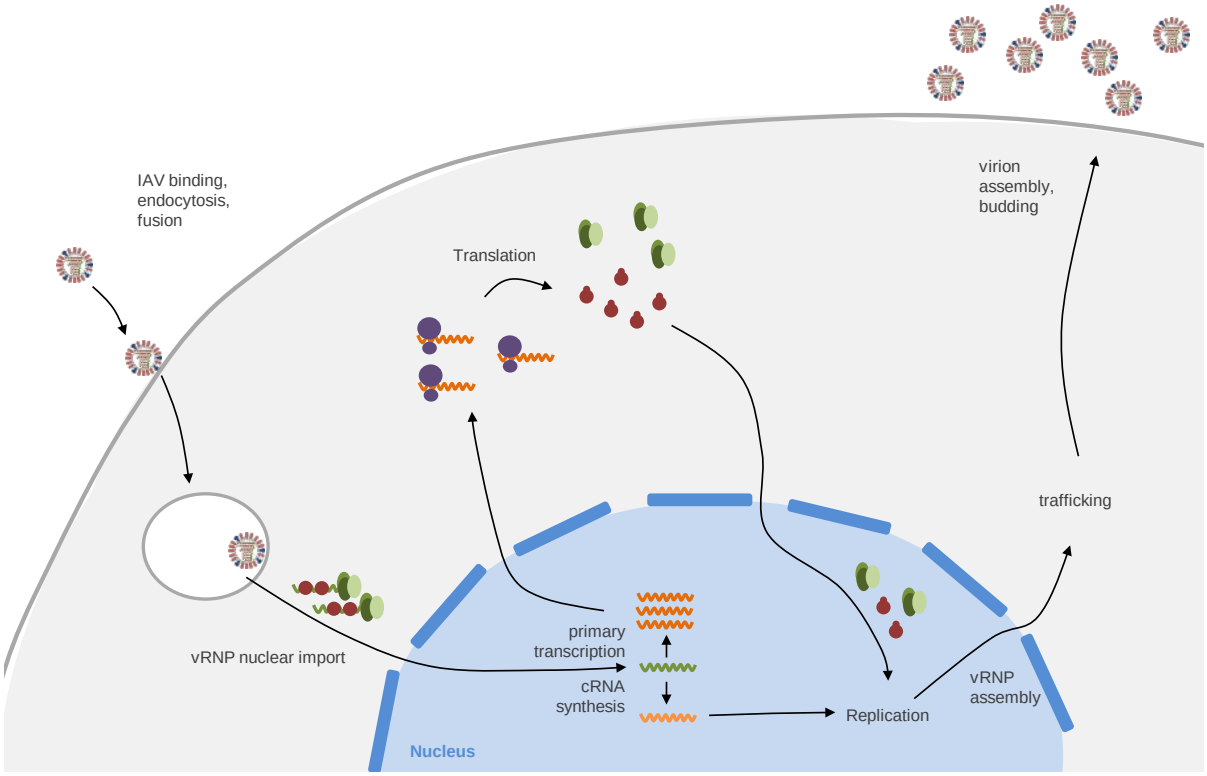

Fig. 1.2. IAV replication cycle. Upon binding of IAV to its receptor sialic acid the virions get internalized via clathrin-mediated endocytosis and travel through the endosomal pathway. Acidification of the endosomes and with the help of the M2 ion channel also of the viral core induces structural changes in HA, which enable the viral envelope and the host endosomal membrane to fuse. After fusion the vRNPs are imported into the nucleus, mRNA transcription is initiated and mRNA is exported to the cytoplasm. After host-dependent translation the viral polymerase complex and the nucleoprotein travel back to the nucleus where they assist in viral genome replication. vRNPs are assembled in the nucleus and reach the plasma membrane through endosomal trafficking. Virions are assembled at the plasma membrane and released by NA activity. HA: hemagglutinin, vRNP: viral ribonucleoprotein complex, NA: neuraminidase

1.1.3 A closer look on the nucleoprotein NP of IAV

NP is a key viral protein, involved in many processes during the viral replication cycle. NP is the major component of vRNPs and an RNA-binding binding protein. Its affinity to bind to RNA is high but unspecific, meaning not selective for viral RNA[34,35]. NP also interacts with

two other components of the vRNP: PB1 and PB2, two of the three subunits of the viral polymerase[36,37]. NP enables the vRNPs to reach the nucleus via its nuclear localization signals (NLS)[38]. Those NLS motifs associate with importin-α and are subsequently transported through the nuclear pore[39]. NP stabilizes viral RNA by concomitant encapsidation during cRNA synthesis and vRNA production[40]. This encapsidation is initiated by binding of an NP monomer to the RNA-bound polymerase. Subsequent addition of NP molecules during RNA elongation is achieved through NP-NP binding and homo-oligomerization[41-43]. Intriguingly, it has also been suggested that vRNP CRM1-dependent export prior to virion assembly is mediated by NP[44]. NP is further required for packaging of some RNA segments[45]. The various functions of NP are regulated via post-translational modifications such as phosphorylation (prevents premature NP oligomerization[41,46]), SUMOylation (important for intracellular trafficking of NP[47]), ubiquitination (affecting its binding affinity to nascent cRNA[48]) and acetylation (affecting polymerase activity and virion release [49]).

NP has been shown in vitro to form homo-oligomers: trimers[50-52], tetramers[51] and even higher oligomers[50]. The oligomerization capacity of NP is dispensable for initiation and termination of viral genome replication, however, it is crucial for the elongation and assembly of the nascent vRNA[52-54]. It has further been suggested, that NP needs to be kept in the monomeric state previous to binding to and polymerizing on the vRNA[29,55,56]. This function is exerted by the cellular chaperone UAP56[29,57] and possibly also by its close relative URH49[57].

NP is highly conserved between different strains of IAV, nevertheless, some structural differences are obvious. So far, H1N1 and H5N1 NP have been crystallized[50,51], which resulted in trimers. They harbor a C-terminal tail loop, important for the formation of oligomers and an insertion groove, the binding site for the tail loop (Fig. 1.3). The positively charged RNA-binding groove is located opposite of the insertion groove. When comparing H5N1 (Fig. 1.3A) and H1N1 (Fig. 1.3B) NP, it is obvious that the angle at which the tail loop is protruding from the body of the protein is different. Even though the trimeric structure of H5N1 and H1N1 (Fig. 1.3C) NPs therefore differ considerably, the interaction of the tail loops with the insertion grooves are virtually the same[51] (Fig. 1.3D). NP can be rendered monomeric via point mutations: R416A (in the tail loop), E339A (in the insertion groove) and S165D (in the insertion groove, phosphomimetic) (shown in yellow in fig. 1.3 A and B). Introducing the R416A mutation, the positive charge of the RNA-binding groove is reduced concomitantly[55]. In contrast to R416A and E339A, IAV harboring NP(S165D) can be grown, although strongly attenuated, which indicates that this substitution does not render NP exclusively monomeric[46,58].

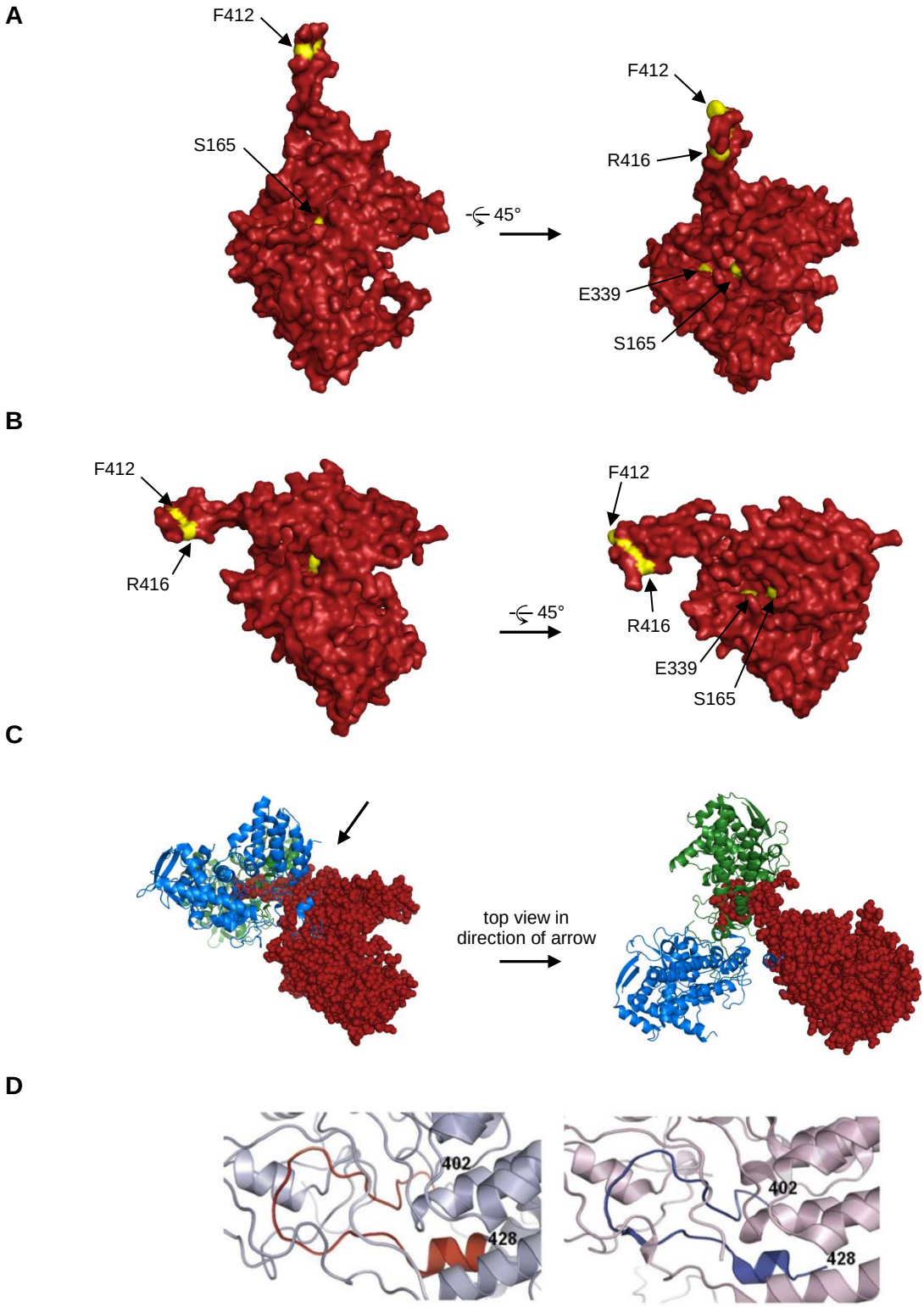

Fig. 1.3. Structure of H5N1 and H1N1 nucleoprotein. Crystal structure of a single NP protomer. Residues, which were shown to influence the oligomeric state of NP are marked in yellow. **A)** H5N1 NP crystal structure (RCSB ID: 2q06, A/HK/483/97) of one protomer adapted from [51]. **B)** H1N1 crystal structure (RCSB ID: 2iqh, A/WSN/1933) of one protomer from [50]. **C)** Trimeric H1N1 NP as in B). Single NP molecules are shown in different colors. **D)** Comparison of H5N1 (left) and H1N1 (right) interactions domains (adapted from [51]). The stalk of one NP monomer (red or blue, respectively)

inserts into the insertion groove of another NP molecule (light blue or rose, respectively). The structures of the trimeric interaction domains are virtually identical.

1.2 Innate immune system

The cell has evolved two main systems to defend against pathogens: the fast and broadly acting innate immune system and the slow but more specialized adaptive immune system. The first line of defense of a cell against an incoming virus is the interferon system[59] (Fig. 3), a part of the innate immunity. Viral proteins or nucleic acids, harboring so-called pathogen-associated molecular patterns (PAMPs) thereby bind to pattern recognition receptors (PRRs). These are either Toll like receptors (TLRs) in endosomes or RIG-I like receptors (RLRs) in the cytoplasm[60-62]. For IAV, TLR 3 and TLR7, which recognize viral dsRNA and ssRNA in endosomes, respectively, and RIG-I, sensing viral 5' triphosphate RNA[63,64], are of particular importance. The binding to their target molecules activates the downstream effectors, eventually leading to the activation and nuclear translocation of interferon regulatory factors 3 and 7 (IRF3 and IRF7). These transcription factors subsequently activate the expression of interferons of the type I and III (interferon (IFN) α, β and λ), their levels depending on the cell type[65]. Secreted IFNs then bind in an auto- and paracrine manner to their cognate receptor, interferon-α or -λ receptor (IFNAR or IFNLR). Receptor subunit dimerization activates Janus Kinase (JAK) family tyrosine-protein kinases Janus Kinase 1 (Jak1) and Tyrosine Kinase 2 (TYK2). These two kinases phosphorylate the receptor tail, forming a binding site for Signal Transducers and Activators of Transcription 1 and 2 (STAT1 and STAT2) proteins[66]. Bound STATs in turn get phosphorylated by JAKs and form heterodimers. These dimers associate with IFN regulatory factor 9 (IRF9) and translocate to the nucleus[59], where they activate transcription of over 300 interferon-stimulated genes (ISGs), many of them with intrinsic antiviral activity. There are many well-characterized ISGs in the battle against IAV and the three most prominent examples are protein kinase R (PKR), 2'-5' oligoadenylate-synthetase (OAS) and IFN-induced transmembrane (IFITM) protein family members. PKR is a Ser/Thr protein kinase, which is activated by double-stranded RNA (dsRNA)[67,68]. Activation of PKR leads to auto-phosphorylation, which further results in phosphorylation of downstream target proteins[69]. One of those target proteins is the translation initiation factor eIF2. Phosphorylated eIF2 is inactive, thus translation of cellular and viral mRNAs is blocked[70] and hence the virus is unable to perform genome replication. OAS is also stimulated by dsRNA, inducing the production of 2'-5' oligoadenylic acid from ATP[71,72]. These ATP species in turn activate RNase L, which cleaves viral and cellular single-stranded RNA (ssRNA)[73]. Activation of RNase L additionally stimulates autophagy[74] and apoptosis[75] further enhancing the antiviral effect. IFITM3, the major anti-IAV protein of

the IFITM protein family inhibits IAV even before the virus undergoes uncoating and entry into the host cell due to its transmembrane nature[76-78]. The mechanism is poorly defined so far[79], but for HIV it has been shown, that IFITMs get incorporated into the viral membrane and decrease virus infectivity[80,81]. It has also been shown that IFITMs specifically target the viral envelope protein (Env) during assembly impairing the incorporation of Env into the virions[82]. The human myxovirus resistance protein 1 (MxA) is another well-known ISG, which plays an important role in the struggle against many different viruses including IAV[59]. A detailed description can be found in chapter 1.3.

Since the innate immune system is a very potent and fast acting antiviral mechanism, IAV has also evolved means to counteract it. The multifunctional NS1 protein plays a major role thereby. It can bind directly to RIG-I and thus inhibit the downstream activation of IRF3 and eventually IFN production[83-86]. NS1 can also indirectly inhibit RIG-I activation by binding to dsRNA and thereby shielding it from the recognition by cellular sensors[85-88]. Recently it has been shown that the virus carries RIG-I antagonizing factors in the virions: the polymerase subunits PB1 and PA suppress IFN induction possibly through direct interaction with RIG-I[89]. NS1 also is capable of blocking the function of OAS and PKR by out-competing those two proteins for dsRNA binding[90,91] or even through direct interaction with PKR[14,69,91].

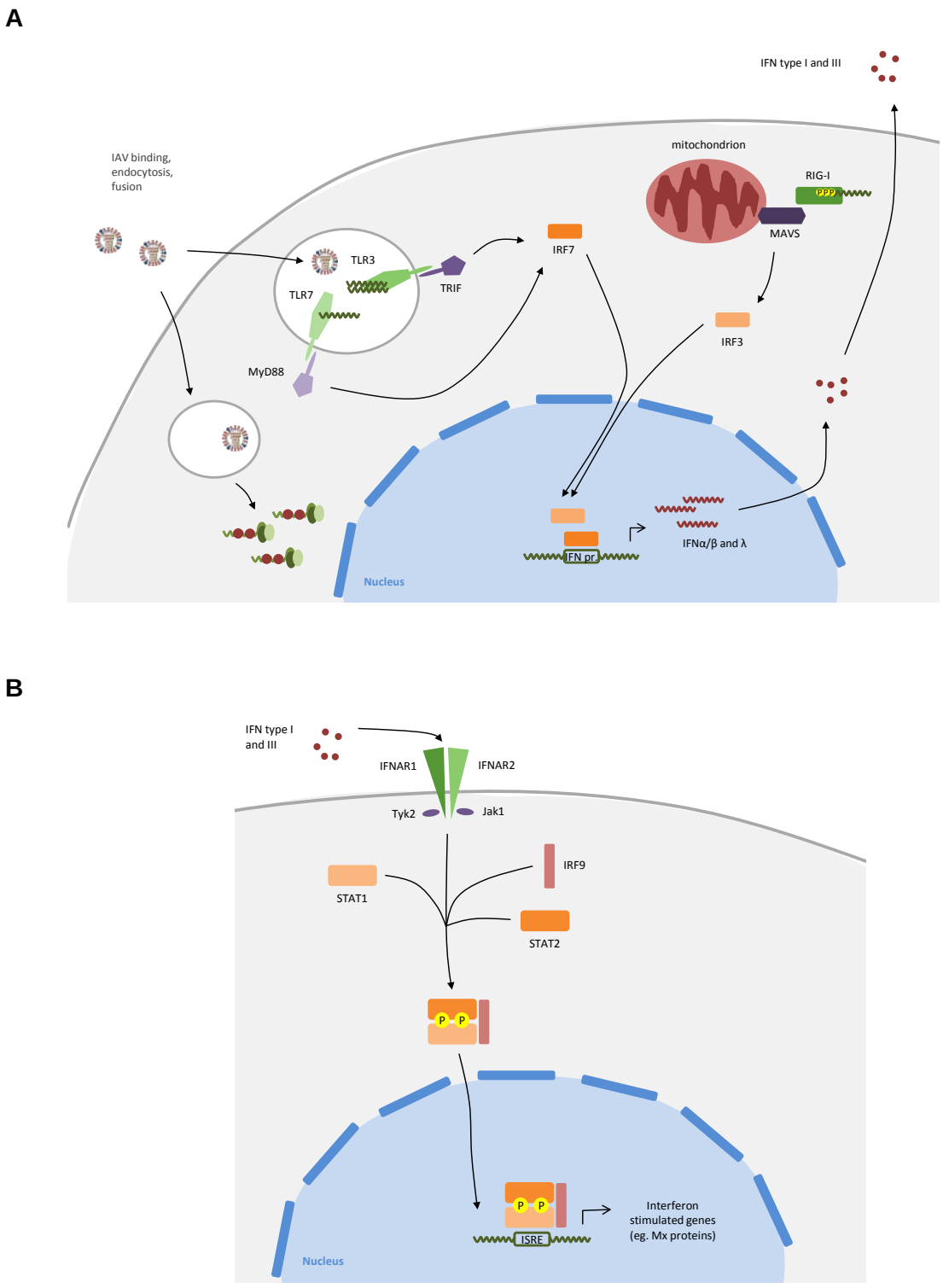

Fig. 1.3. IFN induction and the JAK/STAT pathway. A) Stimulation of PRRs TLR3 and 7 and RIG-I leads to the activation of downstream effectors IRF3 and 7. Binding of those transcription factors to an ISRE activates transcription of the IFN gene. IFN protein is secreted and auto- and paracrine signaling is activated. **B)** IFN produced as in A) binds to its receptor subunit 2 (IFNAR2) and triggers dimerization of subunit 1 and 2. The following activation of Jak and Tyk leads to the phosphorylation and activation of STAT1 and STAT2. STAT1 and STAT2 form heterodimer, associate with IRF9, translocate to the nucleus and activate the transcription of various ISGs. PRR: pattern recognition

receptor, TLR: toll-like receptor, RIG-I: retinoic-inducible gene 1, TRIF: TIR-domain-containing adapter-inducing interferon-β, MyD88: myeloid differentiation primary response 88, IRF: interferon regulatory factor, MAVS: mitochondrial antiviral-signaling protein, IFN: interferon, ISRE: interferon-stimulated response element, JAK: Janus kinase, STAT: signal transducers and activators of transcription, Tyk: tyrosine kinase, IFNAR/IFNGR: interferon alpha/gamma receptor

1.3 Mx proteins

In 1962, a protein called myxovirus resistance protein 1 or Mx1 (myxovirus is an outdated term to describe viruses, which infect the respiratory tract) was discovered in inbred mouse strains[92]. This interferon-inducible protein protected mice very potently against lethal doses of IAV. Two years later the coding region for this protein was mapped to a single gene, *Mx1*, on chromosome 16[93]. In humans the *Mx1* locus on chromosome 21 codes for a protein named MxA, which shares some, but not all features of Mx1. Another gene, most likely arisen through gene duplication[94], codes for yet another closely related Mx protein: Mx2 (in mice) or MxB (in humans). This protein, however, is very different from Mx1/MxA in that until recently there has not been any antiviral function associated with it. *Mx* genes can be found in all mammals but also in many other species like birds and fish[95,96].

1.3.1 Structure and function

Mx proteins belong to the dynamin family of large GTPases. They resemble the structure of cellular dynamin[97], which is a protein involved in endocytosis. According to the crystal structure, Mx proteins have a globular GTPase domain (G domain) head and an elongated stalk consisting of five α-helices. G domain and stalk are linked via a bundle-signaling element (BSE) built of three α-helices[98], which confers structural changes of the G-domain after GTP hydrolysis to the stalk. Between the α3- and α4-helix the unstructured L4 loop is localized. This loop has been shown previously to be involved in the recognition of Thogoto vRNPs and to be important for the antiviral activity against IAV and La Crosse virus[99-101]. If this loop is replaced in Mx1 with the one from MxA, this chimeric protein is then able to inhibit THOV replication[100].

MxA's expression is induced exclusively by interferon type I and III. MxA localizes to the cytoplasm and there is evidence that it associates with the smooth endoplasmic reticulum (smooth ER) [102]. Mx1, however, localizes to the nucleus and forms distinct dots, which were shown to be closely associated with promyelocytic leukemia (PML) nuclear bodies[103]. PML bodies form distinct nuclear dots 5-15 in number with a diameter of 0.1-1 µm[104]. The function of PML is highly diverse ranging from tumor suppression[105] over regulating apoptosis[106] to

the protection against a variety of viruses[107-109]. There are two isoforms of MxB, a longer isoform, which harbors a nuclear localization signal (NLS) and the other isoform lacking this NLS. The former therefore localizes to the nucleus, but interestingly to the cytoplasmic face of the nuclear envelope and the latter is dispersed throughout the cytoplasm.

MxA exhibits potent antiviral activity against many RNA[110] viruses, most thoroughly investigated Thogotovirus (THOV), a member of the bunya virus family, and IAV, but also two DNA viruses (Hepatitis B Virus (HBV) and African Swine Fever Virus (ASFV))[111,112]. It is interesting to note here, that despite MxA being localized to the cytoplasm it inhibits IAV and THOV, viruses that replicate in the nucleus, but also viruses whose replication takes place in the cytoplasm, whereas Mx1 only inhibits viruses which replicate in the nucleus. MxB on the other hand is only restricting HIV-1 and HSV-1. In 2013, Goujon and colleagues were able to show for the first time that human MxB indeed harbors anti-HIV activity[113] and this year MxB was characterized to be a Herpes virus restriction factor[114].
When cells are stimulated with interferon-α2, endogenous MxA is present as a tetramer in the cell[115]. There are several mutants available, which lock MxA in a defined oligomeric state[115]: monomeric (M527D, L612K) or dimeric (L617D, R640A) variants, which retain their antiviral potential. Inactive GTPase domain mutants, abolishing GTP-hydrolysis function only or in combination with GTP-binding, are additionally available (Δ81-84, T103A, D250N, D253N). It has also been shown *in vitro* under high salt concentrations that MxA can form higher order oligomers and ring-like structures similar to dynamin[116].

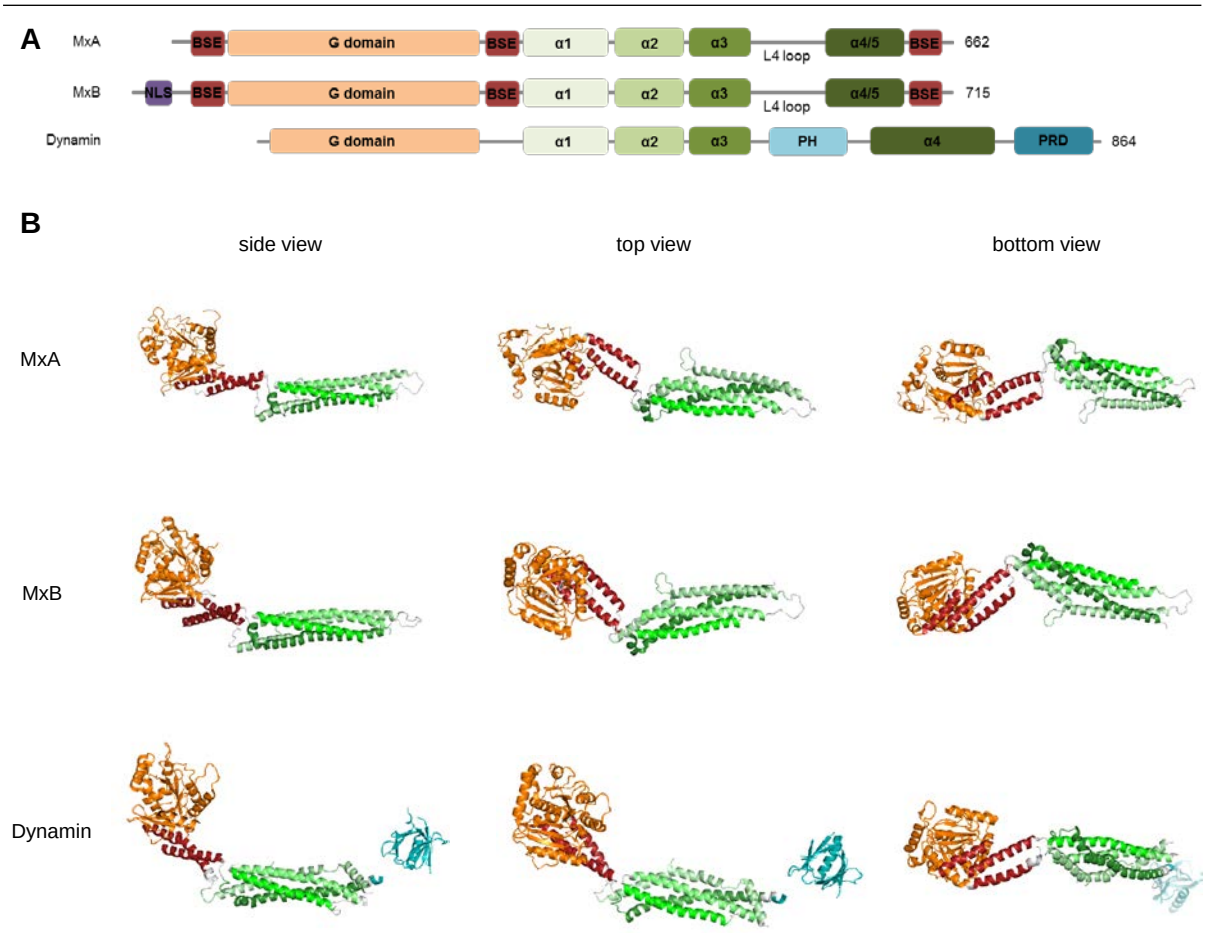

Fig. 1.4. Structural comparison of human MxA, MxB and dynamin. A) Schematic representation of the indicated proteins and their length in number of amino acid residues. G domain: GTPase domain, BSE: bundle-signaling element, α1-5: α-helices 1-5, NLS: nuclear localization signal, PH: pleckstrin homology domain, PRD: proline-rich domain. **B)** Crystral structures visualized with Pymol (RCSB protein database ID: MxA: 3szr, MxB: 4whj, dynamin: 3zvr)

1.3.1 Mx proteins and IAV

MxA and Mx1 inhibit their target viruses at different stages of the viral replication cycle. Focusing on IAV and bunyaviruses, Mx1, as opposed to MxA, generally inhibits earlier steps in the virus replication cycle. More specifically, in the presence of Mx1 primary transcription of both viruses is already inhibited. On the other hand, MxA does not interfere with primary transcription or the export of the primary transcripts[117], but targets a step after viral protein synthesis. MxA associates with IAV and bunyavirus nucleoproteins, but the mechanisms of action are not completely understood to date[118,119]. For bunyaviruses, however, it is thought that binding of MxA to the nucleoprotein (N) leads to its sequestration and missorting, which makes it inaccessible for the viral replication complex. Intriguingly, if the localization of MxA

is artificially changed from cytoplasmic to nuclear, IAV primary transcription is inhibited as seen with Mx1[120].

MxA efficiently inhibits the replication of a number of different IAV strains. Avian strains of IAV are generally more sensitive while human IAV strains have adapted to MxA and exhibit at least partial resistance[121,122]. Recent evidence through mutational scanning of single amino acid residues indicates that NP of IAV represents the target of MxA[122,123]. This was shown by the introduction of amino acid substitutions in the NP of MxA-sensitive H5N1 IAV strain originating from the resistant pH1N1 strain. These substitutions gradually decreased the sensitivity of H5N1 NP to MxA in the mini replicon assay[122].

The GTPase domain of Mx1 and MxA are highly conserved and also essential for the proteins antiviral activity. If the capability to hydrolyse GTP is abrogated the antiviral effect is lost as well. Intriguingly, the question of what the functions of GTP-binding and -hydrolysis are is still not resolved. On the other hand, MxB's G-domain function is dispensable for its anti-HIV activity[124] but crucial for the inhibition of HSV1 and HSV2 replication[114].

1.4 Cellular RNA helicase UAP56 (or DDX39B)

UAP56 belongs to the DEAD-box family of RNA helicases. This is a family of RNA helicases, which are found in all eukaryotes and also most prokaryotes. The name originates from a conserved motif consisting of the four amino acids aspartic acid (Asp, D), glutamic acid (Glu, E) and alanine (Ala, A) in the order D-E-A-D[125-127]. This family of ATP-dependent RNA helicases are involved in a variety of processes ranging from unwinding of dsRNA, nuclear RNA export, RNA folding, remodeling of RNA-protein complexes to performing RNA chaperone functions and being involved in splicing and translation initiation[125].

UAP56 in particular is a nucleo-cytoplasmic shuttling protein[128], since it is part of the transcription export (TREX) complex[129] and involved in the nuclear export of spliced cellular mRNAs[130]. UAP56 is composed of two globular domains, which are connected by a flexible linker[131] and is intracellularly present as a dimer. In humans, there is a closely related gene coding for the UAP56-Related Helicase URH49 (or DDX39A) [132]. The two proteins share 90% sequence homology, however, the DEAD-box RNA helicase motifs are fully conserved. The least conserved parts can be found at the N-terminus[128]. The two proteins have very similar functions but they differ in the expression level. In most tissues UAP56 mRNA levels are much higher than URH49 levels[132].

In the context of IAV infection it has been shown that UAP56 knock-down results in reduced viral titers (as well as URH49 knock-down, although to a lesser extent)[133] and impaired mRNA export of several viral genome segments[134]. Additionally, dsRNA accumulation can be

observed in the cytoplasm[133]. This may indicate that UAP56 plays a role in preventing the interferon system from being activated through inhibition of dsRNA formation.
UAP56 also appeared as a potential hit in an siRNA screen, where it was screened for loss of anti-IAV activity of MxA through a knock-down of a panel of different cellular proteins[135].
UAP56 (and URH49) have further been shown to interact with Mx1[57], MxA[57] and UAP56 also interacts with free (not bound in the vRNPs) NP[136,137]. UAP56-NP complexes, however, dissociate when challenged with increasing amounts of RNA[136] and NP-RNA complexes are formed. This could indicate a chaperone function for UAP56 to prevent the aggregation of NP and promote the assembly of NP molecules onto the elongating vRNA during replication. It has indeed been shown in 2011 that long nascent cRNA production *in vitro* was stimulated in the presence of UAP56 as opposed to NP alone[29]. So as a model the authors proposed a chaperone function of UAP56, whereby NP is co-replicationally added to the growing cRNA chain to prevent the formation of secondary structure formation and therefore premature termination of cRNA synthesis.

1.5 Aims of this work

MxA is an interferon- induced protein, which potently protects cells from invading pathogens, such as, most importantly for this work, IAV. The *Mx1* gene was identified more than 50 years ago and (human) MxA's high antiviral potential against IAV and vesicular stomatitis virus (VSV) was first shown in 1990[138]. In the following decades a lot of work was performed to shed light on the antiviral mechanism of MxA but to so far the exact mechanism of action on the molecular level still remains elusive. The viral target protein of MxA is thought to be NP and there has also been experimental evidence of the involvement of the cellular RNA helicase UAP56 in MxA's antiviral function.
We therefore investigated the interplay between the three proteins MxA, NP and UAP56, with respect to the importance of the proteins' stoichiometry and/or enzymatic activity. We also aspired to map the binding sites in each protein to its two interactors. We further aimed at finding viral and cellular determinants of the antiviral action of Mx proteins also in conjunction with UAP56. Additionally, we investigated the antiviral potential of MxB against IAV, a protein closely related and very similar in structure to MxA.

2 Nuclear MxB variant blocks influenza A virus replication

Fiona Steiner[1,2] , Michel Crameri[1,2], Jovan Pavlovic[1]

[1] Institute of Medical Virology, University of Zurich, Winterthurerstrasse 190, 8057 Zürich, Switzerland

2 Life Science Graduate School, University of Zurich, Zurich, Switzerland

2.1 Abstract

Mx proteins are a group of proteins with potent antiviral potential. Different Mx proteins localize to different subcellular compartments and also inhibit different viruses in seemingly different ways. Human MxA localizes to the smooth endoplasmic reticulum in the cytoplasm and exerts potent anti-IAV activity at a step after primary transcription and export of viral mRNAs. However, if it is artificially re-localized to the nucleus IAV replication is still inhibited but at an earlier step before primary transcription. This inhibition of primary transcription is also seen in cells expressing Mx1, a mouse homolog of MxA localizing to the nucleus. However, mouse Mx1 does not inhibit IAV when mis-localized to the cytoplasm. We thus investigated the structurally very similar human MxB protein, which is primarily localized to the cytoplasm and the cytoplasmic face of the nuclear envelope in terms of its antiviral potential when located to the nucleus.

We showed that nuclear MxB inhibits IAV replication at the level of or before primary transcription similar to mouse Mx1. This suggests a conserved antiviral mechanism between different Mx proteins, which is dependent on the exact subcellular localization. We further observed the capability of TMxB to bind to IAV NP. This and the fact that also wildtype MxB co-precipitated with NP suggests that NP-binding is not sufficient to exert anti-IAV activity.

2.2 Introduction

Mx proteins are dynamin-related GTPases that play key roles in the interferon type I and III mediated innate immune response against viruses (reviewed in[96]). They interfere with the replication of many RNA and DNA viruses by inhibiting early steps of their life cycle. The two MX genes (MX1 and MX2) of the human genome encode the two proteins MxA and MxB (also designated Mx1 and Mx2). MxA protein restricts a broad spectrum of viruses, primarily negative-stranded RNA viruses and DNA viruses but also some positive-stranded RNA viruses (for a review see[95]). The subcellular localization determines in part the antiviral specificity of Mx proteins[120,139]. MxB has recently been shown to inhibit the replication of primate (non-human and human) lentiviruses and herpesviruses[113,114]. Mammalian Mx proteins accumulate in different subcellular compartments. Human MxA accumulates in the cytoplasm and has been reported to be associated with the plasma membrane as well as the smooth endoplasmic reticulum[102,140]. MxB exists as at least two isoforms of 715 and 690 amino acids in length. The longer isoform represents the full-length form including the amino terminal NLS, while the shorter isoform engages the second methionine (M26) downstream of the NLS as translation start site[141,142]. The full length MxB is localized primarily on the cytoplasmic face of the nuclear membranes but when expressed ectopically it can also be found in the cytoplasm or in the nucleus in a granular pattern in the heterochromatin region beneath the nuclear envelope[114,142,143]. The short isoform is expressed in the cytoplasm[144,145]. The mouse genome carries two Mx genes encoding nuclear Mx1 and cytoplasmic Mx2[93,146]. Mouse Mx1 protein contains an NLS in the carboxy-terminal region and is thus exclusively expressed in the cell nucleus[93,147]. Mouse Mx1 exclusively inhibits members of the orthomyxovirus family including influenza A virus (IAV), which replicates in the cell nucleus. By contrast, Mx2 restricts vesicular stomatitis virus (VSV) and Hantaan virus, both negative-stranded RNA viruses replicating in the cytoplasm[146,148,149]. Intriguingly, MxA restricts not only various RNA viruses replicating in the cytoplasm such as VSV, La Crosse virus or Semliki forest virus (SFV) but also several members of the orthomyxoviruses, including IAV (reviewed in[95,96]). Mx proteins require a functional G-domain to inhibit Mx-sensitive viruses; exceptions are MxB when targeting lentiviruses[113] and MxA blocking HBV[150]. Although the viral targets of Mx proteins are known for many Mx-sensitive viruses to be nucleoproteins (or vRNP complexes) or nucleocapsids (reviewed in[95]), the molecular mechanism(s) of action of Mx proteins remain to be elucidated. In the case of IAV the prevailing model predicts that Mx1 as well as MxA attach to the IAV vRNPs by forming oligomeric “ring-like” structures thereby blocking the activity of the viral polymerase[151-153]. However, this mode of action does not explain the pronounced inhibition of the IAV based mini-replicon system where replication occurs from vRNPs formed in the nucleus[154]. Hence, MxA must act at an additional step of the viral replication cycle. We have recently shown that the mouse Mx1 as well as human

MxA bind to the cellular DEAD-box RNA helicase UAP56[57]. Intriguingly, UAP56 is required for efficient replication of IAV at multiple steps of the viral life cycle, which include predicted efficient export of viral RNAs (as for other viruses[155,156]) to the cellular translation machinery as well as a chaperone function for newly synthesized NP to be incorporated into newly formed vRNPs in the nucleus of infected cells[29,57,133,137]. Hence, it is conceivable that MxA targets the UAP56-NP complex in the cytoplasm and thereby restricting the availability of NP for the replication process by a yet to be identified mechanism. MxA is thought to exert a gate keeper function in the cytoplasm, blocking or modifying NP of incoming vRNPs and/or newly synthesized NP in the cytoplasm of infected cells. Similarly, for MxB evidence also points to a gate keeper function by preventing the nuclear import of genomic DNA of human lentiviruses and herpesviruses into the nucleus[114,157].

The fact that Mx proteins inhibit a wide variety of RNA and DNA viruses at different subcellular locations raises the question whether (i) Mx proteins act via a largely common mechanism and the observed virus specificity is a consequence of distinct subcellular localization or (ii) Mx proteins act through distinct molecular mechanisms.

When MxA was ectopically expressed in the nucleus by virtue of an artificial NLS attached to its amino terminus (TMxA) it exhibited a pronounced restriction of IAV already at the stage of primary transcription of viral mRNAs[120], the same phenotype which is seen in Mx1-expressing cells. However, the cytoplasmic variant of Mx1 mMx(R614E) that lacks a functional NLS is not able to adopt the activity of MxA. Mx1(R614E) exhibited no antiviral activity neither against IAV nor VSV[139]. These data suggest that the mode of action of human MxA and mouse Mx1 differ and that MxA has the ability to block IAV in the cytoplasm as well as in the nucleus by employing distinct mechanisms. Nevertheless, this study did not take into account that Mx proteins may have to localize to specific sites in the cytoplasm in order to exert antiviral activity against a given virus. Hence, it may be possible that the different Mx proteins from different mammalian species act by using the same mechanism.

To address this issue we made use of human MxB predominantly accumulating in the perinuclear region. This protein exerts antiviral activity against HIV and herpesviruses but not IAV. We reasoned that if our hypothesis was correct a nuclear form of MxB should restrict IAV replication. To this end we chose the NLS of the large T antigen of SV40, since cytoplasmic MxA directed to the nucleus by the same NLS exhibits pronounced anti-IAV activity. We show here that MxB targeted to the nucleus indeed blocks IAV replication at a step prior to primary transcription.

2.3 Experimental procedures

2.3.1 Cell lines

All cell lines were cultured in DMEM supplemented with 10% FCS, 1 mg/ml Penicillin/Streptomycin and 2 mM GlutaMAX™ (Thermo Fisher Scientific) (complete DMEM) at 37°C and 5% CO_2. HEp-2 (HeLa-derived human epithelial cells) and HEK-293T (human embryonic epithelial kidney cells) were purchased from ATCC.

2.3.2 Plasmids

As previously described MxA wt cDNA was cloned into pcDNA3.1(+)neo (Invitrogen)[158]. MxA(R640A) cDNA in pcDNA3.1(+)neo plasmids was kindly provided by Georg Kochs, Freiburg, Germany. MxA mutant D250N was generated using the QuikChange II Site-Directed Mutagenesis Kit (Agilent). Primers were designed using http://www.bioinformatics.org/primerx/ with the QuikChange protocol.
pCAGGS-NP plasmid (NP cDNA derived from A/Thailand/1(*KAN-1*)/2004 (H5N1), was kindly provided by Martin Schwemmle, Freiburg, Germany.
MxB cDNA with an N-terminal FLAG-peptide sequence or MxB cDNA with an N-terminal large T antigen NLS peptide plus FLAG-peptide were cloned into pcDNA3.1(+)neo (Invitrogen) using the *NotI* and *XbaI* restriction sites. FLAG-Mx1 or FLAG-Mx1(K49A) encoding plasmids were previously described[159]. TMx1 encoding plasmid was described previously[139]. Mutants Mx1(R614E) and TMx1(R614E) were generated using the QuikChange II Site-Directed Mutagenesis Kit (Agilent). Primers were designed using http://www.bioinformatics.org/primerx/ with the QuikChange protocol.

2.3.3 Viruses

Infection experiments were carried out using Influenza A/Seal/Massachusetts/1/1980 H7N7 (≡rSC35M). Infections were carried out in PBS supplemented with 0.02 mM Mg^{2+}, 0.01 mM Ca^{2+}, 0.3% BSA and 1% penicillin/streptomycin (PBSi) for 1 h at 37°C. Inoculum was removed, cells were washed with PBS and DMEM supplemented with 20mM HEPES, 0.2% bovine serum albumin (BSA), 1 mg/ml Penicillin/Streptomycin and 2 mM GlutaMAX™ (Thermo Fisher Scientific) (piDMEM) was added.

2.3.4 Immunofluorescence assay

Cells were seeded in 24-well format on glass cover slides. After transfecting with jetPRIME® (Polyplus transfection), cells were fixed with 3% paraformaldehyde (PFA) in PBS for 10 min at RT and permeabilized with 0.1% or 0.5% Triton-X100 in PBS for 10 min at RT. Staining was performed in PBS with 5% goat serum for 1 h at RT (mouse α-MxA (hybridoma ab143, 1:5), mouse α-MxB (Santa Cruz, sc 271527, 1:50), mouse α-FLAG M2 (Sigma, F1804, 1:1000), rabbit α-PML (Bethyl laboratories, A301-167A, 1:500).

2.3.5 Minimal replicon reconstitution assay

The mini replicon assay has been described before[154]. Basically, pcDNA3.1(+)neo vectors harboring cDNA sequences of the viral polymerase subunits PB1,PB2 and PA and viral NP derived from the A/Thailand/1(*KAN-1*)/2004 (H5N1) strain were transfected into 293T cells. Additionally, the firefly luciferase (FFLuc) reporter plasmid pPOLI-Luc-RT (Zimmermann et al, 2011) and the constitutively active *Renilla reniformis* luciferase (RRLuc) plasmid pRL-SV40-R*luc* (Promega) as a read-out and for transfection efficiency were co-transfected using jetPRIME® (Polyplus transfection) according to the manufacturer's instructions. 10 ng PB1, PB2 and PA and 50 ng NP, FFLuc and RRLuc plasmids plus varying amounts of plasmids coding for Mx proteins were transfected. For the read-out, cells were lysed 24 h after transfection in 60 µl 1X passive lysis buffer and incubated at room temperature for 15 min on a shaker. A dual-luciferase read-out was performed using the Dual-Luciferase® Reporter Assay System (Promega). 15 µl lysate was mixed with 45 µl LARII and immediately read on a Perkin Elmer Envision 2104 plate reader for the Firefly luciferase signal and additional 45 µl Stop&Glo was added for the Renilla luciferase read-out.

2.3.6 Cell-Titer-Glo assay

293T cells were transfected and 48 h post transfection half the volume of the medium was aspirated. An equal volume of Cell-Titer-Glo reagent (as medium was aspirated) was added to the wells, incubated for 2 min at room temperature on a shaker and additional 10 min without shaking and luminescence was measured on a Perkin Elmer Envision 2104 plate reader.

2.3.7 Co-immunoprecipitation (co-IP)

HEp-2 cells were transfected with ViaFect™ (Promega) according to the manufacturer's instructions. 24 h post-transfection cells were lysed in 300 µl lysis buffer (20 mM Tris-HCl pH 7.5, 150 mM NaCl, 5 mM MgCl2, 50 mM NaF, 1 mM Na3VO4, 1% NP-40, 50 mM β-glycerophosphate, 100 nM iodoacetamide, 1x Roche cOmplete Protease Inhibitor Cocktail)

in the dark on ice for 30 min. Lysates were homogenized using QiaShredder columns (Qiagen). 100 µl of each lysate was incubated with antibody (α-NP (in-house, 50 µl, HB65, hybridoma) at 4°C over night on a rotating wheel. 15 µl lysate was used for the whole cell lysate (WCL) control. 20 µl Dynabeads protein G magnetic beads (Thermo Fisher Scientific) per sample were pre-adsorbed over night at 4°C on a rotating wheel using untransfected HEp-2 cell lysate. Pre-adsorbed beads were washed once with lysis buffer and incubated with the lysates for 1 h at 4°C on a rotating wheel. Beads were washed once with 1 ml followed by five times 0.5 ml lysis buffer. Beads were briefly vortexed in between the washing steps. Proteins were eluted from the beads with 20 µl 1x Laemmli buffer at 95°C for 10 min. 15 µl WCL/IP sample was loaded on a 10% SDS-PAGE gel and analysed by Western blot (α-NP (rabbit serum, in-house, 1:10'000), α-FLAG (mouse, Sigma, F-3165, 1:1000).

2.3.8 qRT-PCR

293T cells were transfected using jetPRIME® (Polyplus transfection) according to the manufacturer's instructions. 24 h post-transfection cells pre-treated for 1 h with 100 µg/ml cycloheximide (CHX) or DMSO. Cells inoculated with virus in PBSi for 1 h at 37°C with rSC35M or SFV V42 at MOI5. The inoculum was aspirated and piDMEM was added. 5 hpi the medium was removed and cells were lysed with 200 µl TRIzol™ reagent (Thermo Fisher Scientific) per well of a 24-well plate. After the addition of 40 µl chloroform the samples were mixed thoroughly by inverting the tubes several times and centrifuged at 13'000xg at 4°C for 15 min. The resulting upper aqueous phase (~120 µl) was transferred to a new tube and RNA extraction was subsequently performed using the RNeasy Mini Kit (Qiagen) starting with the addition of 1 volume of 70% EtOH. cDNA synthesis was performed with 1 µg RNA using SuperScript™ III Reverse Transcriptase (Thermo Fisher Scientific) and random primers. The qPCR reaction was performed with 2.5 µl of the 1:10 diluted cDNA and EvaGreen® fluorescent nucleic acid dye in a total volume of 20 µl. The cycling conditions were as follows: initial denaturation: 95°C for 5 min, denaturation: 95°C for 15 sec, annealing and extension: 60°C for 60 sec. A dissociation step starting at 55°C was added in the end to confirm the specificity of the primers. The primer sequences are: rSC35M PB2 forward primer: 5'-GCAATGGGCTTGAGGATT, rSC35M PB2 reverse primer 5'-CAATCTCCTGGTTGCCTT. GAPDH forward primer: 5-CTGGCGTCTTCACCACCATGG, GAPDH reverse primer 5-CATCACGCCACAGTTTCCCGG. Fold change of PB2 mRNA normalized to GAPDH mRNA was calculated according to[160]. In short: first ΔCt was calculated (Ct(CHX) - Ct(DMSO)) of a given sample, then ΔΔCt was assessed (ΔCt(Mx)-ΔCt(mCherry)) and the final values for plotting were shown as 2^(-ΔΔCt) (in percentage).

2.4 Results

We first tested whether full-length MxB encoding the NLS of the large T antigen at its amino terminus would be expressed in the cell nucleus (Fig. 2.1 A). We transiently transfected HEp2 cells with plasmids coding for MxB (negative control), FLAG-tagged TMxB, FLAG-tagged Mx1, the cytoplasmic mutant Mx1(R614E) lacking a functional NLS, or the FLAG-tagged mutant TMx1(R614E) redirected to the nucleus. As expected, TMxB accumulated in the nucleus forming different size speckles. Mx1 and the redirected mutant TMx1(R614E) showed a very similar punctuated pattern in the nucleus, omitting the nucleoli. The Mx1 mutant lacking a functional NLS accumulated predominantly in a punctate pattern in the cytoplasm. Since Mx1 assemblies have often been observed to be distributed in juxtaposition to PML bodies in the nucleus[103,161], we co-transfected HEp-2 cells with plasmids encoding Flag-tagged TMxB, TMx1, TMx1(R614E) or Mx1 and immuno-stained PML bodies and the FLAG peptide in parallel. Indeed, independent of the NLS used (heterologous or endogenous) PML bodies were often found next to Mx1 assemblies (Fig 2.1B).

Next, we tested whether TMxB would exert antiviral activity against IAV. To this end, we transfected HEK293T cells with plasmids encoding MxB wt, TMxB and MxA or with the control plasmids coding for mCherry or GST and infected them 24 h post transfection with 0.01 MOI of the A/Seal/Massachusetts/1/1980 (H7N7) strain of IAV. 24 h post infection the culture supernatants were harvested and subjected to plaque assay analysis (Fig. 2.2A). Surprisingly, TMxB expression restricted IAV to a similar extent than MxA, resulting in a 50 fold reduction of viral titers. Cell viability assays performed in parallel revealed that the observed reduction in titers was not due to possible cytotoxic effects of TMxB expression (Figure 2.2B).

In order to corroborate the antiviral activity of TMxB against IAV we tested its activity using the Kan1 based mini replicon system[121]. HEK293T cells were co-transfected with increasing amounts of plasmids (22ng, 66ng, 200ng and 600ng) encoding either mCherry (negative control), wild type MxA, the inactive G-domain mutant MxA(D250N), wild type mouse Mx1, the cytoplasmic mutant Mx1(R614E), Mx1 with the amino terminal NLS TMx1, or TMx1(R614E) together with plasmids encoding PB1, PB2, PA, and NP of the A/Thailand/1(KAN-1)/2004 (H5N1) strain, *Renilla* luciferase under a constitutive promoter and the firefly luciferase reporter. The data clearly indicate that TMxB restricted IAV replication at least as strongly as MxA while MxB showed only marginal activity at high concentration of the transgene (Fig. 2.2C). As expected the G-domain mutant MxA(D250N) and the cytoplasmic variant of Mx1 Mx1(R614E) exhibited no inhibitory activity against IAV. Mx1 and TMx1 exerted a very strong inhibition of the mini-replicon driven reporter gene expression. Surprisingly, however, TMx1(R614E) over-expression only marginally affected efficiency of the mini replicon system. The reason for this observation is not clear and

contradicts previously published data obtained in mouse 3T3 cells[139]. Since Mx proteins which localize to the nucleus such as Mx1 and TMxA inhibit IAV replication at or before primary transcription of viral mRNAs[117,139], we tested whether this is also the case for TMxB. We transiently transfected HEK293T cells with plasmids encoding mCherry, GST, Mx1, the G-domain mutant Mx1(K49A), MxA, MxB or TMxB and infected the cells with 5 MOI of the avian strain rSC35M for 6 hours in the presence or absence of cycloheximide (CHX). In the presence of cycloheximide IAV vRNPs are still able to enter the nucleus and to produce viral transcripts by the vRNP-associated viral polymerase. However, later steps are blocked by the translational inhibition exerted by cycloheximide[162]. Overall mRNA levels are thus reduced in CHX- versus DMSO-treated samples since the viral proteins PB1, PB1, PA and NP, which are crucial for viral genome replication, are not translated. As expected mRNA levels are 35- to 100-fold lower in CHX-treated samples in contrast to DMSO-treated controls (data not shown). Synthesis of viral mRNA was determined by RT-qPCR with primers specific for PB2. Indeed, TMxB inhibited viral RNA synthesis at a step prior to or during primary transcription to a very similar extent as Mx1 (Fig 2.3B). As expected, Mx1(K49A), lacking a functional G-domain, failed to inhibit viral mRNA synthesis in the presence or absence of cycloheximide (Fig. 2.3A).

We next tested whether MxB has the capacity to form stable complexes with NP. We transiently transfected HEp-2 cells with plasmids encoding FLAG-tagged MxA(R640A), wildtype MxB and TMxB together with a plasmid encoding NP of the Kan1 strain. The cells were lysed 24 h post transfection and the lysates subjected to co-immunoprecipitation using a monoclonal mouse anti-NP antibody. For MxA we employed the dimeric variant MxA(R640A) previously shown to exhibit antiviral activity and form a stable complex with NP[115] Surprisingly, MxB as well as TMxB were efficiently co-precipitated with NP indicating that MxB has the capacity to bind NP independently of its subcellular localization (Fig. 2.4A).

2.5 Discussion

The fact that Mx proteins, in particular MxA, are able to exhibit a very broad antiviral specificity inhibiting many RNA as well as DNA viruses at different steps of their replication cycle suggests that Mx proteins are multi-functional proteins exerting different strategies to block viral replication. For instance, MxA blocks the replication of viruses as diverse as VSV and HBV at different steps of their life cycle (reviewed in[95]). Moreover, Mx proteins can be found in different subcellular compartments. Human MxA resides in the cytoplasm where it is partially associated with internal membranes, in particular the smooth endoplasmic reticulum, whereas the human MxB accumulates primarily in the perinuclear region associated with the outer membrane of the nucleus but can also be found in the cytoplasm[102,114,140,142].

In this study we addressed the question whether the apparent diversity of antiviral activities of Mx proteins is a consequence of distinct subcellular localizations rather than a multitude of molecular mechanisms. To test this hypothesis we employed the human MxB protein with well-defined antiviral activities against HIV and HSV but not IAV. We reasoned that if our hypothesis were correct redirecting MxB into the nucleus by attaching a classical NLS should enable it to block the replication of IAV occurring in the nucleus. Indeed, ectopic expression of TMxB inhibited infection with IAV (Fig 2.2A). Moreover, TMxB but not MxB efficiently blocked the expression of a luciferase reporter gene driven by the mini-replicon system based on the avian IAV strain Kan1 indicating that MxB has the capacity of interfering with IAV when located in the nuclear compartment. We also re-tested a cytoplasmic variant of Mx1 harboring a mutation, which disrupts the endogenous NLS. This mutant has previously been reported to be inactive in the cytoplasm but active when redirected to the nucleus by a heterologous amino-terminal NLS. According to our hypothesis of a universal Mx mechanism, a cytoplasmic variant of Mx1 should exhibit a similar activity as MxA. We found that indeed the cytoplasmic Mx1(R614E) lost its capacity to interfere with IAV replication, however, surprisingly the redirected nuclear form TMx1(R614E) did not exhibited strong activity either. The R614 residue of the Mx1 NLS resides in the carboxy-terminal part of the tripartite BSE that is critical for the proper function of Mx proteins. Hence, we believe that a drastic change of a negatively charged K residue to a positively charged E residue reduces the antiviral function of Mx1 per se and does not reflect inactivity due to an altered subcellular localization. The observed differences between the present study and the study by Zürcher and colleagues are most likely due to the use of different cell culture (human versus mouse) and assay systems[139].

As expected, expression of the TMxB reduced the synthesis of primary viral PB2 mRNA to a similar extent than Mx1 strongly suggesting that TMxB like Mx1 interfered directly with viral mRNA transcription by interfering with the activity of the viral transcriptase complex[163,164]. Surprisingly, cells expressing the cytoplasmic MxA also showed reduced levels of viral primary transcripts. Evidence suggests that MxA can inhibit IAV replication at two different steps (i) during cell entry by blocking incoming vRNPs in the cytoplasm preventing nuclear import of vRNPs or (ii) by interfering with the integrity or transport of newly synthesized NP, a step following primary viral mRNA synthesis. It is therefore conceivable that in this experimental setting overexpression of MxA led to a pronounced block of vRNP import into the nuclei of infected cells, preventing initial viral mRNA synthesis.

Since the antiviral activities of Mx1 and MxA are associated with at least a transient interaction with their viral target NP[115,122,123,151] it came as no surprise that MxB has the capacity to bind NP (Fig 2.4). Intriguingly, we observed that wild type MxB was able to form a stable complex with NP as opposed to MxA, which can only stably interact with NP in the

dimeric state (variants MxA(R640A) or MxA(L617D)) but not in its wildtype form existing as a tetramer. The fact that MxB appears to predominantly form dimers[141] most likely explains this apparent difference.

Moreover, like mouse Mx1 and human MxA, MxB has also the capacity to form a complex with UAP56. The DEAD-box RNA helicase UAP56 is indispensable for IAV replication at several steps of its life cycle. Recently, several reports showed that UAP56 acts as a chaperone for newly synthesized NP directing it to the site of viral transcription and replication in the nucleus where NP acts as a co-factor for the viral polymerase and protects the nascent vRNA chains[29]. Hence it is tempting to speculate that Mx proteins interfere with this process by sequestering newly synthesized NP from the replication site. However, firm proof for this proposed mode of action of Mx proteins is still lacking.
Interestingly, wild type MxB which exhibited no inhibitory activity against IAV was able to form stable complexes with NP as efficiently as TMxB, which exerts a pronounced restriction of IAV. These findings strongly suggest that the ability of MxB to form a complex with UAP56 and NP is not sufficient for exhibiting antiviral activity. Evidently, an additional factor provided in the nucleus but not in the perinuclear region is required for its activity against IAV.
In this context it is interesting to note that MxB accumulating in the perinuclear region also forms stable complexes with UAP56 (Fig 2.4B). Hence, the complex formation of MxB with UAP56 may represent an integral functional feature, independent of its activity against IAV. Possibly the association with UAP56 is a necessary prerequisite for MxB to inhibit additional as yet not identified viruses. The positive selection of amino acid residues at the amino terminus of MxB in higher primates, that are not associated with a known antiviral function yet, point in this direction[165].

Here we report for the first time that nuclear MxB has the potential to restrict IAV replication. In the future it would be of great interest to further characterize this antiviral activity on the mechanistic level. Also, MxA and MxB are very similar in structure; however, they vary greatly in their anti-IAV activity. More insights into the factors that determine this essential difference would likely shed more light on the general antiviral mechanism of Mx proteins and are thus much sought after.

Fig. 2.1

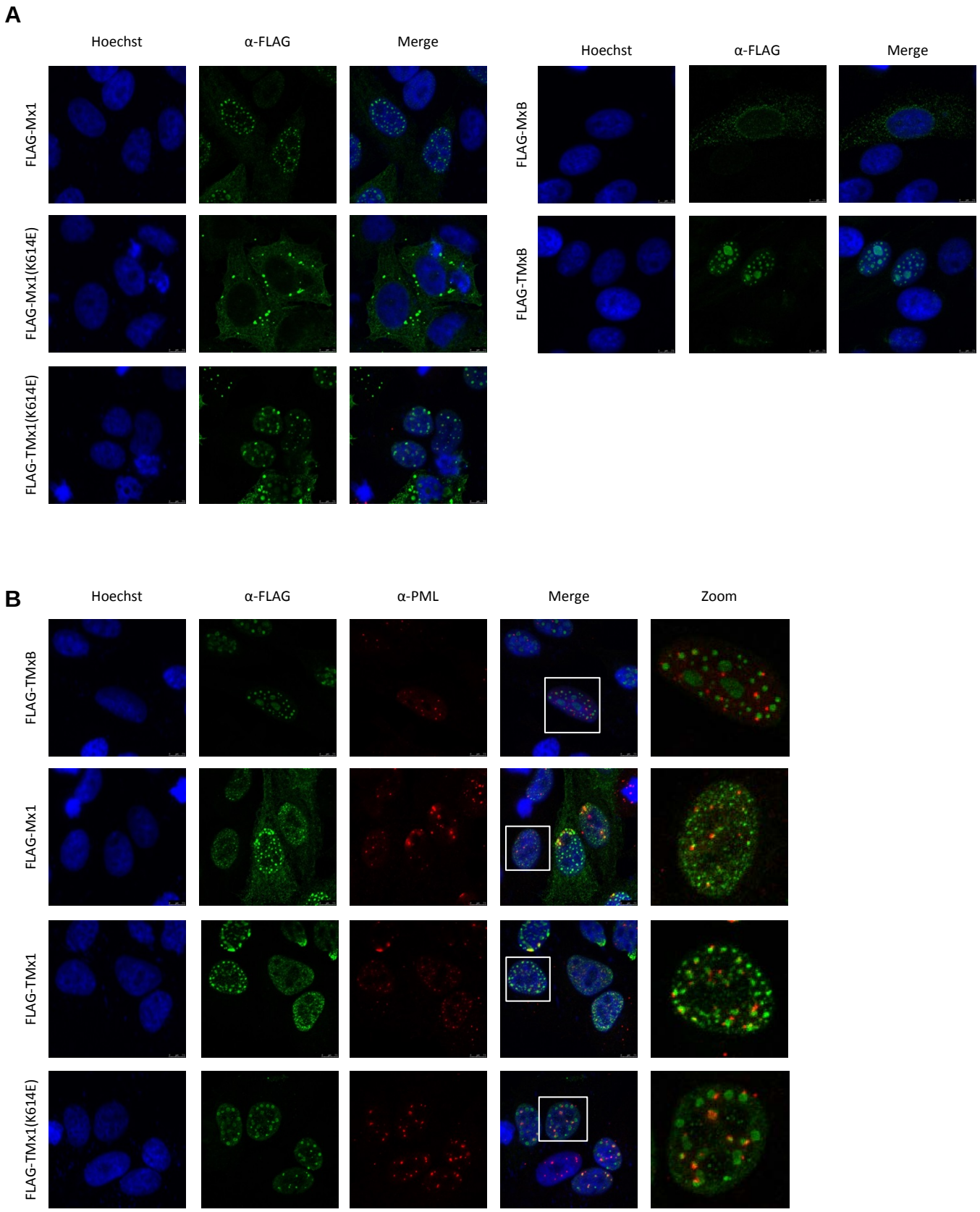
A
Hoechst
α-FLAG
Merge
FLAG-Mx1
FLAG-Mx1(K614E)
FLAG-TMx1(K614E)
Hoechst
α-FLAG
Merge
FLAG-MxB
FLAG-TMxB
B
Hoechst
α-FLAG
α-PML
Merge
Zoom
FLAG-TMxB
FLAG-Mx1
FLAG-TMx1
FLAG-TMx1(K614E)

2.1 Mx1 and nuclear MxB (TMxB) are associated with PML bodies. A HEp-2 cells were transfected with plasmids coding for wildtype MxB, nuclear MxB (TMxB), wildtype Mx1, cytoplasmic Mx1 (Mx1(K614E)) and TMx1(K614E). Cells were fixed and immune-stained as indicated. **B** HEp-2 cells were transfected with plasmids coding for TMxB, Mx1, TMx1 and Mx1. Cells were fixed and immuno-stained with the indicated antibodies. PML bodies: promyelocytic leukaemia nuclear bodies.

Fig. 2.2

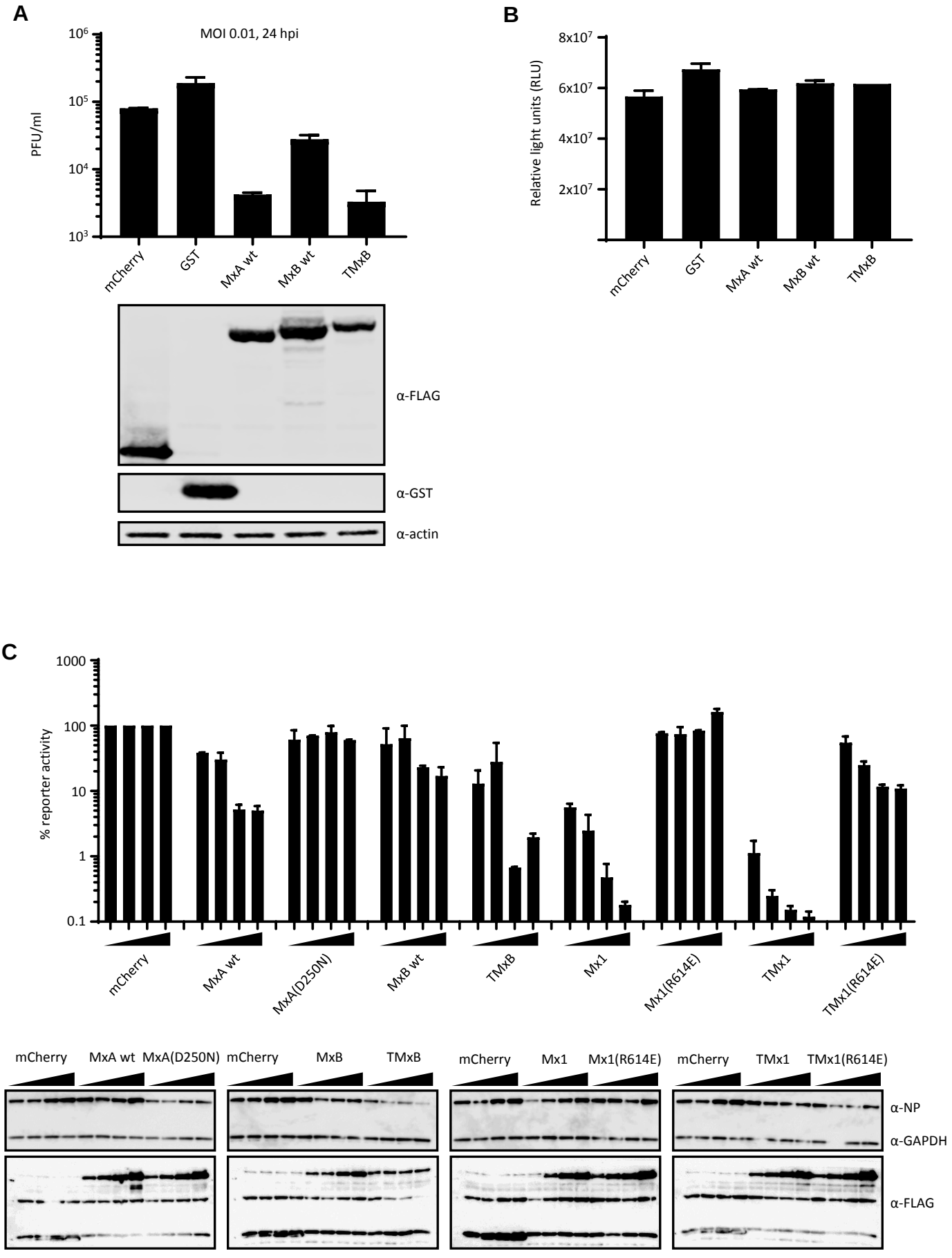
A
MOI 0.01, 24 hpi
PFU/ml
10^6
10^5
10^4
10^3
mCherry
GST
MxA wt
MxB wt
TMxB
α-FLAG
α-GST
α-actin
B
Relative light units (RLU)
8x10^7
6x10^7
4x10^7
2x10^7
mCherry
GST
MxA wt
MxB wt
TMxB
C
% reporter activity
1000
100
10
1
0.1
mCherry
MxA wt
MxA(D250N)
MxB wt
TMxB
Mx1
Mx1(R614E)
TMx1
TMx1(R614E)
mCherry
MxA wt
MxA(D250N)
mCherry
MxB
TMxB
mCherry
Mx1
Mx1(R614E)
mCherry
TMx1
TMx1(R614E)
α-NP
α-GAPDH
α-FLAG

2.2 A nuclear variant of MxB (TMxB) shows restriction of IAV replication. A left: Plaque assay titration of supernatants harvested from 293T cells transiently transfected with plasmids coding for the indicated control protein or Mx proteins and infected with MOI 0.01 for 24 h. Supernatants were titrated on MDCK cells. Data are represented as mean ±SEM of duplicates. Right: expression control. Samples were harvested at the same time as supernatants were collected for the plaque assay. Immunostaining was performed using the indicated antibodies (bottom panel). **B** Cell-Titer-Glo cell viability assay. 293T cells were transfected as in **A** and cells were lysed at the same time as supernatant was collected for the plaque assay from an identical plate. Luminescence was measured and absolute values were plotted. Data are represented as mean ±SEM of duplicates. **C** Mini replicon assay of 293T cells transfected with plasmids encoding the mini replicon constituents and increasing amounts of mCherry or various Mx proteins. Cells were lysed and a dual luciferase assay was performed. Values are presented in percent firefly luciferase activity normalized to *Renilla* luciferase relative to the mCherry control for each condition individually (22ng, 66ng, 200ng 600ng). Values of mCherry-expressing samples are set to 100%. Data are represented as mean ±SEM of duplicates. Western blot analysis was performed on pooled lysates for each condition and immunostaining was performed with the indicated antibodies (bottom panel).

Fig. 2.3

A

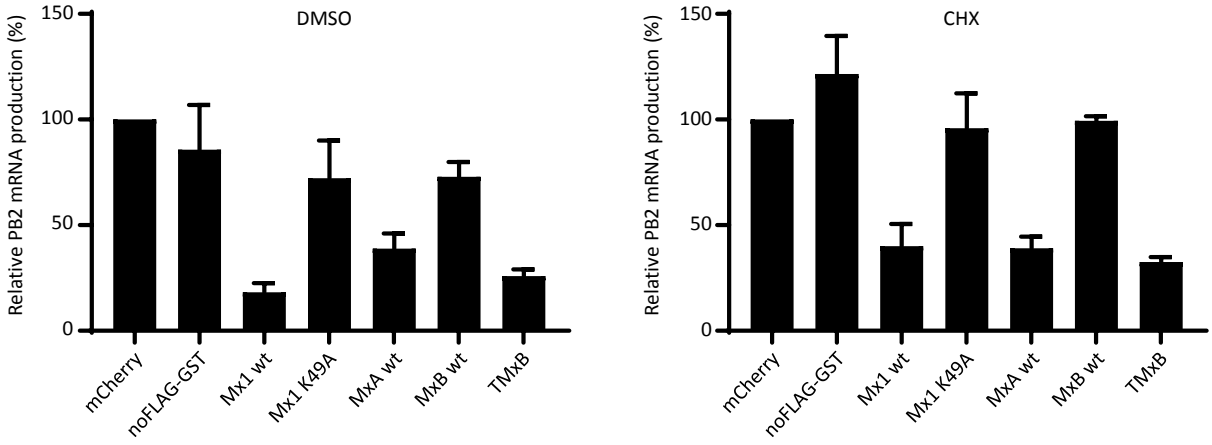
DMSO
CHX
Relative PB2 mRNA production (%)
150
100
50
0
mCherry
noFLAG-GST
Mx1 wt
Mx1 K49A
MxA wt
MxB wt
TMxB

B

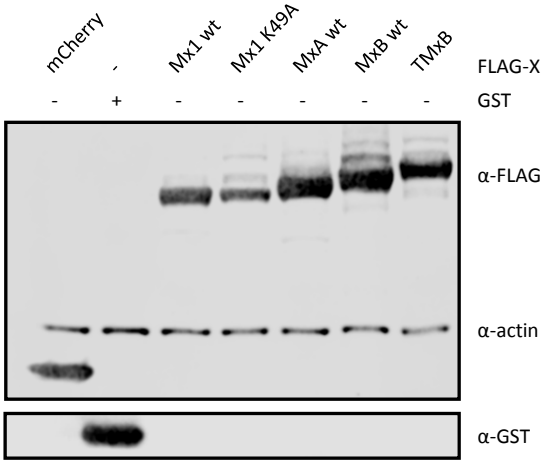
mCherry
-
Mx1 wt
Mx1 K49A
MxA wt
MxB wt
TMxB
FLAG-X
- + - - - - -
GST
α-FLAG
α-actin
α-GST

2.3 Primary transcription of IAV is inhibited by TMxB. A 293T cells were transfected with plasmids coding for the indicated control or Mx proteins and infected with rSC35M(H7N7) at MOI5 for 6 h. RNA was isolated and reverse transcribed into cDNA using random primers. RT-qPCR analysis was performed and PB2 mRNA normalized to GAPDH mRNA is shown. Cells were pre-treated with 100 µg/ml cycloheximide (CHX) or the same volume of solvent (DMSO) for 1 h prior to infection. Infection was carried out in the presence of CHX. Values are relative to the mCherry control, which was set to 100%. Data are represented as mean ±SEM of triplicates. **B** Western blot analysis of 293T cells transfected and lysed at the same time as in **A**. Immunostaining was performed with the indicated antibodies.

Fig. 2.4

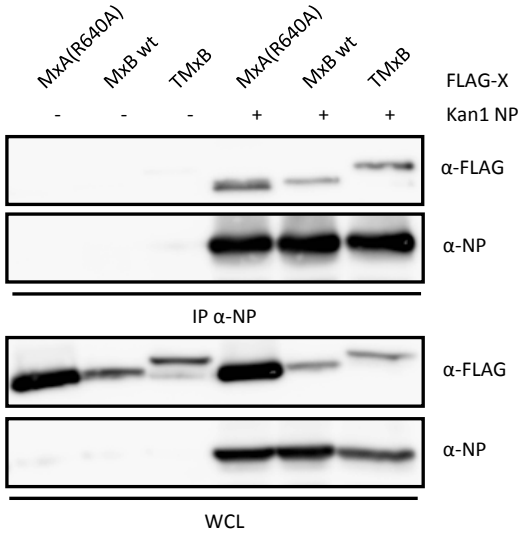
MxA(R640A)
MxB wt
TMxB
MxA(R640A)
MxB wt
TMxB
FLAG-X
- - - + + +
Kan1 NP
α-FLAG
α-NP
IP α-NP
α-FLAG
α-NP
WCL

2.4 TMxB interacts with Kan1 NP. A HEp-2 cells were transfected with plasmids coding for the indicated Mx proteins and either a Kan1 NP-expressing plasmid or the empty vector only. Immunoprecipitation was performed with an α-FLAG antibody. IP fractions and WCL samples were subjected to Western blot analysis using the indicated antibodies.

3 The trimeric MxA-NP-UAP56 complex: Identifying molecular determinants to unravel their interplay

Fiona Steiner[1,2] and Jovan Pavlovic[1]

[1] Institute of Medical Virology, University of Zurich, Winterthurerstrasse 190, 8057 Zürich, Switzerland

2 Life Science Graduate School, University of Zurich, Zurich, Switzerland

3.1 Abstract

MxA exerts potent activity against a panel of RNA- and DNA-viruses with influenza A virus (IAV) being one of those target viruses. IAV replication is inhibited by MxA through a yet uncharacterized mechanism targeting the viral nucleoprotein (NP). Evidence suggests, however, that incoming vRNPs as well as a later less defined step between viral protein translation of viral proteins and replication are inhibited. Here we show that import of newly translated NPs was not affected by MxA. The mechanism of action further appeared not to be indirect by separating NP from its chaperone the cellular DEAD-box helicase UAP56. We further showed that the potential of MxA to inhibit IAVs of different origin does not correlate with its binding strength to the respective NPs. Also, the dimeric state of MxA, as opposed to its wildtype tetrameric form, is the determinant of stable binding to viral NP independent of its antiviral activity. The enzymatic activities of UAP56 are similarly dispensable to enable binding to MxA and NP. Lastly, we found two residues in NP, which are involved in NP oligomerization, to abrogate binding to MxA as well as UAP56 when mutated to alanine. Our results suggest MxA to modify NP, UAP56 or the NP-UAP56 complex prior to nuclear translocation and thereby abrogating functional integrity.

3.2 Introduction

The human organism has evolved various means to fight the multitude of pathogens, which constantly threaten its health. One of such means is the interferon system, a fast and broadly acting defense mechanism present in virtually all human cells. When activated trough pathogen recognition the innate immune system induces the expression of a variety of interferon stimulated genes (ISGs) with potent activities against a variety of invading pathogens. In the context of influenza A virus (IAV) infection there are several well described ISG products such as 2′,5′-oligoadenylate synthetase (OAS) and RNase L, protein kinase R (PKR) and interferon-inducible transmembrane (IFITM) proteins (reviewed in[166]). Another protein that plays a major role in restricting IAV infections is the myxovirus resistance protein 1 (MxA). MxA is a cytoplasmic dynamin-like large GTPase, which is induced by interferon (IFN) type I (α/β) and type III (λ)[112,158,167,168] and although it has been discovered over 50 years ago[92,169] its mechanism of action against IAV is still not very well characterized. The crystal structure of MxA reveals an N-terminal globular GTPase-domain (G-domain) and a C-terminal elongated stalk domain, which is connected to the G-domain via a tripartite bundle signaling element (BSE)[98,170]. In IFN-stimulated cells MxA presents itself as a tetramer[115] but it has also been shown *in vitro* to form higher order oligomeric structures[116,171]. An enzymatically active G-domain is indispensable for its antiviral activity[159,172,173] however a functional role for GTP hydrolysis in relation to MxA function has not been assigned yet.

A vast effort has been made in the past decades to shed more light on the detailed antiviral mechanism of MxA not only against IAV but against a variety of RNA and DNA viruses. For Thogoto virus (THOV), an orthomyxovirus virus like IAV, it has been shown that primary transcription is inhibited by binding to and blocking the transport of the viral nucleocapsids into the cell nucleus[174,175]. Furthermore, an unstructured loop (loop L4) in the stalk domain of MxA has been associated with this function[100]. This loop also seems to be the determinant for antiviral specificity[99] and is responsible for the localization of MxA to the smooth endoplasmic reticulum (ER)[116]. Considering the viral replication cycle of IAV (see fig. 3.6), one of the earliest steps at which IAV could be inhibited is primary transcription and export of the mRNA transcripts. However, it has been shown that these processes are unaffected in MxA-expressing cells[115,117]. Viral replication, on the other hand, is highly reduced. It has further been shown, that the viral target protein of MxA is the nucleoprotein (NP)[115,123], an abundant protein in in the nucleocapsids of IAV virions, which envelops the viral genomic RNA segments. If certain residues are exchanged between NPs derived from human and avian strains, with human strains generally being more resistant to MxA, inhibition of IAV replication by MxA can be altered dramatically[122]. Binding of viral NP to MxA has additionally been shown[115], which strengthens the hypothesis of NP being the major target of MxA.

Cellular factors are further involved in the antiviral function of MxA. The DEAD-box helicase UAP56 (also designated DDX39B) was shown to interact with MxA[57]. This helicase is part of the transcription export (TREX) complex, which is involved among other processes in mRNA transcription and nuclear export[176]. UAP56 is a dimeric nucleo-cytoplasmic shuttling protein but it localizes mainly to the nucleus in fixed cells[57]. There is further evidence that UAP56-expression is crucial to maintain the antiviral potential of MxA, since MxA loses its activity when UAP56 is downregulated[135]. UAP56 has also been implicated in being a proviral factor[133] acting co-translationally as a chaperone for IAV NP. This ensures safe transport of NP to the nucleus, where it is delivered to viral RNA and supports viral replication[29].

In this work we aimed at resolving the inhibitory mechanism of MxA against IAV in more detail. It is currently under debate, whether viral primary transcription is affected in MxA-expressing cells[115,117,177,178] (Fig.2.3A, Martin Schwemmle, personal communication). It is clear, however, that MxA engages with viral NP[115]. This occurs either very early with NP incorporated in incoming vRNPs or at a later step after primary transcription with newly translated NP. The proposed antiviral mechanism through binding of MxA to incoming vRNPs is based on a ring-like model of MxA. This model, however, is solely based on crystal structures and *in vitro* oligomerization assays[98,153,170]. We thus hypothesized that following primary mRNA transcription, nuclear export and translation, the translocation step of newly generated viral proteins to the nucleus could be affected in the presence of MxA. Additionally, we reasoned that there may be a correlation of the binding strength of NPs of various viral strains with the respective MxA-sensitivity of those viral strains. To our surprise we were not able to support either of those hypotheses. We further characterized the structural and enzymatic features of MxA, NP and UAP56 that contribute to the maintenance of their interaction capacities. We have observed that the dimeric state of MxA is sufficient to induce binding to NP of active as well as inactive MxA mutants. ATPase and helicase functions of UAP56 are negligible for the interaction with MxA and NP. The F412A/R416A mutant of H5N1 NP lost MxA- and UAP56-binding capacity.

3.3 Experimental procedures

3.3.1 Cell lines

All cell lines were cultured in DMEM supplemented with 10% FCS, 1 mg/ml Penicillin/Streptomycin and 2 mM GlutaMAX™ (Thermo Fisher Scientific) (complete DMEM) at 37°C and 5% CO_2. HEp-2 (HeLa-derived human epithelial cells), HeLa (human adenocarcinoma cells), Vero (African green monkey epithelial kidney cells), HEK-293T (human embryonic epithelial kidney cells), MDCK (Madin Darby Canine kidney cells) were purchased from ATCC.

3.3.2 Plasmids

As previously described MxA wt cDNA was cloned into pcDNA3.1(+)neo (Invitrogen)[158]. MxA(R640A) and MxA(T103A) cDNA in pcDNA3.1(+)neo plasmids were kindly provided by Georg Kochs, Freiburg, Germany. MxA mutants Δ81-84, Δ81-84/R640A, T103A/R640A, D250N, D250N/R640A, D253N, D253N/R640A, F561A, F561A/R640A, I577A and I577A/R640A were generated using the QuikChange II Site-Directed Mutagenesis Kit (Agilent). Primers were designed using http://www.bioinformatics.org/primerx/ with the QuikChange protocol.

pCAGGS-NP plasmids (NP cDNAs derived from A/Thailand/1(*KAN-1*)/2004 (H5N1), swl A/California/04/2009 H1N1 (≡pH1N1)), A/Seal/Massachusetts/1/1980 H7N7 (≡rSC35M), A/Puerto Rico/8/1934 H1N1 (≡PR8)) were kindly provided by Martin Schwemmle, Freiburg, Germany. pcDNA3.1(+)neo-FPV-NP (derived from A/fowl/Dobson(H7N7)), pcDNA3.1(+)neo-PR8-NP (derived from A/Puerto Rico/8/1934 H1N1) and pcDNA3.1(+)neo-WSN-NP (derived from A/Wilson-Smith/1933(H1N1)) were kindly provided by Silke Stertz, Zürich, Switzerland.

pcDNA3.1(+)neo-UAP56 was described before[133]. UAP56(K49A) and UAP56(D199A) mutants were generated by QuikChange as described above. cDNA of GFP β-sheet 10 or 11[179] plus and unstructured linker sequence of 32 or 25 amino acids, respectively was cloned into pcDNA3.1(+)neo. These constructs were designed to be suitable as either N- or C-terminal protein tags. For the detector fragment consisting of the complementing β-sheets 1-9, cDNA of GFP1-9 was cloned into pcDNA3.1(+)neo[179]. To obtain GFP10- or GFP11-tagged MxA, NP or UAP56 variants, the respective cDNA was cloned into these vectors using PacI and BamHI.

3.3.3 siRNA transfection

Transfection was performed in suspension using Lipofectamine® RNAiMAX Transfection Reagent. 30 nM siRNA and 5 µl RNAi max was used per well of a 6-well plate (siBAT1/DDX39A: 5'-GAAUAUGAGCGCUUCUCUATT-3', gene accession: NM_004640). 24 h post-transfection IAV NP was transfected using ViaFect™ (Promega) according to the manufacturer's instructions. Cells were lysed for co-IP and Western blot analysis 24 h later. If DNA and siRNA was transfected simultaneously 500 ng DNA, 30 nM siRNA and 2 µl Lipofectamine® 2000 were used per well of a 24-well plate. Cells were lysed 48 h post-transfection for co-IP and WB analysis.

3.3.4 Tripartite split-GFP complementation assay

HEp-2 or HeLa cells were seeded in an ibidi µ-slide 4-well chamber (Cat. No 80427). Cells were transfected with 500 ng DNA (180 ng plasmid of each GFP10- or GFP11-tagged construct and 90 ng GFP1-9 detector fragment) using ViaFect™ (Promega) according to the manufacturer's instructions. 24 h later growth medium was changed to FluoroBrite DMEM medium (Thermo Fisher Scientific) and Hoechst 33342 (1:5000) and analysed at a Leica SP5 confocal laser scanning microscope.

3.3.5 Non-denaturing PAGE analysis

Vero cells were seeded in 6-well plates and transfected 24 h later with 2 µg DNA with ViaFect™ (Promega) according to the manufacturer's instructions. Cells were lysed 24 hours post-transfection in 200 µl lysis buffer (20 mM Tris-HCl pH 7.5, 150 mM NaCl, 5 mM MgCl2, 50 mM NaF, 1 mM Na3VO4, 1% NP-40, 50 mM β-glycerophosphate, 100 nM iodoacetamide, Roche cOmplete Protease Inhibitor Cocktail) in the dark on ice for 30 min. Lysates were centrifuget at 13'000xg for 20 min at 4°C and dialysed (20 mM Tris-HCl pH6.8, 10% glycerol, 5 mM MgCl2, 0.1% CHAPS and 0.5 mM DTT) for 4 h at 4°C using Slide-A-Lyzer MINI dialysis devices with a 10K molecular weight cut-off (Thermo Scientific). Samples were again centrifuged at 13'000xg for 20 min at 4°C and run on a 4-16% TGX gradient gel (BioRad) (running buffer: 25 mM Tris-HCl pH8.3, 192mM glycine, 0.5 mM DTT and 0.1% CHAPS, sample loading buffer: 300 mM Tric-HCL pH 6.8, 0.05% bromophenol blue, 50% glycerol) for 4 h at 4°C with a constant electric current of 25 mA/gel. Gels were incubated in SDS-containing buffer right before blotting (25 mM Tris-HCl pH8.3, 192 mM glycine and 0.1% SDS) for 15 min at room temperature.

3.3.6 Minimal replicon reconstitution assay

The mini replicon assay has been described before[154]. Basically, pcDNA3.1(+)neo vectors harboring cDNA sequences of the viral polymerase subunits PB1,PB2 and PA and viral NP derived from the A/Thailand/1(*KAN-1*)/2004 (H5N1) strain were transfected into 293T cells. Additionally, the firefly luciferase (FFLuc) reporter plasmid pPOLI-Luc-RT (Zimmermann et al, 2011) and the constitutively active *Renilla reniformis* luciferase (RRLuc) plasmid pRL-SV40-R*luc* (Promega) as a read-out and for transfection efficiency were co-transfected using JetPRIME (Polyplus transfection) according to the manufacturer's instructions. 10 ng PB1, PB2 and PA and 50 ng NP, FFLuc and RRLuc plasmids plus varying amounts of MxA plasmids were transfected. For the read-out, cells were lysed 24 h after transfection in 60 µl 1X passive lysis buffer and incubated at room temperature for 15 min on a shaker. A dual-

luciferase read-out was performed using the Dual-Luciferase® Reporter Assay System (Promega). 15 µl lysate was mixed with 45 µl LARII and immediately read on a Perkin Elmer Envision 2104 plate reader for the Firefly luciferase signal and additional 45 µl Stop&Glo was added for the Renilla luciferase read-out.

3.3.7 Co-immunoprecipitation (co-IP)

HEp-2 cells were transfected with Viafect (Promega) according to the manufacturer's instructions. 24 h post-transfection cells were lysed in 300 µl lysis buffer (20 mM Tris-HCl pH 7.5, 150 mM NaCl, 5 mM MgCl2, 50 mM NaF, 1 mM Na3VO4, 1% NP-40, 50 mM β-glycerophosphate, 100 nM iodoacetamide, 1x Roche cOmplete Protease Inhibitor Cocktail) in the dark on ice for 30 min. Lysates were homogenized using QiaShredder columns (Qiagen). 100 µl of each lysate was incubated with antibody (α-NP (50 µl, HB65, hybridoma, in-house, α-FLAG (0.75 µl, rabbit, Sigma, F7425)) at 4°C over night on a rotating wheel. 15 µl lysate was used for the whole cell lysate (WCL) control. 20 µl Dynabeads protein G magnetic beads (Thermo Fisher Scientific) per sample were pre-adsorbed over night at 4°C on a rotating wheel using untransfected HEp-2 cell lysate. Pre-adsorbed beads were washed once with lysis buffer and incubated with the lysates for 1 h at 4°C on a rotating wheel. Beads were washed once with 1 ml followed by five times 0.5 ml lysis buffer. Beads were briefly vortexed in between the washing steps. Proteins were eluted from the beads with 20 µl 1x Laemmli buffer at 95°C for 10 min. 15 µl WCL/IP sample was loaded on a 10% SDS-PAGE gel and analysed by Western blot (α-NP (rabbit serum, in-house, 1:10'000), α-FLAG (mouse, Sigma, F-3165, 1:1000), α-MxA (ab143, hybridoma, in-house, 1:10)).

3.3.8 Subcellular fractionation

HEp-2 cells were trypsinized and centrifuged at 700xg for 5 min. All following steps were performed on ice unless stated otherwise. Trypsin was removed and cells were washed with ice-cold PBS. Pellet was lysed for 20 min in 100 µl cytoplasmic extraction buffer (0.5% Triton-X100, 5 mM Na_3VO_4, 20 mM β-glycerophosphate, 10 mM HEPES pH 7.4, 2 mM DTT, 0.1 mM EGTA, 0.01 mM KCl, 0.01 mM EDTA, 1x Roche cOmplete Protease Inhibitor Cocktail) under rotation. Nuclei were sedimented by centrifugation at 3000xg for 5 min. 100 µl supernatant (cytoplasmic fraction) was transferred into a new tube. Nuclei were washed twice in 1.5 ml cytoplasmic extraction buffer for 15 min under rotation. An additional washing step with wash buffer (5 mM Na_3VO_4, 20 mM β-glycerophosphate, 10 mM HEPES pH 7.4, 2 mM DTT, 0.01 mM KCl, 1x Roche cOmplete Protease Inhibitor Cocktail) was performed for 5 min under rotation. Nuclei were incubated with 20 µl wash buffer, 20 µl DNase I (1 U/µl) and 5 µl of 10x DNase I buffer and incubated for 10 min at 27°C under

gentle shaking. 5x 10 µl nuclear extraction buffer (1% Triton-X100, 5 mM Na_3VO_4, 20 mM β-glycerophosphate, 10 mM HEPES pH 7.4, 2 mM DTT, 420 mM KCl, 1x Roche cOmplete Protease Inhibitor Cocktail) was added to the samples and the nuclei were lysed for 15 min at RT under rotation. Insoluble components were removed through centrifugation at 6000xg for 5 min through QiaShredder columns (Qiagen). The samples were subjected to Western blot analysis.

3.4 Results

3.4.1 Assessment of the general binding capacity and localization of MxA, viral NP and UAP56

The potential of MxA to inhibit IAV strains of avian origin is generally thought to be much higher compared to IAV strains of human origin[121-123]. It has been shown previously that NP is the target of MxA[115,123]. Thus, we wanted to know whether the binding strength of NP of avian versus human origin to MxA correlates with their sensitivity to MxA. We first verified the sensitivity of various NPs originating from different avian (A/Thailand/1/2004 H5N1 [Kan1], A/FPV/Dutch/1927 H7N1 [FPV], A/Seal/Massachusetts/1/1980 H7N7 [rSC35M]) and human (A/California/04/2009 [pH1N1], A/Wilson-Smith/1933 H1N1 [WSN]) strains against wildtype MxA in a minimal replicon assay (described in[121]). 293T cells were transfected with plasmids coding for the polymerase subunits PB1, PB2 and PA of the A/Thailand/1/2004 (Kan1 (H7N7)) strain, Kan1 NP, the reporter firefly luciferase, *Renilla* luciferase for normalization of transfection efficiency and either wildtype MxA or mCherry. A dual luciferase assay was performed and the resulting firefly luciferase signal was normalized to the luminescence of the *Renilla* luciferase (expressed under a constitutive simian virus 40 (SV40) promoter). The most MxA-sensitive NP thereby was avian Kan1, where replication was reduced to 15% in the presence of MxA compared to cells expressing mCherry (Fig. 3.1A). The NP of pH1N1 exhibited the most resistant, retaining ~60% replication capacity. The sensitivities of the three additional NPs, originating from FPV, rSC35M and WSN to MxA were intermediate, with WSN being slightly more resistant. The two avian NPs FPV and rSC35M retained ~30% replication capacity and WSN NP ~35% (Fig. 3.1A). The two human-derived NPs therefore showed more resistance to MxA than the three avian strains. By performing co-IP experiments in HEp-2 cells stably expressing MxA(R640A) (HEp-2-MxA(R640A)) and transfected with plasmids coding for the above described avian and human NPs we tested the binding affinity of NP to MxA. As shown previously[115], it is not possible to detect binding of wildtype MxA to viral NP (data not shown). In contrast, the dimeric mutant MxA(R640A) efficiently co-precipitates with NP. We performed co-IP experiments in HEp-2-MxA(R640A)

cells, which were transfected with plasmids encoding the above described NPs. MxA(R640A) strongly co-precipitated with pH1N1 NP (Fig. 3.1B, quantification of two independent experiments in the lower panel). Kan1 and FPV NPs show very weak interaction with MxA and rSC35M and WSN NP performing somewhere in between (Fig. 3.1B). In contrast to our expectations the binding strength of the different NP variants did not correlate with the sensitivity of the respective IAV strains to MxA. Since UAP56 has also been implied in MxA's antiviral potential we next tested, if there is a correlation in binding strength of NP with wildtype UAP56. To this end HEp-2 cells were transfected with plasmids encoding FLAG-tagged UAP56 or FLAG-mCherry as a negative control together with the previously described NPs and a FLAG-immunoprecipitation was performed. To our surprise, we could not see a correlation in binding efficiency either (Fig. 3.1C).

NP is a highly conserved protein and the differences in sequence of NPs from various IAV strains are minor. Comparing the PR8 (H1N1) versus Kan1 (H5N1) NP, only 33 out of 498 amino acids differ, which reflects a sequence identity of 93%. However, the introduction of a few amino acid changes can alter the MxA sensitivity of NP dramatically as Mänz and colleagues demonstrated[122]. The introduction of 10 amino acid substitutions from avian (Kan1) to human (pH1N1) residues (E53D, R100V, Y289H, R305K, F313V, I316M, T350K, R351K, V353I, Q357K) (here labelled Kan1 10x) or only the three amino acid substitutions R100V, L283P and F313Y (here labelled Kan1 3x) rendered Kan1 NP 80% replication competent in the presence of MxA compared to approximately 15% in the case of wildtype Kan1 NP[122]. When we transfected HEp-2-MxA(R640A) cells with plasmids encoding those NP mutants and performed co-IP assays we could actually observe a reduction in co-precipitation of MxA(R640A) with NP although moderate (Fig. 3.1D). However, for PR8 3x, which is the complementary mutant to Kan1 3x and thus harbors the mutations V100R, P283L and Y313F, we did not see an increase in binding strength (Fig. 3.1D).

3.4.2 Investigating the capability of MxA to compete for NP binding against UAP56 and the effect of reduced UAP56 levels on MxA-NP binding

To gain more insight into the mechanism of action of MxA we aimed at finding the step in the viral replication cycle, which is inhibited. Since NP is bound by MxA, we hypothesized that MxA might prevent NP to reach the nucleus so that the virus would be unable to perform genome replication. To this end we performed sub-cellular fractionation experiments in stably GST-, MxA wt- or MxA(R640A)-expressing HEp-2 cells (HEp-2-GST, HEp-2-MxAwt, HEp-2-MxA(R640A)), which were transfected with plasmids coding for Kan1 NP. In order to clarify if NP levels in the nuclear fraction in the presence of MxA are reduced, we subjected the nuclear and cytoplasmic fractions to Western blot analysis (Fig. 3.2A). As expected, MxA is

only present in the cytoplasmic fraction. However, there is no reduction of NP protein level apparent in MxA- versus GST-expressing cells (Fig. 3.2A). If the transport of NP is not directly affected, MxA might act more indirectly by separating NP and its chaperone UAP56 from each other. To address this question, we analysed binding of UAP56 to NP in MxA wt- or R640A-expressing cells (Fig. 3.2B and C). FLAG-immunoprecipitation was performed with lysates of HEp-2, HEp-2-MxAwt or HEp-2-MxA(R640A) cells transfected with plasmids coding for Kan1 NP and either FLAG-UAP56 or FLAG-mCherry and revealed that binding of UAP56 to NP is not reduced (Fig. 3.2B). Additionally, by transfecting increasing amounts of a plasmid encoding MxA(R640A) we could not observe any change in binding efficiency between NP and UAP56 either. However, we were able to detect trimeric MxA-NP-UAP56 complex formation (Fig. 3.2C, last lane). Assuming that UAP56's capacity to bind to MxA is essential for the antiviral action of MxA but having observed no impaired UAP56-NP binding in MxA-expressing cells, we decided to investigate the NP-MxA binding kinetics in cells depleted of UAP56 (Fig. 3.2D and E). HEp-2-MxA(R640A) cells were transfected with siRNAs against either UAP56 mRNA or a non-targeting control and 24 h later plasmids encoding for NPs of different viral strains were transfected (Fig. 3.2D). NP immunoprecipitation showed a reduction in co-precipitation of MxA in siUAP56-treated cells (Fig. 3.2D). Staining for NP, however, revealed an ample reduction in protein level in siUAP56-treated samples, which could account for the observed reduction in MxA binding. The involvement of UAP56 in mRNA transcription and export is the obvious explanation for this decrease in NP expression. Therefore, we repeated the experiment but transfected the siRNA and the plasmids at the same time, giving NP enough time to be expressed before UAP56 levels are reduced extensively (Fig. 3.2E). NP expression levels were not affected anymore, albeit a loss of knock-down efficiency was observed. The aforementioned decrease in NP-MxA binding in UAP56 knock-down samples, however, was not detectable anymore.

3.4.3 Molecular determinants of MxA in NP binding and anti-IAV activity

The fact, that we can only see binding of NP to dimeric MxA(R640A) but not wildtype MxA in co-IP experiments led us to investigate the NP-binding capacity of other MxA mutants. We created mutants with substitutions/deletions in the G-domain preventing the binding of GTP (Δ81-84[159,180], D250N[172]) or GTP-hydrolysis only (T103A[173], D253N[172]) (Fig. 3.3A, mutations are highlighted in yellow). We also generated a loop L4 mutant (F561A/Y[100]) (not shown in the crystal structure since this loop was deleted for crystallization purposes) and I577A[100], a residue localized at the third position C-terminal of loop L4. These mutations were all shown to render MxA inactive, except for F561Y. To assess whether the dimeric state of MxA, its

activity or both are needed to bind to NP we further generated double-mutants harboring the R640A substitution in addition to the aforementioned mutations. We started by analyzing the oligomeric state of those mutants in Vero cells transfected with plasmids coding for MxA wildtype and mutants thereof. By non-denaturing PAGE gel electrophoresis and Western blot analysis we could confirm the dimeric nature of the R640A double-mutants (Fig. 3.3B). All the other (single) mutants were present as tetramers like wildtype MxA with the exception of I577A, running as a dimer even in the absence of the R640A substitution (Fig. 3.3B). Unfortunately, we were unable to detect Δ81-84 and Δ81-84/R640A under non-denaturing conditions (not shown).

Next we subjected the MxA-mutants to co-IP analyses in order to monitor binding capacities to NP. To our surprise MxA(Δ81-84) and MxA(D250N9, G-domain mutants unable to bind GTP, co-precipitated with NP in the wildtype background (Fig. 3.3C). Substitution of the R residue at position 640 with an A (R640A) increased the binding strengths of the resulting double mutants to similar levels as MxA(R640A). For the MxA(T103A) and MxA(D253N) mutants binding can only be observed in the R640A background (Fig. 3.3C). For the loop L4 mutants we observed similar phenotypes with the exception of MxA(F561A/R640A), which co-precipitated with NP to a lesser extent. Interestingly, MxA(I577A) did not bind to NP independent of the presence of the R640A substitution and also despite it being dimeric in either case.

We also tested whether these mutants inhibited IAV replication using the Kan1 (H7N7) mini replicon system. 293T cells were transfected with the mini replicon constituents alongside plasmids coding for the above-mentioned MxA mutants or mCherry as a positive control. When assessing the replication efficiency by measuring luminescent signal in a dual-luciferase assay a 10-fold replication reduction was observed in cells expressing wildtype MxA in contrast to the mCherry-expressing cells (Fig. 3.3E). MxA(R640A) showed intermediate inhibition potential and reduced replication about 4-fold. Introduction of the R640A mutation in the aforementioned GTPase mutants did not reverse the loss of function phenotype for any of them. However, for the stalk mutants MxA(F561A/R640A) and MxA(I577A/R640A) an increase in antiviral activity was indeed observed in contrast to the single mutants MxA(F561A) and MxA(I577), respectively, resulting in an inhibitory capacity similar to MxA(R640A) alone (Fig. 3.3E).

3.4.4 Enzymatic activity of UAP56 is not crucial for the binding to MxA and NP

In order to clarify if the enzymatic function of UAP56 is a prerequisite for the MxA-mediated inhibition of IAV, we generated an ATPase/helicase-deficient mutant (K95A) or helicase-deficient mutant (D199A) of UAP56[181]. It has already been shown previously that wildtype

UAP56 is able to bind to MxA[57]. Co-IP experiments were performed in HEp-2-MxAwt and HEp-2-MxA(R640A) cells, which were transfected with FLAG-UAP56 or FLAG-mCherry. We immuno-precipitated with an α-FLAG antibody and observed efficient co-precipitation of wildtype MxA and thus reproducing the finding from Wisskirchen et al. Additionally we showed that MxA(R640A) is able to bind to wildtype UAP56 as well (Fig. 3.4A). When testing the two enzymatically inactive mutants UAP56(K95A) and UAP56(D199A) no difference in binding capacity to wildtype MxA or MxA(R640A) was apparent (Fig. 3.4A and B).

UAP56 is a nucleo-cytoplasmic shuttling protein whereas MxA is exclusively localized to the cytoplasm[128,182]. It is therefore expected and it has also been shown that the binding of those two proteins is occurring in the cytoplasm[57]. We thus adapted the tripartite split-GFP complementation system[179] for the purpose of studying the interaction between MxA, UAP56 and NP, by tagging the three proteins with either β-sheet 10 or 11 of GFP plus a flexible linker (10L-/11L-[protein of interest]). We performed live cell imaging analysis to visualize the interaction sites via the reconstituted GFP signal in HeLa cells transfected with the plasmids encoding the interactor proteins of interest, the detector fragment GFP1-9 and mCherry, which was included as a transfection control. We used the monomeric mutant MxA(M527D) as a negative control. UAP56 and NP show an exclusively nuclear interaction signal with the exclusion of nucleoli (Fig. 3.4C). As expected, UAP56 and wildtype MxA interact in the cytoplasm forming a distinct perinuclear ring-like structure. Assessing the interaction of UAP56(K95A) and UAP56(D199A) with wildtype MxA no obvious difference was observed (Fig. 3.4C). This indeed suggests negligibility of the enzymatic function of UAP56 for the interaction with NP and MxA. Unfortunately, we were unable to study NP-MxA interaction since we could not detect any GFP signal with this experimental approach.

3.4.5 NP F412A/R416A substitutions in NP abrogate binding to MxA and UAP56

We next wanted to identify regions in NP required for binding to MxA and UAP56. NP of the IAV strains A/HK/483/97 (H5N1) and WSN (H1N1) crystallize as trimers[50,51]. *In vitro* NP exists in a dynamic equilibrium changing from monomers to trimers and vice versa[56,183]. Single amino acid substitutions were shown to be sufficient for locking NP in the monomeric state or at least tipping the balance toward the monomeric form, namely R416A, E339A and S165D and also the double mutant F412A/R416A[54,58]. Employing co-IP experiments we assessed the binding of Kan1 NP (H5N1) mutants to UAP56 (Fig. 3.5A) and MxA (Fig. 3.5B). HEp-2 cells were transfected with plasmids coding for wildtype Kan1 NP or mutants thereof and immunoprecipitation of the FLAG peptide revealed that the only NP mutant abrogating binding to UAP56 was NP(F412A/R416A) (Fig. 3.5A). Surprisingly, the R416A substitution alone was not sufficient to abolish the interaction with UAP56 (Fig. 3.5A). We could further

observe increased binding of E339A (Fig. 3.5A). To examine the binding capacities of NP(F412A/R416A) and NP(E339A) to MxA, HEp-2-MxA(R640A) cells were transfected with plasmids encoding NP or empty vector. NP was immuno-precipitated and interaction to MxA(R640A) was only lost with NP(F412A/R416A). We could again observe higher degrees of co-precipitation of MxA(R640A) with the NP(E339A) mutant. The E339 residue lies in the insertion groove for the tail loop and is bound by R416, a residue in the tail loop[58]. To further ensure that the mutations indeed render NP (partially) monomeric, we also deployed those mutants in the tripartite split-GFP system (Fig. 3.5C) and subjected it to non-denaturing PAGE analysis (Fig. 3.5D). For the splitGFP assay HeLa cells were transfected with plasmids encoding 10L-/11L-tagged wildtype Kan1 NP or Kan1 NP oligomeric mutants together with the detector fragment GFP1-9 and mCherry as a transfection control. For non-denaturing PAGE analysis Vero cells were transfected with plasmids encoding wildtype Kan1 NP or the aforementioned oligomeric mutant. Gel electrophoresis under non-denaturing conditions followed by Western blot analysis revealed, surprisingly, that only the F412A/R416A mutant was at least partially monomeric, even though there was also a distinct band running at the expected height of a trimer. Thus, these results could not clarify if F412 and R416 are the residues involved in binding to UAP56 and MxA or if the oligomeric state is the prerequisite for binding instead.

3.5 Discussion

MxA is a potent influenza A virus restriction factor; however, the detailed mechanism of action is still under debate. We addressed this issue by studying the interplay between MxA, NP, the viral target protein of MxA, and UAP56, a cellular helicase associated with MxA and IAV. We found that the dimeric form of MxA binds to NP independently of its activity and we were able to identify residues in NP, which lead to a loss of NP- and UAP56-binding when mutated. We further showed that the enzymatic functions of UAP56 are negligible in order to bind to MxA and NP. Unfortunately, we were not able to characterize the antiviral activity of MxA in more detail from a mechanistic point of view.

Remarkably, the binding strengths of various NPs originating from different viral strains to MxA do not correlate with the MxA-sensitivity of those IAV strains; in other words, NPs of more sensitive strains do not show higher binding capacities to MxA in contrast to NPs of more resistant strains (Fig. 3.1). pH1N1 is the IAV strain which shows the highest resistance to MxA in our assays (Fig. 3.1A), however, its NP bound the strongest to MxA (Fig. 3.1C). We rather observed, at least to some extent, an inverse correlation. We hypothesize that NPs of MxA-resistant strains could bind to MxA and thus sequester it. MxA's normally

transient NP-interaction, which allows it to bind to multiple NP with rapid turnover, would thus be inhibited. These MxA-bound NPs are likely to be released from UAP56-binding, because otherwise UAP56-binding to NP would also be expected to inversely correlate with the MxA-sensitivities of different viral strains, which we have not seen (Fig. 3.1C).

The impact of MxA expression on the IAV replication cycle is the inhibition of viral genome replication (Fig. 3.6) and since NP has been shown to represent the target of MxA[122,123], translation seems not to be inhibited. We thus analyzed which steps of the IAV infection cycle between mRNA translation and replication are targeted by MxA. The obvious mechanism of MxA, a cytoplasmic protein, is the prevention of NP translocation to the nucleus, where NP is indispensable for replication. We showed, however, that NP levels are not reduced in MxA- versus GST-expressing cells (Fig. 3.2A). UAP56's functional link to IAV has been proposed to be a chaperone function for newly synthesized NP[29]. UAP56 thereby delivers NP to the vRNA and stimulates encapsidation of the nascent RNA. We further speculated that the chaperone function might prevent NP to engage with cellular RNA, which would disable it from binding to viral RNA in the nucleus. We imagined that MxA could bind to the UAP56-NP hetero-oligomers and separate them from each other. This separation could be achieved through GTP hydrolysis. This would associate a function with the GTPase activity of the highly conserved G-domain. However, co-IP experiments revealed that UAP56-NP binding is not affected in the presence of MxA (Fig. 3.2B and C), thus, NP-UAP56 complexes seem to translocate to the nucleus together. This is in line with splitGFP data, showing interaction of NP and UAP56 in HEp-2-MxA cells (data not shown). To more conclusively determine if UAP56 is indeed exerting a chaperone function on and thus preventing NP from binding to cellular RNA, an RNA mobility shift assay might provide insights[184].

There is evidence that UAP56 positively influences the antiviral potential of MxA[135]. We tested the effect of NP-MxA binding in cells with reduced UAP56 levels. Our results, however, are inconclusive (compare fig. 3.2D and E) but they rather support the notion that NP-MxA binding remains unchanged in cells transfected with non-targeting versus UAP56-targeting siRNA. We cannot exclude, though, that residual UAP56 levels are high enough to sustain NP-MxA binding. Also, unchanged NP-MxA binding in UAP56 knock-down cells, where MxA is predicted to be less active, might not be surprising after all, since differences in MxA activity against various IAV strains do not correlate with binding to NP of the respective strains either (Fig. 3.1 and[122]).

There is still a debate about the active entity of MxA in term of its oligomeric state. Monomers and dimers have been shown to be inactive in mini replicon assays[170]. This is in contradiction with our results, where we show sustained, even though reduced, activity in particular of the dimeric form (Fig. 3.3E and[115]). We reasoned that different expression levels of MxA are the reason for these seemingly contradictory results, since we also observed a more pronounced inhibition of viral replication with wildtype MxA. The crystal structure of MxA indicates higher order oligomer formation, which might even represent ring-like structures similar to dynamin[97,170]. Gao et al. along with others[151] therefore propose Mx-rings to form around incoming vRNPs, which leads to the retention of vRNPs in the cytoplasm. We, on the other hand, only observed tetrameric MxA in cells overexpressing wildtype MxA or stimulated with IFN-α2 (Fig. 3.3B and[115]). Stable complexes of NP with MxA are only formed with dimeric MxA (Fig. 3.3C) and the dimeric state (through the introduction of the R640A mutation) even increased the antiviral potential of otherwise inactive MxA loop L4/α4-helix mutants to the level of R640A-only mutant activity (Fig. 3.3C). Thus, we rather assume higher oligomers to be a storage form of MxA and dimeric MxA to be the active entity. Interestingly, the inactivity of I577A is reverted in the R640A background and shows the same binding characteristics and antiviral activity as wildtype MxA. R640A is a compensatory mutation in this context. It has already been suggested that an Alanine at position 577 affects folding[100], this, however, would imply a loss of antiviral activity. When analyzing the oligomeric state the MxA(I577A/R640A) band appeared ‘sharper’ in the non-denaturing PAGE analysis (Fig. 3.3B). The R640A mutation in MxA has already been proposed to lead to a more tightly packed and less flexible molecular structure[185] and here this probably has a cumulative effect with the I577A substitution on the tertiary structure of MxA.

We showed UAP56-MxA binding to be independent of the enzymatic functions of UAP56. UAP56 is a protein with RNA-binding activity and has also been shown to interact with other proteins[176,186,187]. UAP56 recruits the adaptor protein Aly the THO complex to intronless mRNA, forming the active TRanscription EXport (TREX) complex, for mRNA nuclear export[176,188]. It was suggested, that the ATPase activity of UAP56 triggers its dissociation from the RNA resulting in an Aly/THO/mRNA complex for nuclear export[188]. Others see the functional TREX complex as UAP56/Aly/THO/mRNA[189,190]. Nevertheless, the ATPase function of UAP56 seems to be indispensable for TREX complex formation[186]. The question is thus raised whether ATPase and helicase activity are needed for NP-UAP56 interaction. Since we assume, that NP-UAP56 complex formation is taking place co-translationally, without the involvement of RNA, we would expect both enzymatic functions to be dispensable for NP-binding.

We assessed, whether the oligomeric state of NP is a prerequisite for binding to MxA and UAP56. It has been shown for H1N1 NP that the double-mutant NP(F412A/R416A) and for H1N1 and H5N1 NP that even the single-mutant NP(R461A) is monomeric[52,55]. We observed that Kan1 NP(R416A) did not show a loss of binding phenotype in UAP65 immuno-precipitation experiments (Fig. 3.5A). NP(F412A/R416A), on the other hand, lost its interaction capacity to both MxA and UAP56 (Fig. 3.5A and B). We further showed, that in Kan1 NP, the single R416A mutation is not sufficient to render NP monomeric (Fig. 3.5D). Kan1 NP(F412A/R416A), however, seemed to be at least partially monomeric (Fig. 3.5D). This is not in accordance with Chan et al[52], who have seen the R461A mutation to render H5N1 NP monomeric. Since the interaction domains of H1N1 and H5N1 NPs are practically identical[51], we expect them to be very similar between different H5N1 strains as well. These differences could thus not be explained by sequence variations. In order to clarify if the monomeric state is indeed crucial for interaction, we would want to assess the oligomeric states and binding capacities of those two mutants in an H1N1 background by using WSN NP.

In summary, we believe that higher order oligomers of MxA represent a storage form and that (likely through a viral trigger) MxA dissociates into its active dimeric form. In our current model MxA engages with NP-UAP56 complexes and changes the functional integrity of either or both proteins in a GTP hydrolysis dependent manner. UAP56-NP hetero-oligomers shuttle to the nucleus where these changes are not compatible with genome replication. This model does by far not explain all the data we have and further investigations are needed to add clarity.

Fig. 3.1

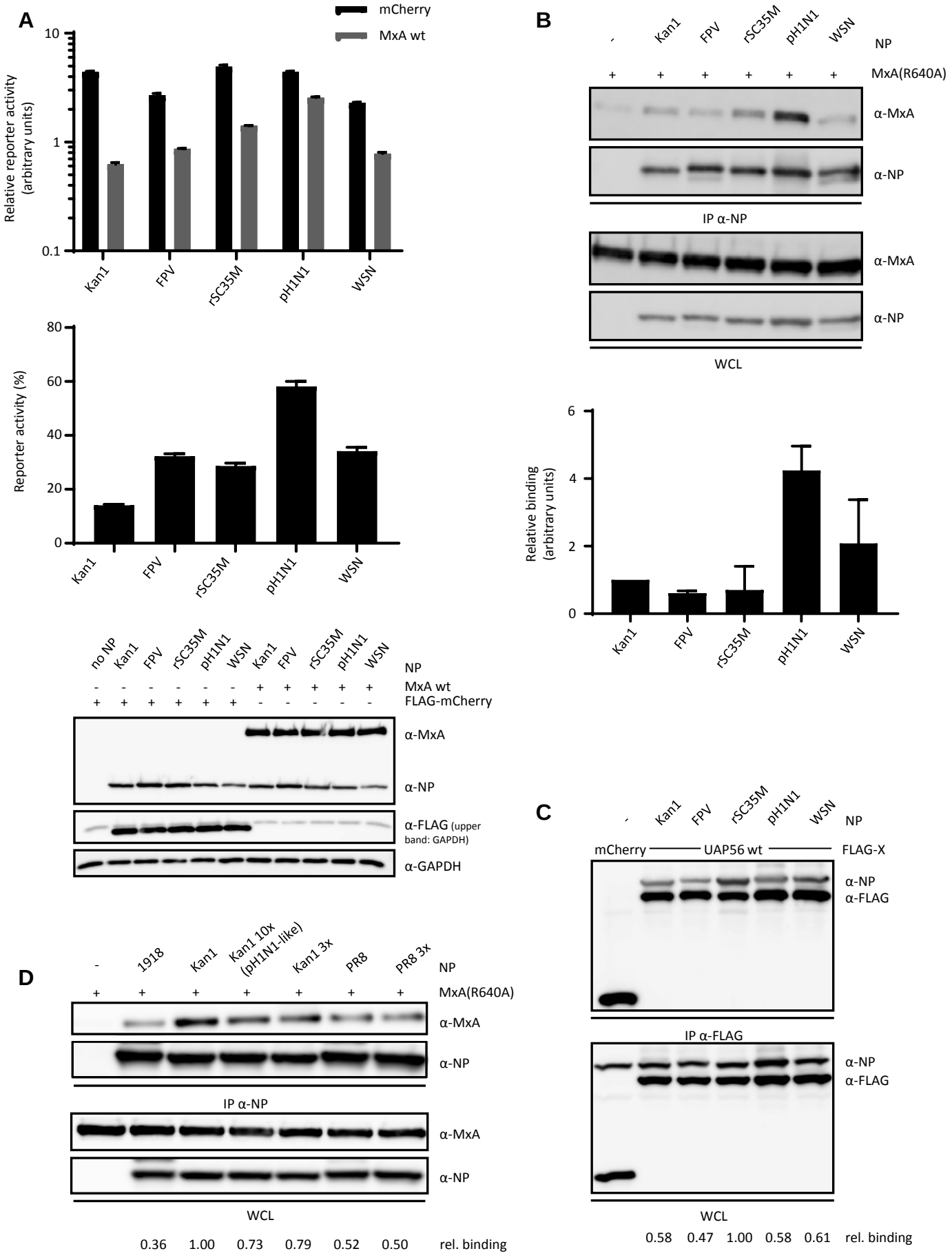
A
mCherry
MxA wt
Relative reporter activity (arbitrary units)
10
1
0.1
Kan1
FPV
rSC35M
pH1N1
WSN
Reporter activity (%)
80
60
40
20
0
B
NP
MxA(R640A)
α-MxA
α-NP
IP α-NP
WCL
Relative binding (arbitrary units)
6
4
2
0
no NP
MxA wt
FLAG-mCherry
α-FLAG (upper band: GAPDH)
α-GAPDH
C
mCherry
UAP56 wt
FLAG-X
α-FLAG
IP α-FLAG
0.58 0.47 1.00 0.58 0.61 rel. binding
D
1918
Kan1 10x (pH1N1-like)
Kan1 3x
PR8
PR8 3x
0.36 1.00 0.73 0.79 0.52 0.50 rel. binding

3.1 Binding capacities of NPs originating from different viral strains do not correlate with their sensitivity to MxA. A HEK293T cells were transfected with plasmids coding for the mini replicon constituents (originating from the Kan1[H5N1] strain) and NPs of different viral strains together with either mCherry or wildtype MxA. Luciferase activities were determined by dual-luciferase read-out. Relative activities of the firefly reporter normalized to *Renilla* are shown in the top panel. Replication capacities are shown in percent (middle panel) by normalization of the MxA wt to mCherry values from the top panel. Expression of the indicated proteins was confirmed by Western blot analysis of pooled samples for each condition using the indicated antibodies (bottom panel). Data are represented as mean ±SEM of duplicates **B** Stable HEp-2(MxA R640A) cells were transfected with an empty vector control or plasmids coding for the indicated NPs. An NP-immunoprecipitation was performed and the IP fractions and the WCL samples were analysed by Western blot (top panel) using the indicated antibodies. Quantification of two independent replicates is shown in the bottom panel. MxA and NP band intensities of the IP fractions were measured using MultiGauge. MxA band intensities normalized to the band intensities NP are plotted. Kan1 NP was set to 1. Data are represented as mean ±SEM of two independent repeats. **C** HEp-2 cells were transfected with plasmids encoding FLAG-mCherry or FLAG-UAP56 together with plasmids encoding the indicated NP. After FLAG-immunoprecipitation the IP fractions and the WCL samples were analysed by Western blot analysis using the indicated antibodies. Band intensities were measured using MultiGauge. MxA band intensities normalized to the band intensities NP are plotted. The highest value was set to 1.00. All the other values are relative to 1.00 **D** Co-IP was performed as in **B** and calculations as in **C**. WCL: whole cell lysate

Fig. 3.2

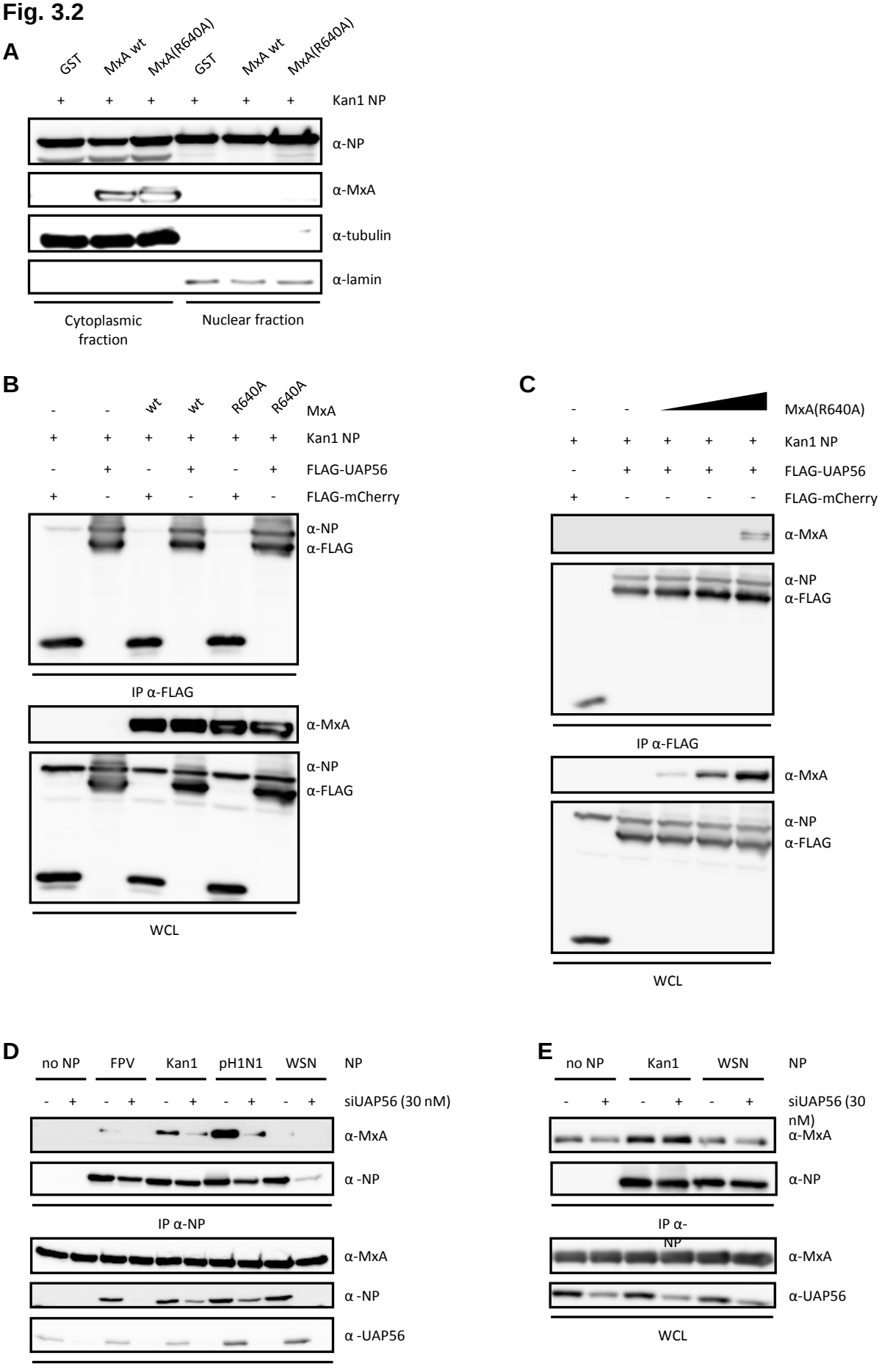
A
GST
MxA wt
MxA(R640A)
GST
MxA wt
MxA(R640A)
Kan1 NP
α-NP
α-MxA
α-tubulin
α-lamin
Cytoplasmic fraction
Nuclear fraction
B
MxA
Kan1 NP
FLAG-UAP56
FLAG-mCherry
α-NP
α-FLAG
IP α-FLAG
α-MxA
α-NP
α-FLAG
WCL
C
MxA(R640A)
Kan1 NP
FLAG-UAP56
FLAG-mCherry
α-MxA
α-NP
α-FLAG
IP α-FLAG
α-MxA
α-NP
α-FLAG
WCL
D
no NP
FPV
Kan1
pH1N1
WSN
NP
siUAP56 (30 nM)
α-MxA
α -NP
IP α-NP
α-MxA
α -NP
α -UAP56
WCL
E
no NP
Kan1
WSN
NP
siUAP56 (30 nM)
α-MxA
α-NP
IP α-NP
α-MxA
α-UAP56
WCL

3.2 Monitoring sub-cellular localization of NP and its binding capacity to UAP56 when challenged with MxA(R640A). A HEp-2-GST, HEp-2-MxAwt and HEp-2-MxA(R640A) cells were transfected with Kan-1 NP. Cells were lysed under low salt conditions, the nuclei were pelleted, washed and under high salt condition lysis was performed. Cytoplasmic and nuclear fractions were analysed by Western blot with the indicated antibodies. **B** HEp-2, HEp-2-MxAwt and HEp-2-MxA(R640A) cells were transfected with plasmids encoding Kan1 NP and either FLAG-mCherry or FLAG-UAP56 as a control. Cells were lysed, a FLAG-immunoprecipitation was performed and the IP fraction and WCL samples were analysed by Western blot using the indicated antibodies. **C** HEp-2 cells were transfected with plasmids coding for Kan1 NP, either FLAG-mCherry or FLAG-UAP56 and increasing amounts of MxA(R640A) expression plasmid (100ng, 250ng, 500ng). Cells were lysed and a FLAG-immunoprecipitation was performed. IP fractions and WCL samples were analysed by Western blot using the indicated antibodies. **D** HEp-2-MxA(R640A) cells were transfected with plasmids encoding different NPs as indicated or empty vector. 24 hours post transfection cells were transfected with 30 nM siRNA targeting UAP56 mRNA. 48 post siRNA transfection cells were lysed and an NP-immunoprecipitation was performed. IP fractions and WCL samples were analysed by Western blot using the indicated antibodies. **E** HEp-2-MxA(R640A) cells were transfected with siRNA targeting UAP56 mRNA together with plasmids coding for Kan1 or WSN NP or empty. 48 hours post transfection cells were lysed and an NP-immunoprecipitation was performed. IP fractions and WCL samples were analysed by Western blot using the indicated antibodies. WCL: whole cell lysate

Fig. 3.3

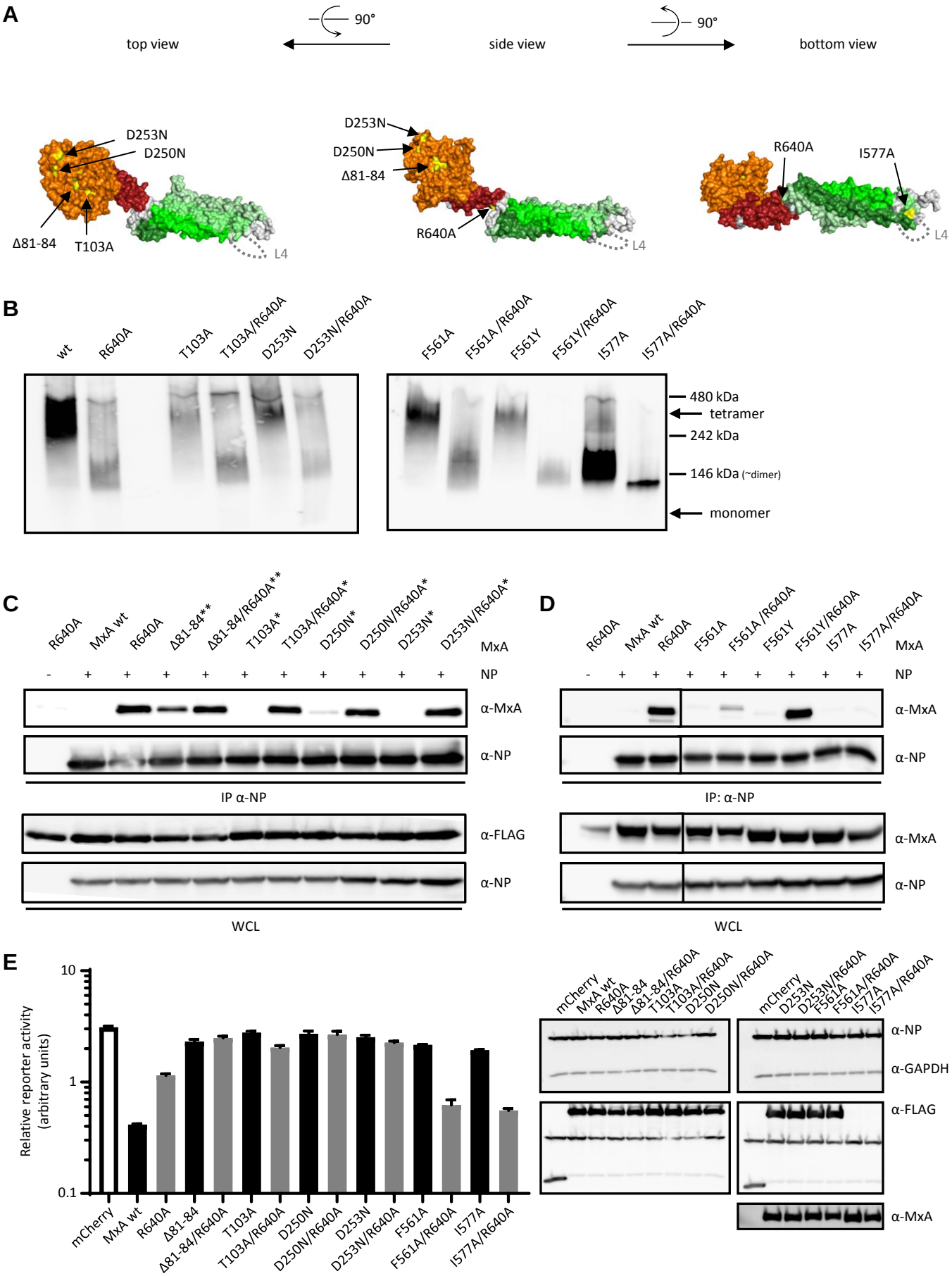
A
top view
90°
side view
90°
bottom view
D253N
D250N
Δ81-84
T103A
L4
D253N
D250N
Δ81-84
R640A
L4
R640A
I577A
L4
B
wt
R640A
T103A
T103A/R640A
D253N
D253N/R640A
F561A
F561A/R640A
F561Y
F561Y/R640A
I577A
I577A/R640A
480 kDa
tetramer
242 kDa
146 kDa (~dimer)
monomer
C
R640A
MxA wt
R640A
Δ81-84**
Δ81-84/R640A**
T103A*
T103A/R640A*
D250N*
D250N/R640A*
D253N*
D253N/R640A*
MxA
NP
α-MxA
α-NP
IP α-NP
α-FLAG
α-NP
WCL
D
R640A
MxA wt
R640A
F561A
F561A /R640A
F561Y
F561Y/R640A
I577A
I577A/R640A
MxA
NP
α-MxA
α-NP
IP: α-NP
α-MxA
α-NP
WCL
E
Relative reporter activity (arbitrary units)
10
1
0.1
mCherry
MxA wt
R640A
Δ81-84
Δ81-84/R640A
T103A
T103A/R640A
D250N
D250N/R640A
D253N
D253N/R640A
F561A
F561A/R640A
I577A
I577A/R640A
mCherry
MxA wt
R640A
Δ81-84
Δ81-84/R640A
T103A
T103A/R640A
D250N
D250N/R640A
mCherry
D253N
D253N/R640A
F561A
F561A/R640A
I577A
I577A/R640A
α-NP
α-GAPDH
α-FLAG
α-MxA

3.3 The dimeric state of MxA highly increases its binding capacity to NP. A Crystal structure of MxA visualized with PyMOL based on Gao et al., Immunity, 2011 (RCSB protein data bank ID: 3SZR). The G-domain is coloured in orange, the BSE in red and the stalk in different shades of green. **B** Non-denaturing PAGE analysis of Vero cells transfected with plasmids coding for different variants of MxA. Lysates were dialysed and run on a gel under non-denaturing conditions. Western blots analysis was performed with an α-MxA antibody. Molecular weight of MxA: 75 kDa. **C and D** HEp-2 cells were transfected with plasmids coding for Kan1 NP or empty vector and different variants of MxA as indicated. Cells were lysed and an NP-immunoprecipitation was performed. IP fractions and WCL samples were analysed by Western blot using the indicated antibodies. **C**: G-domain mutants. **D**: stalk mutants. Pictures in **D** are derived from the same membrane with identical exposure parameters, irrelevant bands were cut out (cut indicated by vertical line). **E** 293Ts were transfected with plasmids coding for the mini replicon constituents and FLAG-mCherry or different variants of FLAG-MxA (except I577A and I577A/R640A, which do not harbour a FLAG-tag) (200 ng). A dual-luciferase read-out was performed and firefly reporter activity is shown normalized to *Renilla* luciferase activity (left panel). Data are represented as mean ±SEM of duplicates. Protein expression is confirmed by Western blot analysis (right panel) of pooled samples for each condition using the indicated antibodies. Note: additional bands seen on the membrane stained with α-FLAG antibody originate from the previous GAPDH and NP staining. WCL: whole cell lysate

Fig. 3.4

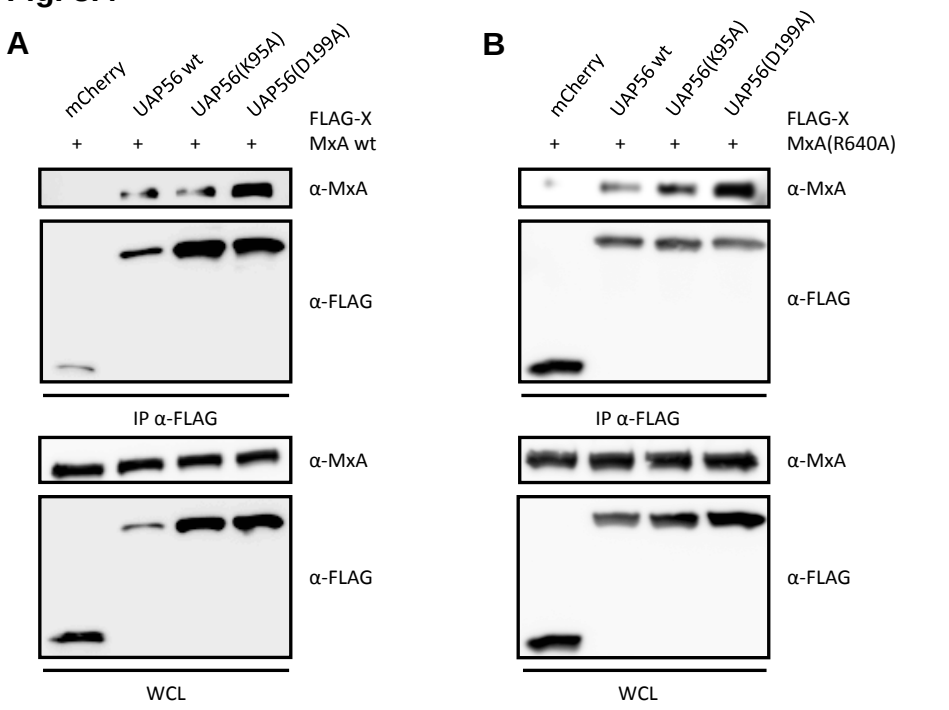
A
mCherry
UAP56 wt
UAP56(K95A)
UAP56(D199A)
FLAG-X
MxA wt
+ + + +
α-MxA
α-FLAG
IP α-FLAG
α-MxA
α-FLAG
WCL
B
mCherry
UAP56 wt
UAP56(K95A)
UAP56(D199A)
FLAG-X
MxA(R640A)
+ + + +
α-MxA
α-FLAG
IP α-FLAG
α-MxA
α-FLAG
WCL

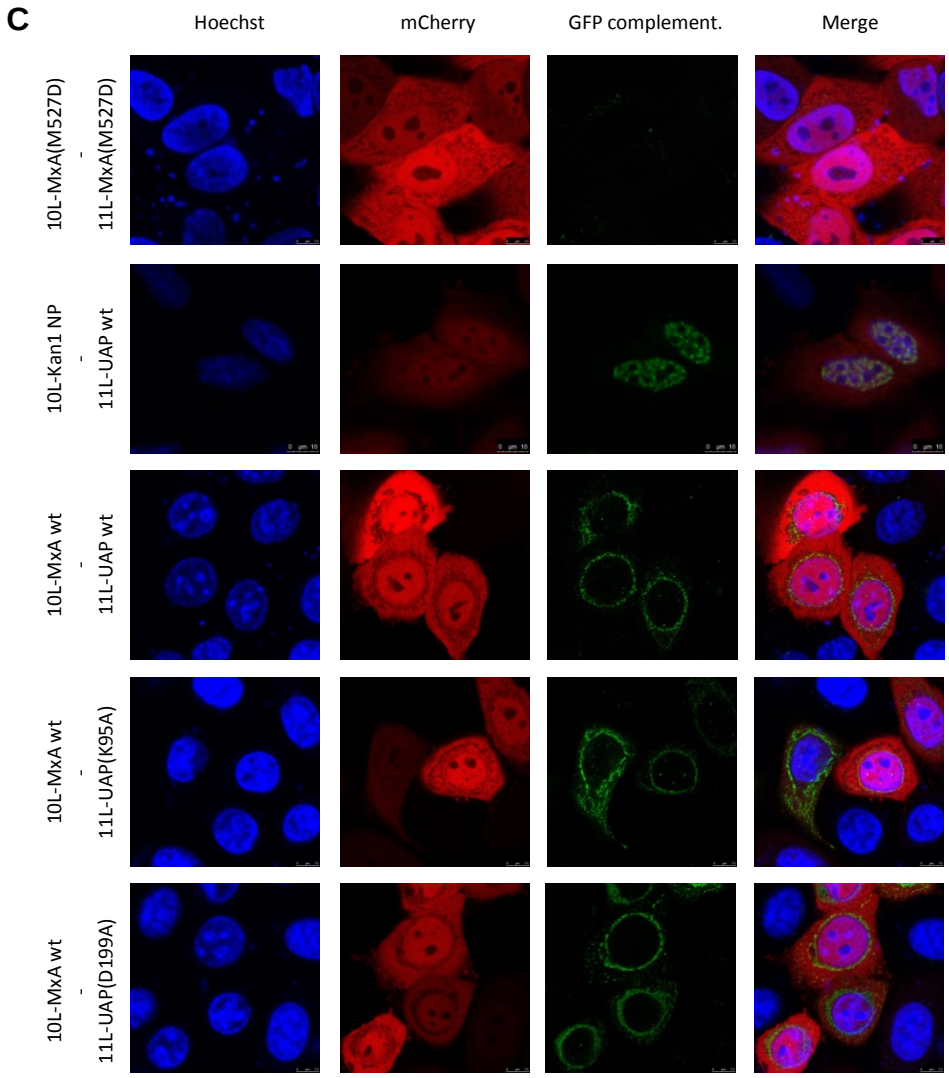
C
Hoechst
mCherry
GFP complement.
Merge
10L-MxA(M527D) - 11L-MxA(M527D)
10L-Kan1 NP - 11L-UAP wt
10L-MxA wt - 11L-UAP wt
10L-MxA wt - 11L-UAP(K95A)
10L-MxA wt - 11L-UAP(D199A)

3.4 ATPase and helicase functions of UAP56 are dispensable for MxA- and NP-binding.
A and B HEp-2-MxAwt (**A**) or HEp-2-MxA(R640A) (**B**) cells were transfected with FLAG-mCherry or FLAG-UAP56wt or different mutants thereof. UAP56(K95A): ATPase- and helicase-activity deficient mutant, UAP56(D199A): helicase-activity deficient mutant. FLAG-immunoprecipitation was performed and IP fractions and WCL samples were analysed by Western blot using the indicated antibodies. **C** HeLa cells were transfected with plasmids coding for the proteins of interest tagged with GFP β-sheet 10 or 11 (10L-X and 11L-X) as indicated, the detector fragment GFP1-9 (GFP β-sheets 1-9) and mCherry as a transfection control. Live cell analysis was performed by confocal microscopy. Monomeric MxA(M527D) served as a negative control. WCL: whole cell lysate

Fig. 3.5

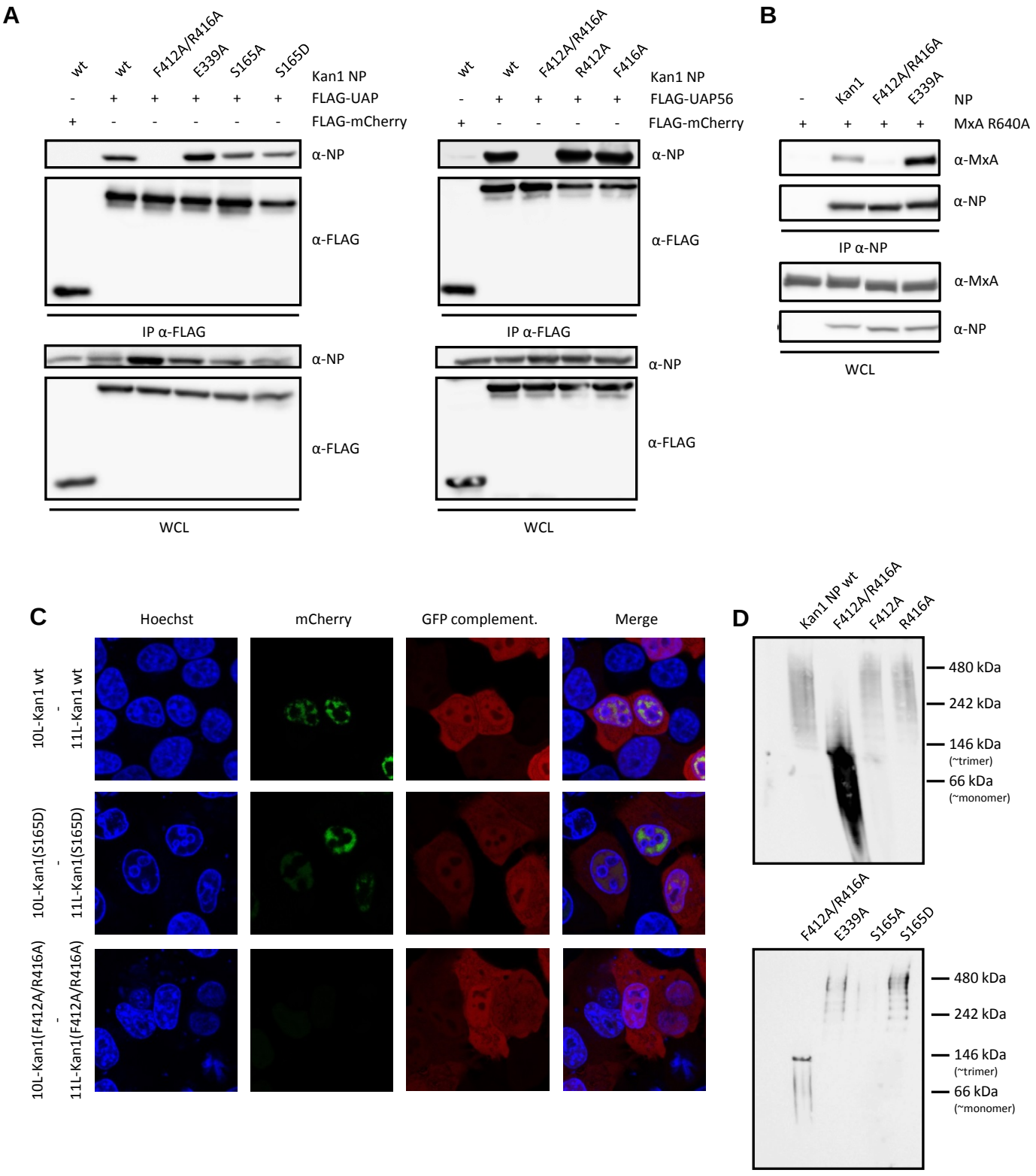
A
wt
wt
F412A/R416A
E339A
S165A
S165D
Kan1 NP
FLAG-UAP
FLAG-mCherry
α-NP
α-FLAG
IP α-FLAG
α-NP
α-FLAG
WCL
wt
wt
F412A/R416A
R412A
F416A
Kan1 NP
FLAG-UAP56
FLAG-mCherry
α-NP
α-FLAG
IP α-FLAG
α-NP
α-FLAG
WCL
B
Kan1
F412A/R416A
E339A
NP
MxA R640A
α-MxA
α-NP
IP α-NP
α-MxA
α-NP
WCL
C
Hoechst
mCherry
GFP complement.
Merge
10L-Kan1 wt - 11L-Kan1 wt
10L-Kan1(S165D) - 11L-Kan1(S165D)
10L-Kan1(F412A/R416A) - 11L-Kan1(F412A/R416A)
D
Kan1 NP wt
F412A/R416A
F412A
R416A
480 kDa
242 kDa
146 kDa
(~trimer)
66 kDa
(~monomer)
F412A/R416A
E339A
S165A
S165D
480 kDa
242 kDa
146 kDa
(~trimer)
66 kDa
(~monomer)

3.5 Kan1 NP(F412A/R416A) loses its binding capacity to MxA as well as UAP56. A HEp-2 cells were transfected with either FLAG-mCherry or FLAG-UAP56 and Kan1 NP wt or different oligomeric Kan1 NP mutants as indicated. FLAG- immunoprecipitation was performed. IP fractions and WCL samples were analysed by Western blot using the indicated antibodies. **B** HEp-2-MxA(R640A) cells were transfected with empty vector or plasmids coding for either wildtype Kan1 NP or monomeric Kan1 NP mutants as indicated. Cells were lysed and an NP- immunoprecipitation was performed. IP fractions and WCL samples were analysed using the indicated antibodies. **C** HeLa cells were transfected with plasmids coding for the proteins of interest tagged with GFP β-sheet 10 or 11 (10L-X and 11L-X) as indicated, the detector fragment GFP1-9 (GFP β-sheets 1-9) and mCherry as a transfection control. Live cell imaging analysis was performed by confocal microscopy. **D** Vero cells were transfected with wildtype Kan1 and the indicated mutants thereof. Cells were lysed and samples were dialysed. The samples were run on a gel under non-denaturing conditions. Western blot analysis was performed using an α-NP antibody. Molecular weight of NP: 50 kDa. WCL: whole cell lysate

4 An attempt at mapping the interaction domains in MxA and UAP56 to each other and to viral NP

4.1 Introduction

The discovery of Mx genes dates back to 1962/64, when Jean Lindenmann found that the protein product of one single gene - namely Mx1 - protected inbred mice from a lethal dose of IAV[92,169]. Later on, Mx genes were found to be present in many other species[95,167]. Humans harbor the two closely related genes Mx1 and Mx2, which express the two structurally but not functionally very similar proteins MxA and MxB, respectively. The most obvious difference is found in their antiviral activity. Whereas MxA has been shown to inhibit many RNA- but also some DNA-viruses[95,96], MxB has only very recently been shown to harbor antiviral potential by antagonizing HIV-1 and other primate lentiviruses[113,141] and various members of the *Herpesviridae* family[114]. Many efforts have been made in the past decades to characterize the antiviral activity of MxA and it is now generally thought that the viral nucleoprotein (NP) represents its target[123]. NP is a major component of the viral ribonucleoproteins (vRNPs), a structure built of the viral RNA genome segments bound to one viral polymerase molecule and covered by multiple copies of NP. These vRNPs are located to the core of IAV virions. However, the mode of action of MxA appears to differ depending on the virus it acts against and the detailed mechanism remains largely unknown for IAV. The MxA-sensitivity of IAVs of different origin varies greatly[121-123]. Generally, avian IAV strains are more sensitive to MxA in contrast to human strains and this sensitivity is dependent on the viral NP. MxA sensitivity is reduced or even lost if certain amino acid substitutions are introduced in the viral nucleoprotein NP of sensitive strains[122,123]. Co-immunoprecipitation (co-IP) experiments revealed the capability of dimeric MxA to bind to NPs of various strains[115] (see fig. 2.1B, 2.2C). In addition to a viral protein partner it has further been shown, that MxA is able to bind to the cellular DEAD-box helicase UAP56 (also designated DDX39B)[57] (see also fig. 2.1C, 2.3A and B), a nucleo-cytoplasmic shuttling protein involved in mRNA biogenesis and nuclear export[128,130,176,186]. This helicase has already been suggested to constitute a pro-viral factor that acts as a chaperone on viral NP[29] but is also required for the anti-IAV activity of MxA[135]. Here, we demonstrate that UAP56 binds IAV NP, which provides a structural link in addition to the already established functional link of UAP56 and IAV. NP-UAP56 interaction was published concomitantly by Hu et al[137].

Apart from the fact that MxA, NP and UAP56 bind to each other no additional information is currently available about the specific regions involved in binding. We thus aimed at mapping the regions that mediate MxA-UAP56 and NP-UAP56 interaction by employing deletion

mutants of MxA and UAP56. To this end we adapted the tripartite splitGFP assay[179] in order to visualize the subcellular localization of the interactions between MxA, UAP56 and NP. In contrast to the standard splitGFP system the tripartite splitGFP has the advantage of smaller tag sizes, higher fluorescence signals and expendability of sample incubation prior to microscopic analysis. The tags consist of GFP β-sheets 10 and 11, respectively, which are fused to our proteins of interest via an unstructured linker sequence. The complementary GFP detector fragment (the remaining β-sheets 1-9), co-expressed from an individual plasmid, assembles with the GFP10 and GFP11 tags and complements GFP fluorescence whenever the tagged proteins are in sufficiently close proximity.

To our disappointment we found that UAP56-deletion mutants are not a feasible tool to study heterotypic UAP56 interactions, due to the recruitment of endogenous UAP56 to most UAP56 deletion mutants. We mapped the domain in UAP56 involved in UAP56 dimerization to the region between amino acid residue 227 and 310. Binding studies with MxA deletion mutants suggested the involvement of loop L4 in UAP56-binding. However, this could not be confirmed, since MxA L4 mutants retained interaction to UAP56. Surprisingly, we were able to show MxB-NP and MxB-UAP56 interactions. Taken together, our observation that both human Mx proteins bind to NP and UAP56 suggests that MxA and MxB share conserved functions that may solely be modulated by their distinct intracellular localization.

4.2 Experimental procedures

4.2.1 Cell lines

All cell lines were cultured in DMEM supplemented with 10% FCS, 1 mg/ml Penicillin/Streptomycin and 2 mM GlutaMAX™ (Thermo Fisher Scientific) (complete DMEM) at 37°C and 5% CO_2. HEp-2 (HeLa-derived human epithelial cells) and HeLa (human adenocarcinoma cells) were purchased from ATCC.

4.2.2 Plasmids

As previously described MxA wt cDNA was cloned into pcDNA3.1(+)neo (Invitrogen)[158]. cDNA of GFP β-sheet 10 or 11[179] plus and unstructured linker sequence of 32 or 25 amino acids ([179] supplemental information), respectively was cloned into pcDNA3.1(+)neo. These constructs were designed to be suitable as either N- or C-terminal protein tags. For the detector fragment consisting of the complementing β-sheets 1-9, cDNA of GFP1-9 was cloned into pcDNA3.1(+)neo[179]. To obtain GFP10- or GFP11-tagged MxA, NP or UAP56 variants, the respective cDNA was cloned into these vectors using PacI and BamHI.

4.2.3 Immunofluorescence assay

Cells were seeded in 24-well format on a cover slide. After transfecting with JetPRIME (Polyplus transfection), cells were fixed with 3% paraformaldehyde (PFA) in PBS for 10 min at RT and permeabilized with 0.1% or 0.5% Triton-X100 in PBS for 10 min at RT. Staining was performed in PBS with 5% goat serum for 1 h at RT (mouse α-MxA (hybridoma ab143, 1:5).

4.2.4 Tripartite split-GFP complementation assay

HEp-2 or HeLa cells were seeded in an ibidi µ-slide 4-well chamber (Cat. No 80427). Cells were transfected with 500 ng DNA (180 ng of each GFP10- or GFP11-tagged construct and 90 ng GFP1-9) using ViaFect^{TM} (Promega) according to the manufacturer's instructions. 24 h later growth medium was changed to FluoroBrite DMEM medium (Thermo Fisher Scientific) + Hoechst (1:5000) and analysed at a Leica SP5 confocal laser scanning microscope.

4.2.5 Co-immunoprecipitation (co-IP)

HEp-2 cells were transfected with Viafect (Promega) according to the manufacturer's instructions. 24 h post-transfection cells were lysed in 300 µl lysis buffer (20 mM Tris-HCl pH 7.5, 150 mM NaCl, 5 mM MgCl2, 50 mM NaF, 1 mM Na3VO4, 1% NP-40, 50 mM β-glycerophosphate, 100 nM iodoacetamide, 1x Roche cOmplete Protease Inhibitor Cocktail) in the dark on ice for 30 min. Lysates were homogenized using QiaShredder columns (Qiagen). 100 µl of each lysate was incubated with antibody (α-NP (50 µl, HB65, hybridoma, in-house) at 4°C over night on a rotating wheel. 15 µl lysate was used for the whole cell lysate (WCL) control. 20 µl Dynabeads protein G magnetic beads (Thermo Fisher Scientific) per sample were pre-adsorbed over night at 4°C on a rotating wheel using untransfected HEp-2 cell lysate. Pre-adsorbed beads were washed once with lysis buffer and incubated with the lysates for 1 h at 4°C on a rotating wheel. Beads were washed once with 1 ml followed by five times 0.5 ml lysis buffer. Beads were briefly vortexed in between the washing steps. Proteins were eluted from the beads with 20 µl 1x Laemmli buffer at 95°C for 10 min. 15 µl WCL/IP sample was loaded on a 10% SDS-PAGE gel and analysed by Western blot (α-NP (rabbit serum, in-house, 1:10'000), α-MxA (ab143, hybridoma, in-house, 1:10)).

4.3 Results

4.3.1 Generating MxA deletion mutants to reveal domains necessary for binding to UAP56 and NP

The C-terminal stalk of MxA has already been shown to be involved in virus specificity[99] and we and others[99,100,191] also have evidence of the importance of the stalk in the antiviral activity of MxA. In order to map the binding sites of MxA to UAP56 and NP we thus decided to focus on the C-terminal region of MxA. We thus designed deletion mutants eliminating an increasing number of the 5 α-helices, which build up the stalk. The last remaining residues of the respective deletions are marked in the schematic representation of MxA in Fig. 4.1A. The expression in HEp-2 cells of those deletion mutants was verified by transfection and immunofluorescent analysis (Fig. 4.1B). Most of the mutants showed a similar expression pattern to wildtype MxA, with the exception of MxA(Δ530-662), which localized to the cytoplasm as well as the nucleus, where MxA is normally excluded from. We visualized the site of interaction of the MxA deletion mutants with UAP56 by means of the tripartite split-GFP complementation assay (described in 3.3 and in[179]). We transfected HEp-2 cells with the proteins of interest fused to a splitGFP tag (‘10L-’ or ‘11L-’), the detector fragment GFP1-9 and mCherry as a transfection control and we observed that interaction to wildtype UAP56 was lost with MxA(Δ530-662) but not with MxA(Δ575-662) (Fig. 4.1C). Amino acids 530-574 comprise the whole of loop L4, an unstructured loop which has been implicated in membrane binding[116] and in the case of mouse Mx1 (a mouse homolog of MxA) in anti-IAV activity[101]. When looking at co-precipitation of the MxA deletion mutants with NP in cells transfected with the indicated plasmids, interaction with both MxA(Δ575-662) and MxA(Δ530-662) was observed, and this interaction is lost with the MxA(Δ497-662) mutant (Fig. 4.1D). As previously described[115] (also see chapter 2.1), only interaction of MxA(R640A) but not wildtype MxA can normally be visualized by co-IP. Intriguingly, here we report interaction of NP with the MxA-deletion mutants, despite the fact that the R640 residue is in the deleted part of the molecule. This renders the results challenging to interpret.

4.3.2 Investigating the potential involvement of MxA loop L4 in its capability to bind to UAP56 and NP

MxA and MxB are two closely related proteins with a very similar 3D structure. However, wildtype MxB does not harbor potent anti-IAV function. In order to clarify the importance of loop L4 of MxA for the interaction with UAP56 and NP, we generated MxA-MxB chimeras. We exchanged loop L4 in MxA with the according structure in MxB and vice versa. The sequence identity of these loops is 32% and the length of the loop in MxB exceeds the one in

MxA by two amino acids. We hypothesized that the binding of MxA to UAP56 is abrogated in MxA harboring the loop from MxB if L4 is indeed crucial for binding. HEp-2 cells were transfected with the splitGFP constituents as indicated in fig. 4.2. To our surprise, UAP56-binding capacity of MxA(L4-MxB) was not affected in the least compared to wildtype MxA (Fig. 4.2A). The complementary chimera MxB(L4-MxA) showed similar binding capacities to UAP56 and even MxA(ΔL4), a mutant where L4 was replaced by an unrelated flexible linker sequence of the same length, retained its binding capacity to UAP56 (Fig. 4.2A). Therefore it is obvious that even if L4 is involved in binding to UAP56 it is clearly not sufficient. Being left with no loss of binding phenotype, we investigated the UAP56- and NP-binding capacity of wildtype MxB. Intriguingly, binding to UAP56 was indeed observed in a manner similar to MxA (Fig. 4.2B) in cells transfected with the indicated plasmids. The interaction was possibly slightly more dispersed throughout the cytoplasm. Furthermore, we were actually able to see splitGFP complementation of 11L-NP and 10L-MxB in contrast to 11L-NP and 10L-MxA expressing cells. The binding to NP could also be confirmed in co-IP experiments (Fig. 3.2B) in cells transfected with the indicated plasmids. Since wildtype MxB does not exert anti-IAV activity, the interaction to UAP56 and NP was unexpected. These differences in antiviral specificity imply, however, that MxA harbors additional features enabling it to counteract IAV infection.

4.3.3 Attempts at finding binding sites in UAP56 to MxA and NP

We further wanted to narrow down the region(s) in UAP56 necessary for the binding to MxA and NP. We aimed at addressing this issue with deletion mutants as well. UAP56 is a crescent shaped protein with two globular domains connected by a flexible linker (Fig. 4.3A). We chose a selection of N- and C-terminal deletion mutants according to Thomas et al.[128] (Fig. 4.3B). We first subjected the C-terminal deletion mutants to split-GFP complementation analysis in order to monitor the interactions with MxA (Fig. 4.3C) and NP (Fig. 4.3D). The perinuclear GFP signal seen in MxA- transfected cells remained unchanged independent of the length of the deletion in UAP56 (Fig. 4.3C). Also, nuclear localization of UAP56-NP interaction was clearly visible using the same UAP56-deletion mutants (Fig. 4.3D). When N-terminal UAP56 deletion mutants were tested in conjunction with NP and MxA a loss of interaction was not observed either (data not shown). We hypothesized that this phenotype is resulting from the interaction of the UAP56 deletion mutants with endogenous UAP56 so that MxA and NP are able to bind to the mutants indirectly via wildtype UAP56. To validate this hypothesis we examined the interaction potential of the deletion mutants with wildtype UAP56 (Fig. 4.4). Cells were transfected with 11L-UAP56wt and various 10L-UAP56 deletion mutants and we saw that complex formation was unaffected for some but not all mutant

UAP56 proteins (Fig. 4.4A). Interaction was only lost with UAP56(Δ201-428) (Fig. 4.4A, schematic representation shown in fig. 4.4B). In conclusion, we narrowed the dimerization domain down to amino acids 227 to 310 of UAP56 (highlighted in orange in fig. 4.4B). Furthermore, the observed loss of UAP56 dimerization but not binding to MxA and NP in N-terminal deletion mutants (compare fig. 4.4A with 4.3C) proposes the N-terminus to being part of the MxA- and NP-binding domain.

4.4 Discussion

In this chapter we aimed at mapping the interaction domains of MxA and the helicase UAP56 to each other as well as to viral NP. We made use of the tripartite splitGFP system described in Cabantous et al[179]. In contrast to the standard splitGFP complementation assay, where the two halves of GFP are used as protein tags, the improved tripartite splitGFP system utilizes only the very last C-terminal β-sheets of GFP as tags for the proteins of interest. This is an easy approach to quickly uncover regions involved in binding of two proteins. We adopted this system to study MxA-UAP56 interactions as well as interactions with NP. We thus generated various deletion mutants of MxA and UAP56. MxA truncation mutants first suggested loop L4 to be part of the UAP56-interaction domain. Further experiments with MxA L4 mutants, however, could not strengthen these data. Unexpectedly, the tripartite splitGFP system did not appear to be a suitable experimental approach to map UAP56 interaction domains. Sustained binding of endogenous UAP56 with the UAP56 deletion mutants interfered with the characterization of UAP56-MxA and UAP56-NP interactions. Nevertheless, we were able to narrow down the region involved in UAP56 dimerization to residues 227-310.

The inability to detect NP-MxA interaction with this approach was unexpected (data not shown), since robust interaction can be observed in NP-pulldown experiments (chapter 2 and 3 and[115]). However, tagging of proteins by attaching additional amino acids can interfere with the ability of those proteins to interact with other partners due to steric hindrance. In this work we used only N-terminally tagged MxA and NP proteins, based on a number of reasons. The N-terminus of MxA comprises the G-domain[170] and it is generally believed that the G-domain confers structural rearrangements to the stalk upon GTP hydrolysis[98,100], thus we believe the stalk offers a more suitable structure for protein binding. Also, the arginine residue at position 640 (R640), which is crucial for dimerization, is located at the C-terminal one part of the bundle-signaling element (BSE) of MxA[170]. MxA in some of our co-IP assays (eg. Fig. 3.3C) harbors an N-terminal FLAG-tag and that did not interfere with NP-binding or activity. The crystal structure of trimeric NP reveals that the N-terminus is not involved in

oligomerization[50,51]. It is situated at the outermost part of trimeric NP where it forms a protrusion. This makes the N-terminus a suitable target for the addition of another peptide as a tag. Not much is known about UAP56 and its dimeric structure so we tested both N- and C-terminal tagging. In the case of UAP56, it does not seem to matter if the tag is at the N- or C-terminus, complex formation of tagged UAP56 with MxA and NP was not affected (data not shown). In contrast to MxA-interaction, NP harboring an N-terminal splitGFP-tag still retains the capacity to interact with UAP56. We thus hypothesized that in the trimeric MxA-UAP56-NP complex, UAP56 is the 'linker' protein between MxA and NP, so that MxA and NP are too far apart from each other to allow splitGFP complementation. Extending the 30 amino acid linker sequence might possibly resolve this issue. On the other hand this could then also increase the rate of false-positives, due to random complementation.

Starting off with mapping the UAP56-interaction domain of MxA by consecutively larger C-terminal deletions, our results suggested loop L4 to be the potential region of interaction (Fig. 4.1C). Loop L4 has already been shown to be a determinant of antiviral activity of MxA against IAV and THOV[100,153]. We speculated that the antiviral activity of MxA is dependent on UAP56 und is thus indirectly mediated via the ability of MxA to bind to UAP56 via loop L4. However, the more elaborate MxA-MxB chimeric mutants showed sustained binding capabilities of all the tested chimera (Fig. 4.2). Swapping of whole domains between MxA and MxB did not result in loss of UAP56-binding and it has also been shown that swapping the loops between Mx proteins of different species is single amino acid mutations in L4, which have been shown to alter the antiviral activity against THOV and IAV[99,191], would be the next mutants to investigate. On top of that we uncovered the ability of MxB to interact with UAP56 in the cytoplasm. This was quite surprising, since MxB is lacking anti-IAV activity. On the other hand, MxA and MxB are very similar, thus the potential of MxB to interact with UAP56 might seem obvious. Nevertheless, binding is certainly not sufficient to exert anti-IAV activity and MxB might lack other characteristics, which are present in MxA, such as possibly the slight differences in tertiary structures or sub-cellular localization, which makes it unsuitable to inhibit IAV replication. We have evidence, though, that nuclear MxB is potent at restricting IAV replication (see chapter 2), which might account for the UAP56- and NP-binding capacity of MxB (Fig. 4.2B and fig. 2.4). It is also in line with reports, show binding of Mx1, a mouse homolog of MxA localized to the nucleus, to UAP56[57] and NP[151].

It is very intriguing that interaction of wildtype MxA cannot be visualized with co-IP experiments. The dimeric MxA(R640A) co-precipitates with NP (see chapter 3). However, this residue is deleted in all the MxA C-terminal deletion mutants used in the NP-pulldown in fig. 4.1D. We were thus lacking a suitable positive control. Nevertheless, we observed NP-

binding with MxA(Δ575-662) and MxA(Δ530-662) (Fig. 4.1D), which suggested the involvement of the α3-helix in NP binding, either directly or indirectly via changes in the tertiary structure of MxA.

So far, we could show that interaction of MxA with NP is highly dependent on the dimeric state of MxA (Fig. 3.3C and D). We have no data on folding and homotypic interactions of the MxA deletion mutants but it might well be that they assemble in dimers and thus form a complex with NP. Alternatively, the C-terminal deletions in MxA may result in an increased accessibility of the NP- and/or UAP56-binding site which may result in stable NP co-precipitation. We hypothesize that wildtype MxA, on the contrary, needs to undergo conformational changes upon NP-binding and possibly GTP hydrolysis, which subsequently releases NP from MxA and leads to a highly transient binding phenotype. Co-IP experiments with a cross linker to stabilize wildtype MxA-NP interaction might is a means to address this issue.

To circumvent the problem with the interference of endogenous UAP56 with our binding assay, cell lines depleted or at least with reduced levels of UAP56 are needed. We suspect, however, that the closely related and partially redundant helicase URH49[189] would then take over some of the functions of UAP56 and its expression might be upregulated. Additionally, due to the ability of URH49 to bind to MxA[57] and UAP56[192], UAP56 and URH49 would need to be downregulated simultaneously. This, however, greatly reduces cell viability (data not shown), which makes those cells unsuitable for splitGFP experiments. Instead of performing mapping studies of UAP56 deletion mutants with MxA and NP we were able to uncover the dimerization site of UAP56, which, according to our data, involves residues 227-310, the flexible linker between the N- and C-terminal globular domains. This is in partial accordance with Zhao et al[193], who proposed the N-terminus (via salt bridge formation between residues R123 and D62, E134 and K138 and K156 and E55 of the first and the second UAP56 molecule, respectively) or amino acids 198 - 244 to harbor a dimerization domain according to UAP56's crystal structure. They state that the likelihood of the second dimer interface being the biologically relevant is lower than the first, because dimer formation in this fashion is "rarely observed in biological systems". We, on the other hand, have experimental evidence that strongly suggests the second interface to be the relevant dimer interface. UAP56 lost dimerization capability, when residues 201-428 of UAP56 were deleted (Fig. 4.4) but this mutant retained its capability to interact with MxA and NP (data not shown). Taken together, these data suggest the C-terminal residues 201-428 to be dispensable for NP and MxA binding.

Another issue is the observed difference in splitGFP complementation signal intensity between different samples. These differences are challenging to interpret and we question the biological relevancy. It is known that due to the irreversibility of GFP complementation, transient or weak interactions are stabilized[179,194]. This stabilization could explain differences in signal intensities. We do not know the extent of this stabilizing feature in our particular set of experiments. But differences in binding strengths between mutants with reduced interaction capacities and mutants still harboring the full binding potential might well be reflected in differences in GFP signal intensities. Thus, the loss of binding mutants we found have most likely completely lost their binding capacity and such mutants are the only feasible candidates for splitGFP experiments.

Taken together, the tripartite splitGFP assay is an easy-to-use system to study protein-protein interactions. It was not suitable, however, for our experimental setup due to complex interactions involving more than one interface. This means first of all oligomerization of MxA, NP and UAP56 and in addition to this, the interaction of those oligomers with each other. We were thus not able to conclusively map binding domains of MxA and UAP56.

Fig. 4.1

A

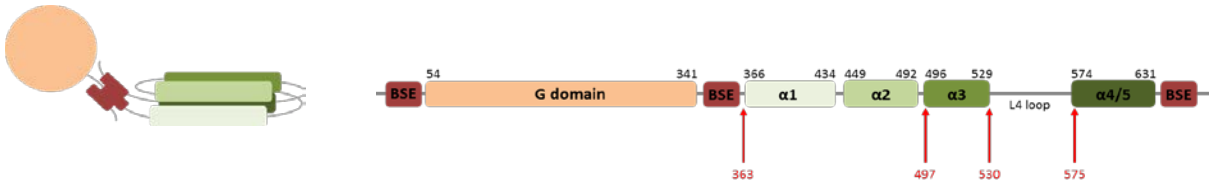
54
341
366
434
449
492
496
529
574
631
BSE
G domain
BSE
α1
α2
α3
L4 loop
α4/5
BSE
363
497
530
575

B

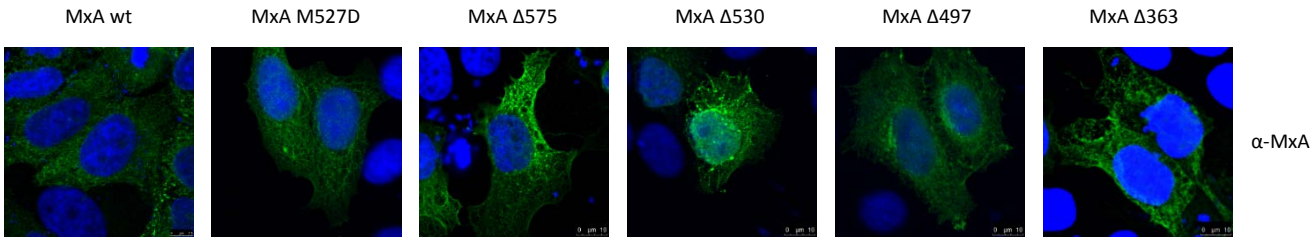
MxA wt
MxA M527D
MxA Δ575
MxA Δ530
MxA Δ497
MxA Δ363
α-MxA

C

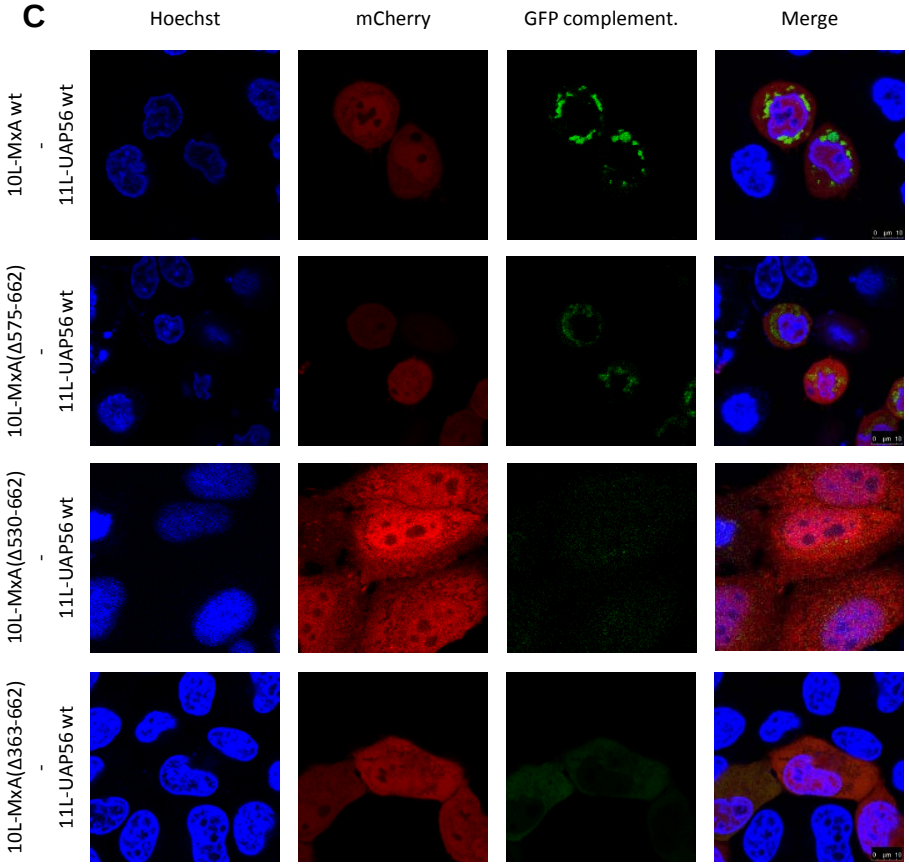
Hoechst
mCherry
GFP complement.
Merge
10L-MxA wt - 11L-UAP56 wt
10L-MxA(Δ575-662) - 11L-UAP56 wt
10L-MxA(Δ530-662) - 11L-UAP56 wt
10L-MxA(Δ363-662) - 11L-UAP56 wt

D

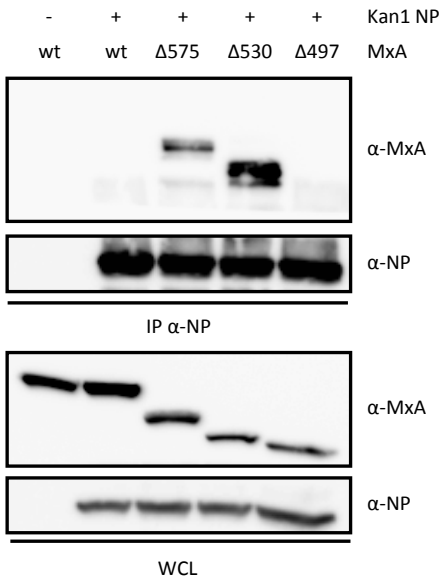
- + + + + Kan1 NP
wt wt Δ575 Δ530 Δ497 MxA
α-MxA
α-NP
IP α-NP
α-MxA
α-NP
WCL

4.1 Binding capacities of C-terminal truncations mutants of MxA to NP and UAP56. A Schematic representation of the 3D structure of MxA (left) and a linear representation (right) with the first residue, which is deleted in the corresponding mutant indicated by a red arrow. **B** HEp-2 cells were transfected with plasmids coding for wildtype MxA or the indicated MxA mutants. Cells were fixed, stained as indicated and analysed by confocal microscopy. **C** HEp-2 cells were transfected with plasmids coding for the proteins of interest tagged with GFP β-sheet 10 or 11 (10L-X and 11L-X) as indicated, the detector fragment GFP1-9 (GFP β-sheets 1-9) and mCherry as a transfection control. Live cell imaging was performed at a confocal microscope. **D** HEp-2 cells were transfected with plasmids encoding wildtype MxA or MxA deletion mutants as indicated together with a Kan1 NP expression plasmid. Cells were lysed and an NP- immunoprecipitation was performed. IP fractions and WCL samples were analysed by Western blot using the indicated antibodies. WCL: whole cell lysate

Fig. 4.2

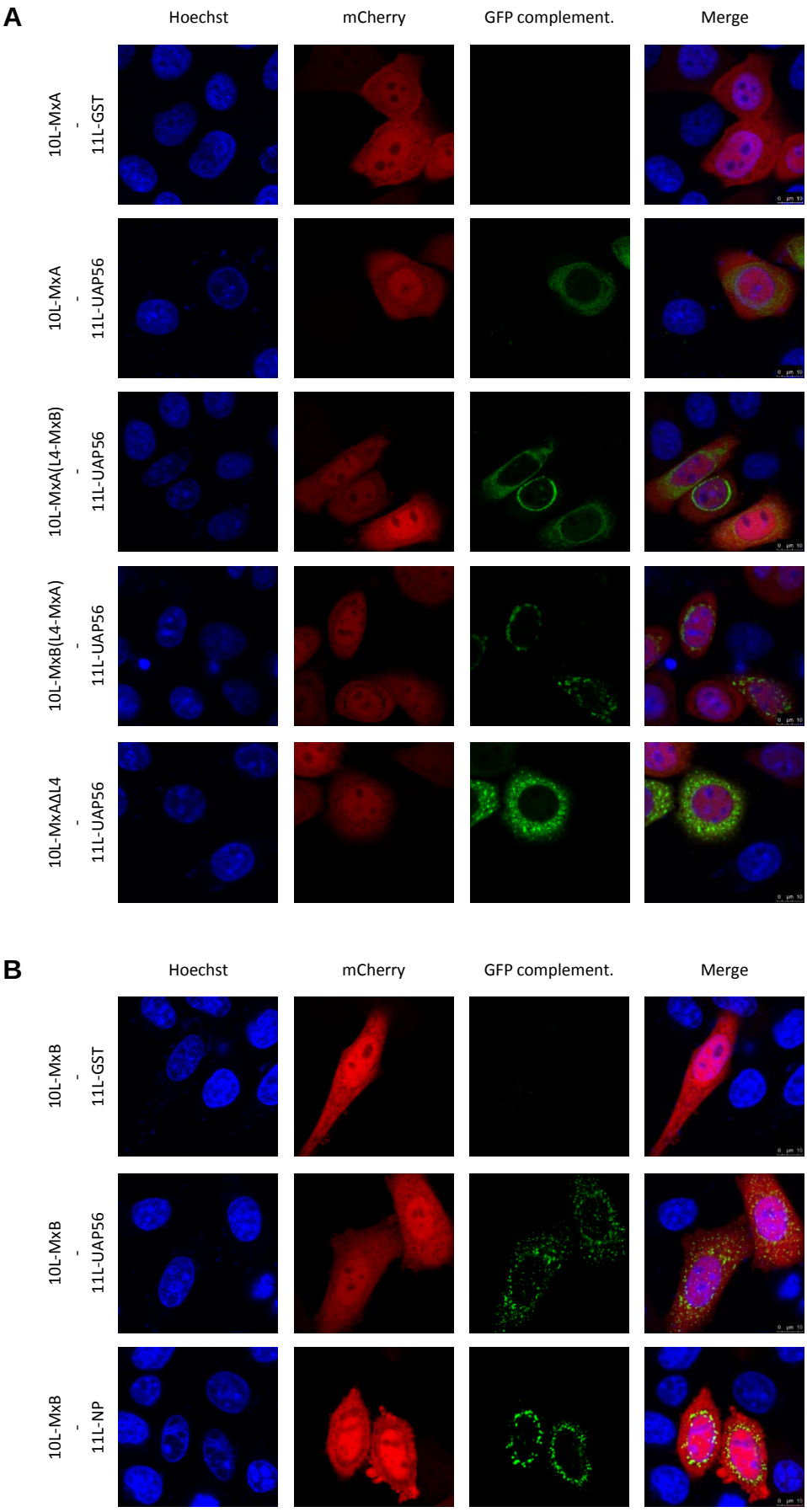
A
Hoechst
mCherry
GFP complement.
Merge
10L-MxA - 11L-GST
10L-MxA - 11L-UAP56
10L-MxA(L4-MxB) - 11L-UAP56
10L-MxB(L4-MxA) - 11L-UAP56
10L-MxAΔL4 - 11L-UAP56
B
Hoechst
mCherry
GFP complement.
Merge
10L-MxB - 11L-GST
10L-MxB - 11L-UAP56
10L-MxB - 11L-NP

4.2 Testing loop L4 of MxA for its potential as a prerequisite for UAP56 binding. A and B HEp-2 cells were transfected with plasmids coding for the proteins of interest tagged with GFP β-sheet 10 or 11 (10L-X and 11L-X) as indicated, the detector fragment GFP1-9 (GFP β-sheets 1-9) and mCherry as a transfection control. Cells were analysed by confocal microscopy. MxAL4-MxB: wildtype MxA harbouring the corresponding loop from MxB instead of loop L4, MxBL4-MxA: wildtype MxB harbouring loop L4 from MxA instead of its corresponding loop, MxAΔL4: wildtype MxA where loop L4 was exchanged with an unstructured linker sequence.

Fig. 4.3 part one

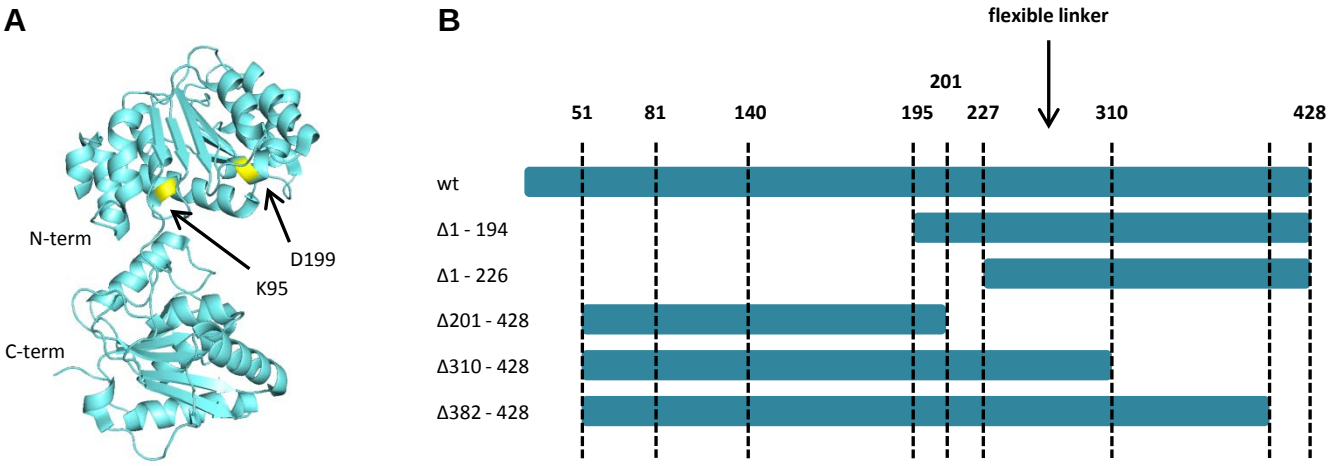

Fig. 4.3 part two

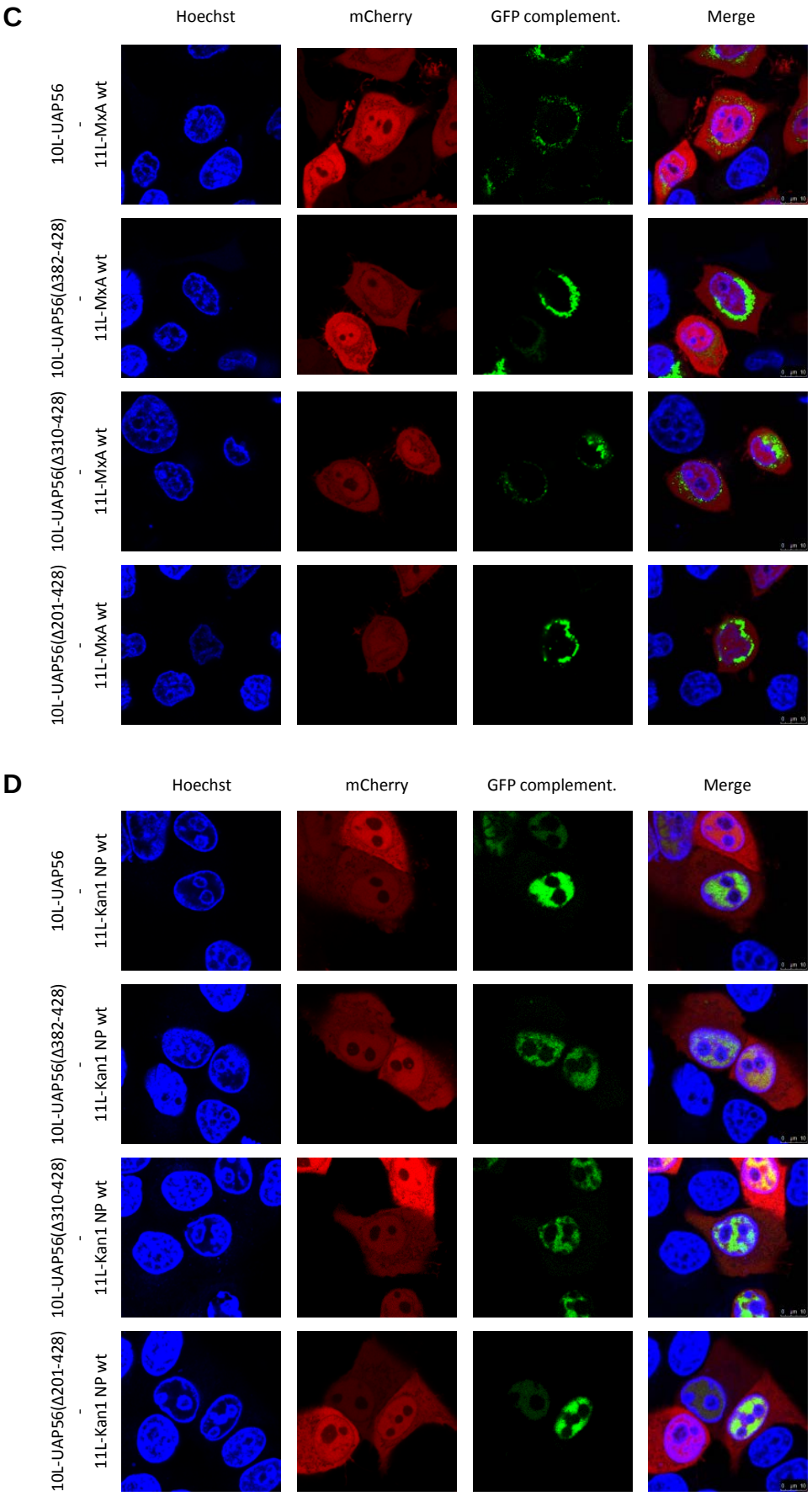

4.3 UAP56 deletion mutants are not feasible to for interaction studies. A Crystal structure according to Shi et al., 2004 visualized with PyMOL (RCSB protein data bank ID: 1xti). Mutations affecting the helicase (D199A) and ATPase/helicase (K95A) functions are highlighted in yellow. **B** Schematic representation of the N- and C-terminal UAP56 deletion mutants based on Thomas et al. The arrow indicates the flexible linker between the N- and C-terminal globular tertiary structures. **C and D** Interaction capacities of wildtype MxA (**C**) or wildtype Kan1 NP (**D**) with wildtype UAP56 or C-terminal deletion mutants thereof. HEp-2 cells were transfected with plasmids coding for the proteins of interest tagged with GFP β-sheet 10 or 11 (10L-X and 11L-X) as indicated, the detector fragment GFP1-9 (GFP β-sheets 1-9) and mCherry as a transfection control. Live cell imaging was performed on a confocal microscope.

Fig. 4.4

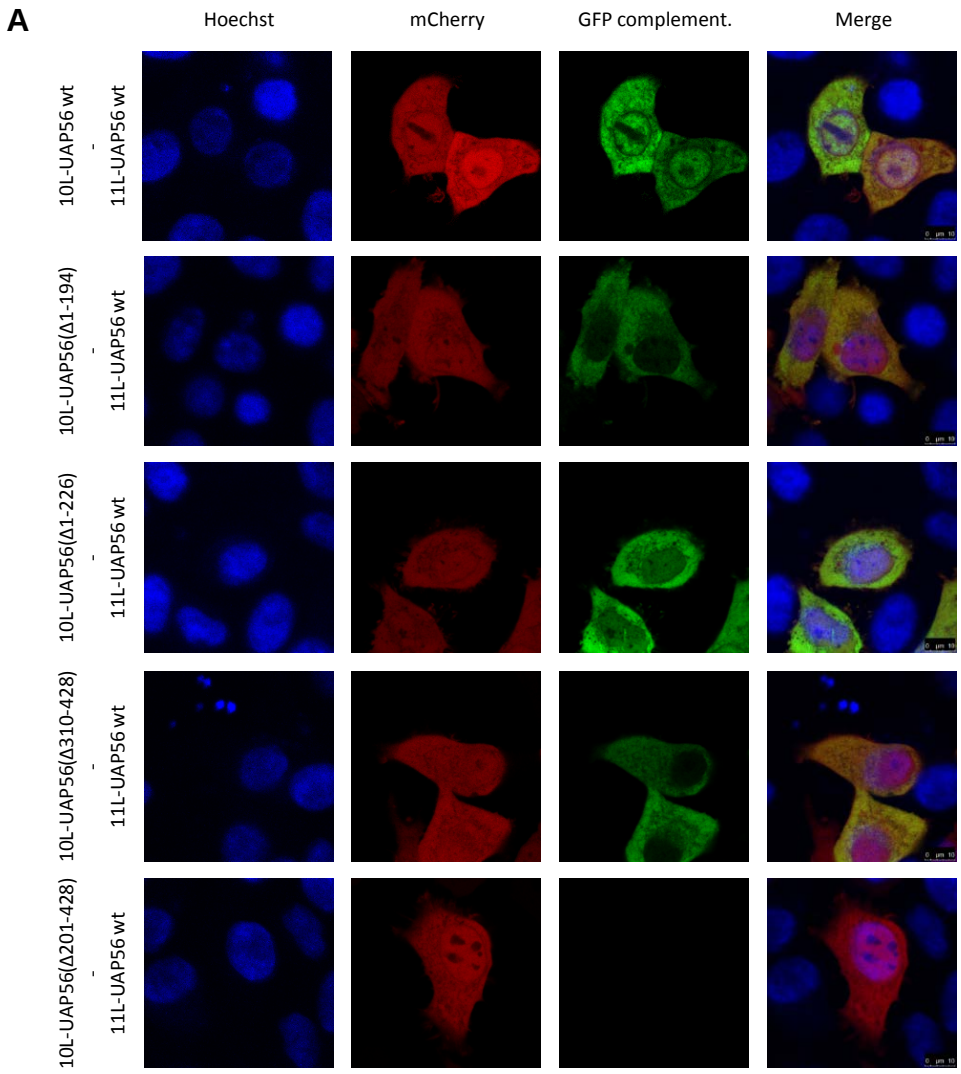
A
Hoechst
mCherry
GFP complement.
Merge
10L-UAP56 wt - 11L-UAP56 wt
10L-UAP56(Δ1-194) - 11L-UAP56 wt
10L-UAP56(Δ1-226) - 11L-UAP56 wt
10L-UAP56(Δ310-428) - 11L-UAP56 wt
10L-UAP56(Δ201-428) - 11L-UAP56 wt

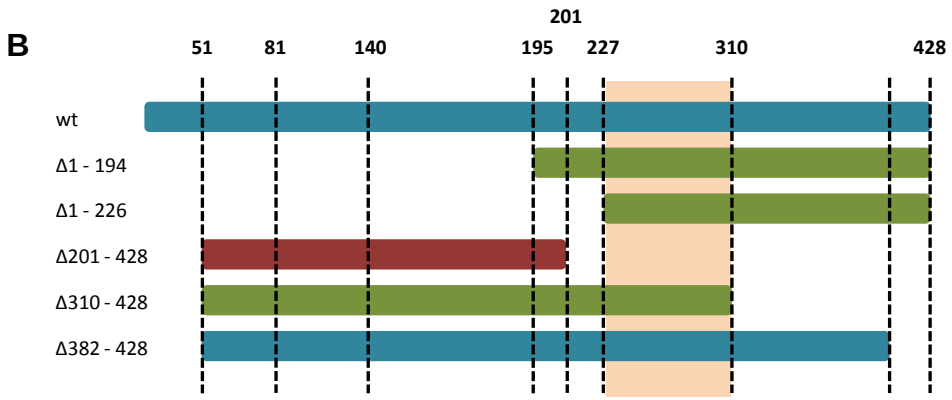
B
201
51
81
140
195
227
310
428
wt
Δ1 - 194
Δ1 - 226
Δ201 - 428
Δ310 - 428
Δ382 - 428

4.4 Mapping the dimerization domain in UAP56 to amino acid residues 227-310. A HEp-2 cells HeLa cells were transfected with plasmids coding for the proteins of interest tagged with GFP β-sheet 10 or 11 (10L-X and 11L-X) as indicated, the detector fragment GFP1-9 (GFP β-sheets 1-9) and mCherry as a transfection control. Live cell imaging was performed on a confocal microscope. **B** Schematic representation of the different UAP56 deletion mutants and their oligomerization capacity. Colours indicate retained ability to form oligomers (green) or a loss thereof (red). The putative dimerization domain is highlighted in orange.

5 General discussion

In response to virus infection the innate immune system induces the production of many proteins with potent antiviral functions. Mx proteins represent a small group of such effector proteins and are present in a variety of species. Almost all mammal genomes harbor two genes: MX1 and MX2[95]. Despite their remarkable structural resemblance, the protein products of those two genes nevertheless harbor some distinct features. Mouse Mx1 and its human homolog MxA restrict a panel of viruses, mainly RNA viruses (reviewed in[95]), among them IAV, but MxA has also been shown to inhibit some DNA viruses[111,195]. They localize to different subcellular compartments and also inhibit IAV at different stages of its replication cycle. The viral targets are known for many viruses to be nucleoproteins, ribonucleoprotein complexes or nucleocapsids (reviewed in[95]). Despite extensive investigations of Mx1 and MxA antiviral functions over the past decades the molecular mechanism of action is still unresolved. Mouse Mx2 and human MxB do not show potent anti-IAV activity and were only shown to inhibit vesicular stomatitis virus (VSV)[149] and Hantaan virus[148] or human immunodeficiency virus type 1 (HIV-1)[113,157,196], other primate lentiviruses[113] and human herpesviruses[114], respectively.
The cellular RNA-helicase UAP56 has been shown to play a role for both IAV infection[133] and the antiviral activity of MxA[135]. This helicase was also found to bind to MxA and Mx1[57] as well as viral NP[136] supposedly exerting a chaperone function. The research topics of this thesis were therefore the following: (i) investigation of nuclear MxB on its anti-IAV activity, (ii) characterization of the proposed MxA-NP-UAP56 trimeric complex and (ii) mapping of binding sites in MxA and UAP56 to each other as well as NP.

In the first part of this work (chapter 2) we showed that nuclear MxB potently inhibits IAV replication at a step prior to or at the level of primary transcription. Work presented in the second manuscript (chapter 3) aimed at shedding more light onto the antiviral mechanism of MxA and its effect on the NP-UAP56 complex. We observed no interference of MxA with the translocation of newly synthesized viral NP to the nucleus or with the binding of NP's chaperone UAP56 to NP. Binding strength of a variety of NPs turned out not to correlate with their respective MxA sensitivity. In addition, the binding capacity of MxA to NP is independent of a functioning G-domain and thus not sufficient to exert its antiviral potential. We further found NP residues F412 and R416, which are involved in NP oligomerization, to be crucial for the binding of NP to MxA and UAP56. In the last part (chapter 4) we aimed at mapping the binding sites of MxA and UAP56 to each other and viral NP with the tripartite splitGFP

assay. However, we were only successful to narrow down the region in UAP56, which is involved in its oligomerization.

5.1 The antiviral mechanism of MxA: an initial model

After viral entry, primary transcription and export of the viral mRNA to the cytoplasm translation of viral proteins takes place. NP is one of the viral proteins, which are subsequently needed in the nucleus for viral replication, since it must be added co-transcriptionally to the growing RNA chain[52-54]. It is an RNA-binding protein without sequence requirements[35] and has been shown to interact with the cellular RNA-helicase UAP56 most likely already during translation[29,57]. This interaction is thought to exert a chaperone function on NP and ensure its proper delivery to the vRNA in the nucleus. We further speculated that the chaperone function of UAP56 is crucial to prevent NP from unspecifically binding cellular RNA, since its affinity for RNA is relatively high[34]. Our initial model for the mechanism of action of MxA (graphically summarized in fig. 6.1) described a scenario in which dimeric MxA would either (i) inhibit NP from reaching the nucleus or (ii) bind to NP-UAP56 hetero-oligomers and separate the chaperone from NP. For the latter concept the conserved G-domain in MxA can be neatly explained by the need for structural rearrangements through GTP hydrolysis to achieve a 'power-stroke' similar to the one described for dynamin[197,198]. In both of those scenarios NP would eventually be unavailable for viral replication: in the first case because of the inability to reach its intended destination and in the second scenario because of consequential binding to cellular RNA and thus unavailability for vRNA encapsidation. Higher order oligomers of MxA would represent a pre-active storage form of MxA.

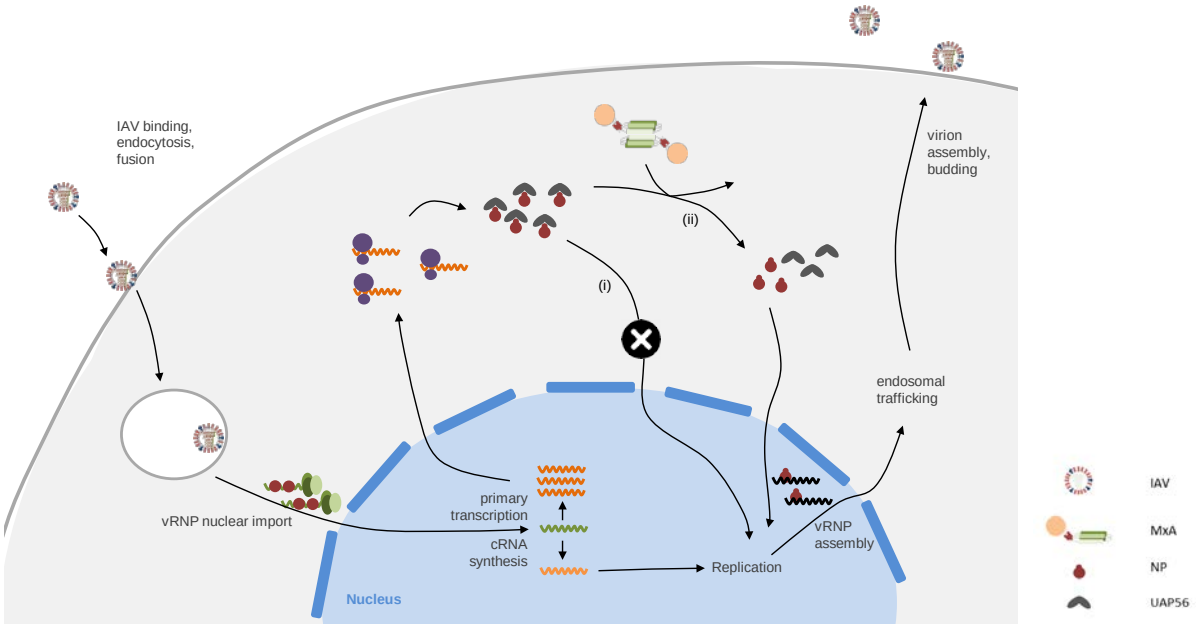

Fig. 6.1. Initial model for the antiviral action of MxA. The model describes two potential mechanism of the anti-IAV activity of MxA: either (i) transport of the UAP56-NP complex to the nucleus is inhibited or (ii) MxA separates NP from its chaperone UAP56 resulting in binding of NP to cellular RNA.

5.2 Adjustments to the model

We showed that MxA does not inhibit translocation of NP from the cytoplasm to the nucleus by a subcellular fractionation approach. Furthermore, NP-UAP56 interaction is undisturbed in the presence of MxA. This suggests that the NP-UAP56 complex does reach the site of viral replication. All the three proteins previously interact with each other in the cytoplasm forming a trimeric complex. We have strong evidence that the site of interaction is the cytoplasm since MxA has never been shown to localize to the nucleus. Furthermore, nuclear forms of Mx (Mx1 and TMxA) proteins interfere with the function of PB2[151,199], which is not seen for MxA[115]. These data thus point towards a more indirect mechanism of MxA to inhibit replication probably through post-translationally modifying NP or UAP56 or both. Alternatively, MxA might induce a transient separation of UAP56 and NP resulting in the binding of NP to cellular RNA.

Furthermore, we cannot exclude the involvement of an additional cellular factor. For human cytomegalovirus it has been shown for example, that the viral regulatory protein pUL69 interacts with UAP56 as well as the cellular protein arginine methyl transferase PRMT6[200]. This interaction resulted in methylation of pUL69. Even though UAP56 and PRMT6 were shown to not directly interact[200], we could envision a similar mechanism for influenza virus

where MxA recruits enzymes that add post-translational modifications (i.e. phosphorylation[41]) or on the contrary remove modifications at defined residues impairing the function of NP or UAP56. It has been shown for instance that acetylation of certain residues in NP is crucial to support viral growth[49]. Phosphorylation at specific residues at the very N-terminus of NP have been shown to impair the binding capacity to importins and thus the import of NP into the nucleus leading to cytoplasmic accumulation of NP[201]. If other residues are phosphorylated, NP loses its ability to oligomerize and vRNP generation is thus impaired. The modification(s) of NP and/or UAP56, which are presumably added in the presence of MxA, have thus to be added at specific residues to lead to the desired effect of viral replication inhibition.

All in all, we propose that the re-localization of the UAP56-NP complex to the nucleus is not perturbed. However, dimeric MxA is likely to destroy the integrity of this complex through the recruitment of a yet unknown factor, which adds post-translational modifications to UAP56, NP or both. These modifications then interfere with the function(s) of UAP56 and/or NP. This is summarized in fig. 6.2. The GTPase activity of MxA could potentially be needed for the recruitment of this additional factor.

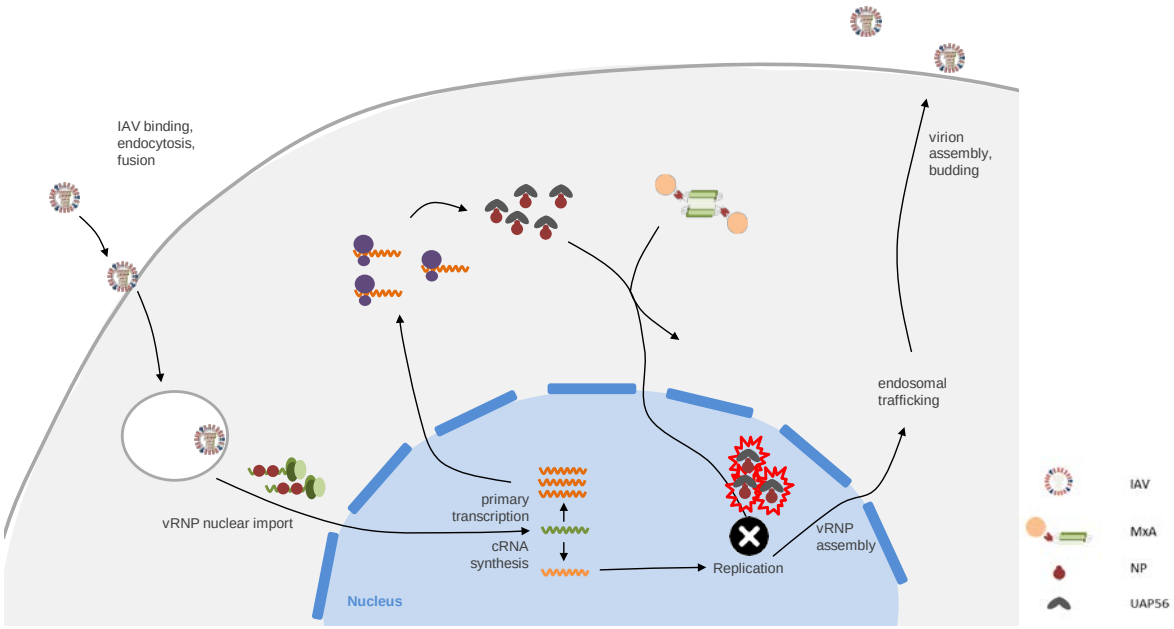

Fig. 6.2. Adjusted model for the antiviral action of MxA. MxA could potentially (with the help of another factor) be involved in the addition of post-translational modifications to the UAP56-NP complex. This renders the complex non-functional.

5.3 Primary transcription: inhibition or not?

Intriguingly, we observed inhibition of viral primary transcription in cells expressing wildtype MxA. Although it has been shown that primary transcription is not affected by MxA[115,117] others have seen that viral transcripts are actually not generated[178]. The assays used in those studies are basically the same, yet the chosen cell lines are different. It is rather doubtful, however, that this explains the seemingly contradictory results. In the case of Thogoto virus, an RNA virus with a segmented ssRNA genome of negative polarity like IAV, MxA interferes with the import of nucleocapsids, which results in the inhibition of primary transcription[175]. UAP56 is thought to function as a chaperone of newly synthesized viral NP and we have previously shown that UAP56 further binds to MxA[57]. UAP56-NP binding, and likely also UAP56-MxA binding, occurs at the step of NP mRNA translation, thus MxA seems to be capable of inhibiting IAV replication at two steps affecting both primary transcription and viral genome replication as previously suggested[122,177]. We could imagine that this is a type of safeguard mechanism of the cell, ensuring that progeny virus formation is indeed inhibited even if MxA fails to inhibit primary transcription of the incoming virus particles.

5.4 Mx proteins and their ability to bind to IAV NP

MxA-sensitivity of a given viral strain is defined through its NP and human IAV strains have evolved their NP to partially escape MxA-restriction. Mutations in only a few specific residues have been shown to greatly affect virus sensitivity to MxA[122,123]. The lack of apparent correlation between virus sensitivity to MxA and NP-MxA binding strength thus came as a surprise to us. We speculated that MxA-sensitivity is rather indirectly determined through UAP56-binding capacities. These UAP56 knock-down data did not clarify the situation, however, since reduced UAP56 levels also negatively affected general protein levels. This is not unexpected, since UAP56 is involved in mRNA export[130,131,181,189,193] and reduced export capacity results in decreased protein production. Also the closely related and partially redundant helicase URH49[189] is likely not able to take over all of the function of UAP56. We were thus unable to resolve the determinants for NP-MxA binding differences. Nevertheless, a common feature to Mx proteins seems to be the oligomeric state in which they bind to NP. The dimeric mutant MxA(R640A), as opposed to tetrameric wildtype MxA, is forming stable complexes with NP as seen in co-IP experiments. There is a tendency of NPs of MxA-resistant IAV strains to bind stronger to MxA than NPs of sensitive strains. This strong binding possibly leads to sequestration of MxA or even inhibition of its “catalytic” activity, allowing the remaining NP to travel safely to the nucleus.

Wildtype MxB, which has been shown to be dimeric[141], also co-precipitated with NP. We further observed binding of TMxB to NP, therefore assuming that TMxB is dimeric as well. When looking at mouse Mx1 it has been shown to bind to IAV NP in vRNPs as well as to NP

only[151]. Analysis of the oligomeric state of Mx1 would thus be of high interest and we would predict it to be dimeric.

5.5 Is there a common antiviral mechanism for all Mx proteins?

Prerequisite for a common mechanism is that Mx proteins have the capacity to bind many different viral structures. Interestingly, so far for none of the target viruses, a binding site on MxA has been determined. It is clear that the L4 loop plays a role for recognizing viral proteins in particular NPs from orthomyxoviruses[99-101]. However, we observed that loop L4 alone is not sufficient for binding and other (carboxy terminal) regions are required. Possibly, Mx proteins recognize a common site on viral proteins that are required for attachment to microtubular intracellular transport mechanisms. Incoming viruses need to transport their capsids vRNPs via microtubular transport processes to their specific site of replication. Mx proteins may interfere with this transport processes. Canine Mx1 has been shown to positively affect the transport of molecules to the apical membrane[202]. VPS1, an Mx-like protein in yeast, was shown to play a crucial role in sorting of soluble vacuolar proteins and the correct organization of intracellular membranes[203].

A common antiviral mechanism would further suggest that Mx proteins, localizing to the same subcellular compartment, should exert similar antiviral activities especially considering the step targeted in the viral life cycle. IAV is thought to be inhibited at two steps of its viral replication cycle: before primary transcription at the step of nuclear translocation of the vRNPs and at a later step after translation by targeting the UAP56-NP complex. MxB was thought not to harbor any anti-IAV function, but we could show that re-located nuclear TMxB potently inhibited IAV replication at the step of primary transcription. This goes in line with data showing that other nuclear Mx proteins, namely mouse Mx1[117] and nuclear MxA (TMxA)[173], abrogate primary transcription as well. Interestingly, in our plaque assay as well as mini replicon assays we observed a slight, but constant decrease of viral replication in the presence of MxB. MxA and MxB do not localize to the same subcellular compartments. MxA as well as a fraction of MxB are present in the cytoplasm, however, MxA has been shown to associate with the smooth ER[102,140]. MxB also associates with the cytoplasmic face of the nuclear envelope. We speculate that the aforementioned weak anti-IAV activity of MxB could be explained by a small fraction of MxB, localizing to the same compartment as MxA. In order to test this hypothesis, MxB re-localization to the same smooth ER sub-compartment as MxA would be needed. The sequence in MxA responsible for smooth ER localization remains elusive[102] though. So far we were not able to confirm this hypothesis with another

approach using a cytoplasmic Mx1 mutant either, due to the fact that this mutation abrogated the antiviral potential of Mx1 in general.

More evidence either for or against a common mechanism is needed. The naturally occurring short isoform of MxB[142], lacking the N-terminal 25 amino acids, loses it perinuclear localization and is only found in the cytoplasm. The pattern of expression is reminiscent of the expression pattern of MxA. This MxB(Δ1-25) mutant might therefore localize to the same subcellular compartment as MxA and possibly restrict IAV replication.

5.6 Outlook

Mx proteins are very similar in structure yet they seem quite different in their antiviral activities. Various pieces of evidence now point towards a general mechanism of action. However, there are still a few big gaps in our knowledge about Mx proteins for instance about the function of the GTPase activity or how exactly Mx proteins inhibit viruses in the cytoplasmic and nuclear compartments. The long held fascination for Mx proteins is far from ceasing and there are still many mysteries to be unraveled.

Acknowledgements

I wish to thank PD Dr. Jovan Pavlovic for his supervision of and motivation for my PhD project. His conversational nature was also highly valued outside of the lab.
Many thanks also go to Prof. Dr. Silke Stertz, who provided invaluable scientific support and Prof. Dr. Alexandra Trkola, head of the Institute of Medical Virology, to give me the opportunity to work in this thriving institute. I thank Prof. Dr. Cornel Fraefel and Prof. Dr. Peter Stäheli, for their highly appreciated ideas and comments during discussions at committee meetings.

I am very grateful to Michel Crameri, whose scientific input was highly appreciated and whose company was greatly enjoyed in the lab as well as beyond.

I owe many thanks to Stefan Spirig, a very talented Master student, with whom I discussed every aspect of my project whenever new ideas were needed and who was also a great help hands-on in the lab.

Patricia Nigg introduced me to the lab and was a great help in my first few weeks and months not only scientifically but also making me feel welcome in the research group. Eva Moritz, our valued lab technician, who lent a helping hand whenever needed, and Raphael Walker and Dominik Müller, past members of the Pavlovic group, completed the nice working atmosphere.

Special thanks go to Eva Spieler, Annika Hunziker and Sira Günther, together with me called “Team red”, who were always up for singing a song or performing a nice dance inside or outside of the lab. I found three irreplaceable friends and lab work was so much more fun with Team red in action!

Additionally, the relaxed but still stimulating atmosphere in our institute created by all its members made me feel at ease and I always looked forward to the next working day.

Lastly and most importantly I thank my parents Heidi Waser and Robert Steiner, my stepmother Béatrice Steiner and my brother Dominik Steiner for their immense support. Being part of such a lovely family is an invaluable gift!

References

1 Barry, J. M. The site of origin of the 1918 influenza pandemic and its public health implications. *Journal of Translational medicine* **2**, 3 (2004).

2 Taubenberger, J. K. & Kash, J. C. Influenza Virus Evolution, Host Adaptation, and Pandemic Formation. *Cell Host & Microbe* **7**, 440-451, doi:10.1016/j.chom.2010.05.009 (2010).

3 Taubenberger, J. K. & Morens, D. M. The Pathology of Influenza Virus Infections. 28 (2008).

4 van Dijk, J. G. B., Verhagen, J. H., Wille, M. & Waldenström, J. Host and virus ecology as determinants of influenza A virus transmission in wild birds. *Current Opinion in Virology* **28**, 26-36, doi:10.1016/j.coviro.2017.10.006 (2018).

5 Boivin, S., Cusack, S., Ruigrok, R. W. & Hart, D. J. Influenza A virus polymerase: structural insights into replication and host adaptation mechanisms. *The Journal of biological chemistry* **285**, 28411-28417, doi:10.1074/jbc.R110.117531 (2010).

6 Steel, J. & Lowen, A. C. Influenza A virus reassortment. *Current topics in microbiology and immunology* **385**, 377-401, doi:10.1007/82_2014_395 (2014).

7 Schrauwen, E. J. & Fouchier, R. A. Host adaptation and transmission of influenza A viruses in mammals. *Emerging microbes & infections* **3**, e9, doi:10.1038/emi.2014.9 (2014).

8 Bouvier, N. M. & Palese, P. The biology of influenza viruses. *Vaccine* **26**, D49-D53 (2008).

9 Tong, S. *et al.* A distinct lineage of influenza A virus from bats. *Proceedings of the National Academy of Sciences* **109**, 4269-4274, doi:10.1073/pnas.1116200109 (2012).

10 Tong, S. *et al.* New World Bats Harbor Diverse Influenza A Viruses. *PLoS Pathogens* **9**, e1003657, doi:10.1371/journal.ppat.1003657 (2013).

11 Wise, H. M. *et al.* Identification of a Novel Splice Variant Form of the Influenza A Virus M2 Ion Channel with an Antigenically Distinct Ectodomain. *PLoS Pathogens* **8**, e1002998, doi:10.1371/journal.ppat.1002998 (2012).

12 Muramoto, Y., Noda, T., Kawakami, E., Akkina, R. & Kawaoka, Y. Identification of novel influenza A virus proteins translated from PA mRNA. *Journal of virology* **87**, 2455-2462, doi:10.1128/JVI.02656-12 (2013).

13 Yamayoshi, S., Watanabe, M., Goto, H. & Kawaoka, Y. Identification of a Novel Viral Protein Expressed from the PB2 Segment of Influenza A Virus. *Journal of virology* **90**, 444-456, doi:10.1128/JVI.02175-15 (2016).

14 Hale, B. G., Randall, R. E., Ortin, J. & Jackson, D. The multifunctional NS1 protein of influenza A viruses. *Journal of General Virology* **89**, 2359-2376, doi:10.1099/vir.0.2008/004606-0 (2008).

15 Nemeroff, M. E., Barabino, S. M., Li, Y., Keller, W. & Krug, R. M. Influenza virus NS1 protein interacts with the cellular 30 kDa subunit of CPSF and inhibits 3'end formation of cellular pre-mRNAs. *Mol Cell* **1**, 991-1000 (1998).

16 Chen, Z., Li, Y. & Krug, R. M. Influenza A virus NS1 protein targets poly(A)-binding protein II of the cellular 3'-end processing machinery. *The EMBO journal* **18**, 2273-2283, doi:10.1093/emboj/18.8.2273 (1999).

17 Burgui, I., Aragon, T., Ortin, J. & Nieto, A. PABP1 and eIF4GI associate with influenza virus NS1 protein in viral mRNA translation initiation complexes. *The Journal of general virology* **84**, 3263-3274, doi:10.1099/vir.0.19487-0 (2003).

18 Chua, Mark A., Schmid, S., Perez, Jasmine T., Langlois, Ryan A. & tenOever, Benjamin R. Influenza A Virus Utilizes Suboptimal Splicing to Coordinate the Timing of Infection. *Cell Reports* **3**, 23-29, doi:10.1016/j.celrep.2012.12.010 (2013).

19 Buehler, J. *et al.* Influenza A Virus PB1-F2 Protein Expression Is Regulated in a Strain-Specific Manner by Sequences Located Downstream of the PB1-F2 Initiation Codon. *Journal of virology* **87**, 10687-10699, doi:10.1128/jvi.01520-13 (2013).
20 Tauber, S., Ligertwood, Y., Quigg-Nicol, M., Dutia, B. M. & Elliott, R. M. Behaviour of influenza A viruses differentially expressing segment 2 gene products in vitro and in vivo. *The Journal of general virology* **93**, 840-849, doi:10.1099/vir.0.039966-0 (2012).
21 Bavagnoli, L. *et al.* The novel influenza A virus protein PA-X and its naturally deleted variant show different enzymatic properties in comparison to the viral endonuclease PA. *Nucleic Acids Research* **43**, 9405-9417, doi:10.1093/nar/gkv926 (2015).
22 Hayashi, T., MacDonald, L. A. & Takimoto, T. Influenza A Virus Protein PA-X Contributes to Viral Growth and Suppression of the Host Antiviral and Immune Responses. *Journal of virology* **89**, 6442-6452, doi:10.1128/JVI.00319-15 (2015).
23 Jagger, B. W. *et al.* An overlapping protein-coding region in influenza A virus segment 3 modulates the host response. *Science* **337**, 199-204, doi:10.1126/science.1222213 (2012).
24 Rogers, G. N. & Paulson, J. C. Receptor determinants of human and animal influenza virus isolates: Differences in receptor specificity of the H3 hemagglutinin based on species of origin. *Virology* **127**, 361-373, doi:10.1016/0042-6822(83)90150-2 (1983).
25 O'Connor, A. M., Pennie, R. A. & Dales, R. E. Framing effects on expectations, decisions, and side effects experienced: The case of influenza immunization. *Journal of Clinical Epidemiology* **49**, 1271-1276, doi:10.1016/s0895-4356(96)00177-1 (1996).
26 van Riel, D. *et al.* Human and avian influenza viruses target different cells in the lower respiratory tract of humans and other mammals. *The American journal of pathology* **171**, 1215-1223, doi:10.2353/ajpath.2007.070248 (2007).
27 Watanabe, T., Watanabe, S. & Kawaoka, Y. Cellular Networks Involved in the Influenza Virus Life Cycle. *Cell Host & Microbe* **7**, 427-439, doi:10.1016/j.chom.2010.05.008 (2010).
28 Mair, C. M., Ludwig, K., Herrmann, A. & Sieben, C. Receptor binding and pH stability — How influenza A virus hemagglutinin affects host-specific virus infection. *Biochimica et Biophysica Acta (BBA) - Biomembranes* **1838**, 1153-1168, doi:10.1016/j.bbamem.2013.10.004 (2014).
29 Kawaguchi, A., Momose, F. & Nagata, K. Replication-Coupled and Host Factor-Mediated Encapsidation of the Influenza Virus Genome by Viral Nucleoprotein. *Journal of virology* **85**, 6197-6204, doi:10.1128/jvi.00277-11 (2011).
30 Ohkura, T., Momose, F., Ichikawa, R., Takeuchi, K. & Morikawa, Y. Influenza A Virus Hemagglutinin and Neuraminidase Mutually Accelerate Their Apical Targeting through Clustering of Lipid Rafts. *Journal of virology* **88**, 10039-10055, doi:10.1128/jvi.00586-14 (2014).
31 Lakdawala, S. S., Fodor, E. & Subbarao, K. Moving On Out: Transport and Packaging of Influenza Viral RNA into Virions. *Annual Review of Virology* **3**, 411-427, doi:10.1146/annurev-virology-110615-042345 (2016).
32 Min, J. Y. & Subbarao, K. Cellular targets for influenza drugs. *Nature biotechnology* **28**, 239-240, doi:10.1038/nbt0310-239 (2010).
33 Hussain, M., Galvin, H. D., Haw, T. Y., Nutsford, A. N. & Husain, M. Drug resistance in influenza A virus: the epidemiology and management. *Infection and drug resistance* **10**, 121-134, doi:10.2147/IDR.S105473 (2017).
34 Yamanaka, K., Ishihama, A. & Nagata, K. Reconstitution of influenza virus RNA-nucleoprotein complexes structurally resembling native viral ribonucleoprotein cores. *The Journal of biological chemistry* **265**, 11151-11155 (1990).
35 Baudin, F., Bach, C., Cusack, S. & Ruigrok, R. W. Structure of influenza virus RNP. I. Influenza virus nucleoprotein melts secondary structure in panhandle RNA and exposes the bases to the solvent. *The EMBO journal* **13**, 3158-3165 (1994).
36 Biswas, S. K., Boutz, P. L. & Nayak, D. P. Influenza virus nucleoprotein interacts with influenza virus polymerase proteins. *Journal of virology* **72**, 5493-5501 (1998).

37 Martin-Benito, J. *et al.* Three-dimensional reconstruction of a recombinant influenza virus ribonucleoprotein particle. *EMBO reports* **2**, 313-317, doi:10.1093/embo-reports/kve063 (2001).
38 Wu, W. W., Sun, Y. H. & Pante, N. Nuclear import of influenza A viral ribonucleoprotein complexes is mediated by two nuclear localization sequences on viral nucleoprotein. *Virology journal* **4**, 49, doi:10.1186/1743-422X-4-49 (2007).
39 O'Neill, R. E., Jaskunas, R., Blobel, G., Palese, P. & Moroianu, J. Nuclear import of influenza virus RNA can be mediated by viral nucleoprotein and transport factors required for protein import. *The Journal of biological chemistry* **270**, 22701-22704 (1995).
40 Vreede, F. T., Jung, T. E. & Brownlee, G. G. Model suggesting that replication of influenza virus is regulated by stabilization of replicative intermediates. *Journal of virology* **78**, 9568-9572, doi:10.1128/JVI.78.17.9568-9572.2004 (2004).
41 Mondal, A., Potts, G. K., Dawson, A. R., Coon, J. J. & Mehle, A. Phosphorylation at the homotypic interface regulates nucleoprotein oligomerization and assembly of the influenza virus replication machinery. *PLoS Pathog* **11**, e1004826, doi:10.1371/journal.ppat.1004826 (2015).
42 Moeller, A., Kirchdoerfer, R. N., Potter, C. S., Carragher, B. & Wilson, I. A. Organization of the influenza virus replication machinery. *Science* **338**, 1631-1634, doi:10.1126/science.1227270 (2012).
43 Honda, A., Ueda, K., Nagata, K. & Ishihama, A. RNA polymerase of influenza virus: role of NP in RNA chain elongation. *Journal of biochemistry* **104**, 1021-1026 (1988).
44 Elton, D. *et al.* Interaction of the influenza virus nucleoprotein with the cellular CRM1-mediated nuclear export pathway. *Journal of virology* **75**, 408-419, doi:10.1128/JVI.75.1.408-419.2001 (2001).
45 Moreira, E. A. *et al.* A conserved influenza A virus nucleoprotein code controls specific viral genome packaging. *Nat Commun* **7**, 12861, doi:10.1038/ncomms12861 (2016).
46 Turrell, L., Hutchinson, E. C., Vreede, F. T. & Fodor, E. Regulation of Influenza A Virus Nucleoprotein Oligomerization by Phosphorylation. *Journal of virology* **89**, 1452-1455, doi:10.1128/jvi.02332-14 (2015).
47 Han, Q. *et al.* Sumoylation of influenza A virus nucleoprotein is essential for intracellular trafficking and virus growth. *Journal of virology* **88**, 9379-9390, doi:10.1128/JVI.00509-14 (2014).
48 Liao, T. L., Wu, C. Y., Su, W. C., Jeng, K. S. & Lai, M. M. Ubiquitination and deubiquitination of NP protein regulates influenza A virus RNA replication. *The EMBO journal* **29**, 3879-3890, doi:10.1038/emboj.2010.250 (2010).
49 Giese, S. *et al.* Role of influenza A virus NP acetylation on viral growth and replication. *Nat Commun* **8**, 1259, doi:10.1038/s41467-017-01112-3 (2017).
50 Ye, Q., Krug, R. M. & Tao, Y. J. The mechanism by which influenza A virus nucleoprotein forms oligomers and binds RNA. *Nature* **444**, 1078-1082, doi:10.1038/nature05379 (2006).
51 Ng, A. K. L. *et al.* Structure of the influenza virus A H5N1 nucleoprotein: implications for RNA binding, oligomerization, and vaccine design. *The FASEB Journal* **22**, 3638-3647, doi:10.1096/fj.08-112110 (2008).
52 Chan, W. H. *et al.* Functional Analysis of the Influenza Virus H5N1 Nucleoprotein Tail Loop Reveals Amino Acids That Are Crucial for Oligomerization and Ribonucleoprotein Activities. *Journal of virology* **84**, 7337-7345, doi:10.1128/jvi.02474-09 (2010).
53 Turrell, L., Lyall, J. W., Tiley, L. S., Fodor, E. & Vreede, F. T. The role and assembly mechanism of nucleoprotein in influenza A virus ribonucleoprotein complexes. *Nature Communications* **4**, 1591, doi:10.1038/ncomms2589 (2013).
54 Elton, D., Medcalf, E., Bishop, K. & Digard, P. Oligomerization of the influenza virus nucleoprotein: identification of positive and negative sequence elements. *Virology* **260**, 190-200, doi:10.1006/viro.1999.9818 (1999).

55 Chenavas, S. *et al.* Monomeric Nucleoprotein of Influenza A Virus. *PLoS Pathogens* **9**, e1003275, doi:10.1371/journal.ppat.1003275 (2013).
56 Tarus, B. *et al.* Oligomerization paths of the nucleoprotein of influenza A virus. *Biochimie* **94**, 776-785, doi:10.1016/j.biochi.2011.11.009 (2012).
57 Wisskirchen, C., Ludersdorfer, T. H., Muller, D. A., Moritz, E. & Pavlovic, J. Interferon-induced antiviral protein MxA interacts with the cellular RNA helicases UAP56 and URH49. *The Journal of biological chemistry* **286**, 34743-34751, doi:10.1074/jbc.M111.251843 (2011).
58 Shen, Y. F. *et al.* E339...R416 salt bridge of nucleoprotein as a feasible target for influenza virus inhibitors. *Proc Natl Acad Sci U S A* **108**, 16515-16520, doi:10.1073/pnas.1113107108 (2011).
59 Killip, M. J., Fodor, E. & Randall, R. E. Influenza virus activation of the interferon system. *Virus Research*, doi:10.1016/j.virusres.2015.02.003 (2015).
60 Yoo, J.-S., Kato, H. & Fujita, T. Sensing viral invasion by RIG-I like receptors. *Current Opinion in Microbiology* **20**, 131-138, doi:10.1016/j.mib.2014.05.011 (2014).
61 Hedayat, M., Netea, M. G. & Rezaei, N. Targeting of Toll-like receptors: a decade of progress in combating infectious diseases. *The Lancet Infectious Diseases* **11**, 702-712, doi:10.1016/s1473-3099(11)70099-8 (2011).
62 Takeuchi, O. & Akira, S. Innate immunity to virus infection. *Immunological Reviews* **227**, 75-86, doi:10.1111/j.1600-065X.2008.00737.x (2009).
63 Weber, M. *et al.* Influenza Virus Adaptation PB2-627K Modulates Nucleocapsid Inhibition by the Pathogen Sensor RIG-I. *Cell Host & Microbe* **17**, 309-319, doi:10.1016/j.chom.2015.01.005 (2015).
64 Lee, N. *et al.* Role of human Toll-like receptors in naturally occurring influenza A infections. *Influenza and Other Respiratory Viruses* **7**, 666-675, doi:10.1111/irv.12109 (2013).
65 Syedbasha, M. & Egli, A. Interferon Lambda: Modulating Immunity in Infectious Diseases. *Frontiers in Immunology* **8**, doi:10.3389/fimmu.2017.00119 (2017).
66 Raftery, N. & Stevenson, N. J. Advances in anti-viral immune defence: revealing the importance of the IFN JAK/STAT pathway. *Cellular and Molecular Life Sciences* **74**, 2525-2535, doi:10.1007/s00018-017-2520-2 (2017).
67 Meurs, E. *et al.* Molecular cloning and characterization of the human double-stranded RNA-activated protein kinase induced by interferon. *Cell* **62**, 379-390 (1990).
68 Galabru, J. & Hovanessian, A. Autophosphorylation of the protein kinase dependent on double-stranded RNA. *The Journal of biological chemistry* **262**, 15538-15544 (1987).
69 Li, S., Min, J. Y., Krug, R. M. & Sen, G. C. Binding of the influenza A virus NS1 protein to PKR mediates the inhibition of its activation by either PACT or double-stranded RNA. *Virology* **349**, 13-21, doi:10.1016/j.virol.2006.01.005 (2006).
70 Gale, M., Jr. & Katze, M. G. Molecular mechanisms of interferon resistance mediated by viral-directed inhibition of PKR, the interferon-induced protein kinase. *Pharmacology & therapeutics* **78**, 29-46 (1998).
71 Samuel, C. E. Host genetic variability and West Nile virus susceptibility. *Proc Natl Acad Sci U S A* **99**, 11555-11557, doi:10.1073/pnas.202448899 (2002).
72 Chakrabarti, A., Jha, B. K. & Silverman, R. H. New insights into the role of RNase L in innate immunity. *Journal of interferon & cytokine research : the official journal of the International Society for Interferon and Cytokine Research* **31**, 49-57, doi:10.1089/jir.2010.0120 (2011).
73 Chakrabarti, A. *et al.* RNase L activates the NLRP3 inflammasome during viral infections. *Cell Host Microbe* **17**, 466-477, doi:10.1016/j.chom.2015.02.010 (2015).
74 Chakrabarti, A., Ghosh, P. K., Banerjee, S., Gaughan, C. & Silverman, R. H. RNase L triggers autophagy in response to viral infections. *Journal of virology* **86**, 11311-11321, doi:10.1128/JVI.00270-12 (2012).
75 Zhou, A. *et al.* Interferon action and apoptosis are defective in mice devoid of 2',5'-oligoadenylate-dependent RNase L. *The EMBO journal* **16**, 6355-6363, doi:10.1093/emboj/16.21.6355 (1997).

76 Bailey, C. C., Zhong, G., Huang, I. C. & Farzan, M. IFITM-Family Proteins: The Cell's First Line of Antiviral Defense. *Annu Rev Virol* **1**, 261-283, doi:10.1146/annurev-virology-031413-085537 (2014).
77 Brass, A. L. *et al.* The IFITM proteins mediate cellular resistance to influenza A H1N1 virus, West Nile virus, and dengue virus. *Cell* **139**, 1243-1254, doi:10.1016/j.cell.2009.12.017 (2009).
78 Li, K. *et al.* IFITM proteins restrict viral membrane hemifusion. *PLoS Pathog* **9**, e1003124, doi:10.1371/journal.ppat.1003124 (2013).
79 Diamond, M. S. & Farzan, M. The broad-spectrum antiviral functions of IFIT and IFITM proteins. *Nature reviews. Immunology* **13**, 46-57, doi:10.1038/nri3344 (2013).
80 Compton, A. A. *et al.* IFITM proteins incorporated into HIV-1 virions impair viral fusion and spread. *Cell Host Microbe* **16**, 736-747, doi:10.1016/j.chom.2014.11.001 (2014).
81 Tartour, K. *et al.* IFITM proteins are incorporated onto HIV-1 virion particles and negatively imprint their infectivity. *Retrovirology* **11**, 103, doi:10.1186/s12977-014-0103-y (2014).
82 Yu, J. *et al.* IFITM Proteins Restrict HIV-1 Infection by Antagonizing the Envelope Glycoprotein. *Cell Rep* **13**, 145-156, doi:10.1016/j.celrep.2015.08.055 (2015).
83 Pichlmair, A. *et al.* RIG-I-Mediated Antiviral Responses to Single-Stranded RNA Bearing 5'-Phosphates. *Science* **314**, 997-1001, doi:10.1126/science.1132998 (2006).
84 Mibayashi, M. *et al.* Inhibition of Retinoic Acid-Inducible Gene I-Mediated Induction of Beta Interferon by the NS1 Protein of Influenza A Virus. *Journal of virology* **81**, 514-524, doi:10.1128/jvi.01265-06 (2007).
85 Kochs, G., Garcia-Sastre, A. & Martinez-Sobrido, L. Multiple Anti-Interferon Actions of the Influenza A Virus NS1 Protein. *Journal of virology* **81**, 7011-7021, doi:10.1128/jvi.02581-06 (2007).
86 Leung, D. W., Basler, C. F. & Amarasinghe, G. K. Molecular mechanisms of viral inhibitors of RIG-I-like receptors. *Trends in Microbiology* **20**, 139-146, doi:10.1016/j.tim.2011.12.005 (2012).
87 Donelan, N. R., Basler, C. F. & Garcia-Sastre, A. A Recombinant Influenza A Virus Expressing an RNA-Binding-Defective NS1 Protein Induces High Levels of Beta Interferon and Is Attenuated in Mice. *Journal of virology* **77**, 13257-13266, doi:10.1128/jvi.77.24.13257-13266.2003 (2003).
88 Talon, J. *et al.* Activation of Interferon Regulatory Factor 3 Is Inhibited by the Influenza A Virus NS1 Protein. *Journal of virology* **74**, 7989-7996, doi:10.1128/jvi.74.17.7989-7996.2000 (2000).
89 Liedmann, S. *et al.* Viral suppressors of the RIG-I-mediated interferon response are pre-packaged in influenza virions. *Nature Communications* **5**, 5645, doi:10.1038/ncomms6645 (2014).
90 Min, J. Y. & Krug, R. M. The primary function of RNA binding by the influenza A virus NS1 protein in infected cells: Inhibiting the 2'-5' oligo (A) synthetase/RNase L pathway. *Proc Natl Acad Sci U S A* **103**, 7100-7105, doi:10.1073/pnas.0602184103 (2006).
91 Min, J. Y., Li, S., Sen, G. C. & Krug, R. M. A site on the influenza A virus NS1 protein mediates both inhibition of PKR activation and temporal regulation of viral RNA synthesis. *Virology* **363**, 236-243, doi:10.1016/j.virol.2007.01.038 (2007).
92 Lindenmann, J. Resistance of mice to mouse-adapted influenza A virus. *Virology*, 203-204 (1962).
93 Staeheli, P., Haller, O., Boll, W., Lindenmann, J. & Weissmann, C. (Cell, 1986).
94 Haller, O. Dynamins Are Forever: MxB Inhibits HIV-1. *Cell Host & Microbe* **14**, 371-373, doi:10.1016/j.chom.2013.10.002 (2013).
95 Verhelst, J., Hulpiau, P. & Saelens, X. Mx Proteins: Antiviral Gatekeepers That Restrain the Uninvited. *Microbiology and Molecular Biology Reviews* **77**, 551-566, doi:10.1128/mmbr.00024-13 (2013).

96 Haller, O., Staeheli, P., Schwemmle, M. & Kochs, G. Mx GTPases: dynamin-like antiviral machines of innate immunity. *Trends in Microbiology*, doi:10.1016/j.tim.2014.12.003 (2015).
97 Ford, M. G. J., Jenni, S. & Nunnari, J. The crystal structure of dynamin. *Nature* **477**, 561-566, doi:10.1038/nature10441 (2011).
98 Gao, S. *et al.* Structure of myxovirus resistance protein a reveals intra- and intermolecular domain interactions required for the antiviral function. *Immunity* **35**, 514-525, doi:10.1016/j.immuni.2011.07.012 (2011).
99 Mitchell, Patrick S. *et al.* Evolution-Guided Identification of Antiviral Specificity Determinants in the Broadly Acting Interferon-Induced Innate Immunity Factor MxA. *Cell Host & Microbe* **12**, 598-604, doi:10.1016/j.chom.2012.09.005 (2012).
100 Patzina, C., Haller, O. & Kochs, G. Structural Requirements for the Antiviral Activity of the Human MxA Protein against Thogoto and Influenza A Virus. *Journal of Biological Chemistry* **289**, 6020-6027, doi:10.1074/jbc.M113.543892 (2014).
101 Verhelst, J. *et al.* Functional Comparison of Mx1 from Two Different Mouse Species Reveals the Involvement of Loop L4 in the Antiviral Activity against Influenza A Viruses. *Journal of virology* **89**, 10879-10890, doi:10.1128/jvi.01744-15 (2015).
102 Stertz, S. *et al.* Interferon-induced, antiviral human MxA protein localizes to a distinct subcompartment of the smooth endoplasmic reticulum. *Journal of interferon & cytokine research* **26**, 650-660 (2006).
103 Engelhardt, O. G., Ullrich, E., Kochs, G. & Haller, O. Interferon-Induced Antiviral Mx1 GTPase Is Associated with Components of the SUMO-1 System and Promyelocytic Leukemia Protein Nuclear Bodies. *Experimental Cell Research* **271**, 286-295, doi:10.1006/excr.2001.5380 (2001).
104 Lallemand-Breitenbach, V. & de The, H. PML nuclear bodies. *Cold Spring Harbor perspectives in biology* **2**, a000661, doi:10.1101/cshperspect.a000661 (2010).
105 Bernardi, R. & Pandolfi, P. P. Structure, dynamics and functions of promyelocytic leukaemia nuclear bodies. *Nature reviews. Molecular cell biology* **8**, 1006-1016, doi:10.1038/nrm2277 (2007).
106 Bernardi, R., Papa, A. & Pandolfi, P. P. Regulation of apoptosis by PML and the PML-NBs. *Oncogene* **27**, 6299-6312, doi:10.1038/onc.2008.305 (2008).
107 Everett, R. D., Parada, C., Gripon, P., Sirma, H. & Orr, A. Replication of ICP0-null mutant herpes simplex virus type 1 is restricted by both PML and Sp100. *Journal of virology* **82**, 2661-2672, doi:10.1128/JVI.02308-07 (2008).
108 Everett, R. D. *et al.* PML contributes to a cellular mechanism of repression of herpes simplex virus type 1 infection that is inactivated by ICP0. *Journal of virology* **80**, 7995-8005, doi:10.1128/JVI.00734-06 (2006).
109 Tavalai, N., Papior, P., Rechter, S., Leis, M. & Stamminger, T. Evidence for a role of the cellular ND10 protein PML in mediating intrinsic immunity against human cytomegalovirus infections. *Journal of virology* **80**, 8006-8018, doi:10.1128/JVI.00743-06 (2006).
110 Landis, H. *et al.* Human MxA Protein Confers Resistance to Semliki Forest Virus and Inhibits the Amplification of a Semliki Forest Virus-Based Replicon in the Absence of Viral Structural Proteins. *J. VIROL.* **72**, 7 (1998).
111 Gordien, E. *et al.* Inhibition of Hepatitis B Virus Replication by the Interferon-Inducible MxA Protein. *Journal of virology* **75**, 2684-2691, doi:10.1128/jvi.75.6.2684-2691.2001 (2001).
112 Haller, O. & Kochs, G. Human MxA Protein: An Interferon-Induced Dynamin-Like GTPase with Broad Antiviral Activity. *Journal of Interferon & Cytokine Research* **31**, 79-87, doi:10.1089/jir.2010.0076 (2011).
113 Goujon, C. *et al.* Human MX2 is an interferon-induced post-entry inhibitor of HIV-1 infection. *Nature* **502**, 559-562, doi:10.1038/nature12542 (2013).
114 Crameri, M. *et al.* MxB is an interferon-induced restriction factor of human herpesviruses. *Nat Commun* **9**, 1980, doi:10.1038/s41467-018-04379-2 (2018).

115 Nigg, P. E. & Pavlovic, J. Oligomerization and GTP-binding Requirements of MxA for Viral Target Recognition and Antiviral Activity against Influenza A Virus. *Journal of Biological Chemistry* **290**, 29893-29906, doi:10.1074/jbc.M115.681494 (2015).
116 von der Malsburg, A., Abutbul-Ionita, I., Haller, O., Kochs, G. & Danino, D. Stalk Domain of the Dynamin-like MxA GTPase Protein Mediates Membrane Binding and Liposome Tubulation via the Unstructured L4 Loop. *Journal of Biological Chemistry* **286**, 37858-37865, doi:10.1074/jbc.M111.249037 (2011).
117 Pavlovic, J., Haller, O. & Staeheli, P. Human and mouse Mx proteins inhibit different steps of the influenza virus multiplication cycle. *Journal of virology* **66**, 2564-2569 (1992).
118 Kochs, G., Janzen, C., Hohenberg, H. & Haller, O. Antivirally active MxA protein sequesters La Crosse virus nucleocapsid protein into perinuclear complexes. *Proceedings of the National Academy of Sciences* **99**, 3153-3158, doi:10.1073/pnas.052430399 (2002).
119 Reichelt, M., Stertz, S., Krijnse-Locker, J., Haller, O. & Kochs, G. Missorting of LaCrosse Virus Nucleocapsid Protein by the Interferon-Induced MxA GTPase Involves Smooth ER Membranes: Membrane Association of Antivirally Active MxA GTPase. *Traffic* **5**, 772-784, doi:10.1111/j.1600-0854.2004.00219.x (2004).
120 Zurcher, T., Pavlovic, J. & Staeheli, P. Mechanism of human MxA protein action: variants with changed antiviral properties. 5.
121 Dittmann, J. *et al.* Influenza A Virus Strains Differ in Sensitivity to the Antiviral Action of Mx-GTPase. *Journal of virology* **82**, 3624-3631, doi:10.1128/jvi.01753-07 (2008).
122 Mänz, B. *et al.* Pandemic Influenza A Viruses Escape from Restriction by Human MxA through Adaptive Mutations in the Nucleoprotein. *PLoS Pathogens* **9**, e1003279, doi:10.1371/journal.ppat.1003279 (2013).
123 Zimmermann, P., Manz, B., Haller, O., Schwemmle, M. & Kochs, G. The Viral Nucleoprotein Determines Mx Sensitivity of Influenza A Viruses. *Journal of virology* **85**, 8133-8140, doi:10.1128/jvi.00712-11 (2011).
124 Goujon, C. *et al.* Transfer of the Amino-Terminal Nuclear Envelope Targeting Domain of Human MX2 Converts MX1 into an HIV-1 Resistance Factor. *Journal of virology* **88**, 9017-9026, doi:10.1128/jvi.01269-14 (2014).
125 Cordin, O., Banroques, J., Tanner, N. K. & Linder, P. The DEAD-box protein family of RNA helicases. *Gene* **367**, 17-37, doi:10.1016/j.gene.2005.10.019 (2006).
126 Linder, P. & Jankowsky, E. From unwinding to clamping — the DEAD box RNA helicase family. *Nature Reviews Molecular Cell Biology* **12**, 505-516, doi:10.1038/nrm3154 (2011).
127 Jarmoskaite, I. & Russell, R. DEAD-box proteins as RNA helicases and chaperones: DEAD-box proteins. *Wiley Interdisciplinary Reviews: RNA* **2**, 135-152, doi:10.1002/wrna.50 (2011).
128 Thomas, M., Lischka, P., Müller, R. & Stamminger, T. The Cellular DExD/H-Box RNA-Helicases UAP56 and URH49 Exhibit a CRM1-Independent Nucleocytoplasmic Shuttling Activity. *PLoS ONE* **6**, e22671, doi:10.1371/journal.pone.0022671 (2011).
129 Viphakone, N. *et al.* TREX exposes the RNA-binding domain of Nxf1 to enable mRNA export. *Nature Communications* **3**, doi:10.1038/ncomms2005 (2012).
130 Robin Reed, M.-J. L. Pre-mRNA splicing and mRNA export linked by direct interactions between UAP56 and Aly. *Nature* **413**, 644-647 (2001).
131 Shi, H., Cordin, O., Minder, C. M., Linder, P. & Xu, R.-M. Crystal structure of the human ATP-dependent splicing and export factor UAP56. *Proceedings of the National Academy of Sciences of the United States of America* **101**, 17628-17633 (2004).
132 Pryor, A. Growth-regulated expression and G0-specific turnover of the mRNA that encodes URH49, a mammalian DExH/D box protein that is highly related to the mRNA export protein UAP56. *Nucleic Acids Research* **32**, 1857-1865, doi:10.1093/nar/gkh347 (2004).
133 Wisskirchen, C., Ludersdorfer, T. H., Muller, D. A., Moritz, E. & Pavlovic, J. The Cellular RNA Helicase UAP56 Is Required for Prevention of Double-Stranded RNA

Formation during Influenza A Virus Infection. *Journal of virology* **85**, 8646-8655, doi:10.1128/jvi.02559-10 (2011).
134 Read, E. K. C. & Digard, P. Individual influenza A virus mRNAs show differential dependence on cellular NXF1/TAP for their nuclear export. *Journal of General Virology* **91**, 1290-1301, doi:10.1099/vir.0.018564-0 (2010).
135 Dornfeld, D. *et al.* SMARCA2-regulated host cell factors are required for MxA restriction of influenza A viruses. *Sci Rep* **8**, 2092, doi:10.1038/s41598-018-20458-2 (2018).
136 Momose, F. *et al.* Cellular splicing factor RAF-2p48/NPI-5/BAT1/UAP56 interacts with the influenza virus nucleoprotein and enhances viral RNA synthesis. *Journal of virology* **75**, 1899-1908, doi:10.1128/JVI.75.4.1899-1908.2001 (2001).
137 Hu, Y., Gor, V., Morikawa, K., Nagata, K. & Kawaguchi, A. Cellular splicing factor UAP56 stimulates trimeric NP formation for assembly of functional influenza viral ribonucleoprotein complexes. *Scientific Reports* **7**, doi:10.1038/s41598-017-13784-4 (2017).
138 Pavlovic, J., Zürcher, T., Haller, O. & Staeheli, P. Resistance to Influenza Virus and Vesicular Stomatitis Virus Conferred by Expression of Human MxA Protein. *J. VIROL.* **64**, 6 (2018).
139 Zürcher, T., Pavlovic, J. & Staeheli, P. Nuclear localization of mouse Mx1 protein is necessary for inhibition of influenza virus. *Journal of virology* **66**, 5059-5066 (1992).
140 Accola, M. A. The Antiviral Dynamin Family Member, MxA, Tubulates Lipids and Localizes to the Smooth Endoplasmic Reticulum. *Journal of Biological Chemistry* **277**, 21829-21835, doi:10.1074/jbc.M201641200 (2002).
141 Fribourgh, J. L. *et al.* Structural insight into HIV-1 restriction by MxB. *Cell Host Microbe* **16**, 627-638, doi:10.1016/j.chom.2014.09.021 (2014).
142 Melen, K. *et al.* Human MxB protein, an interferon-alpha-inducible GTPase, contains a nuclear targeting signal and is localized in the heterochromatin region beneath the nuclear envelope. *The Journal of biological chemistry* **271**, 23478-23486 (1996).
143 King, M. C., Raposo, G. & Lemmon, M. A. Inhibition of nuclear import and cell-cycle progression by mutated forms of the dynamin-like GTPase MxB. *Proc Natl Acad Sci U S A* **101**, 8957-8962, doi:10.1073/pnas.0403167101 (2004).
144 Matreyek, K. A. *et al.* Host and viral determinants for MxB restriction of HIV-1 infection. *Retrovirology* **11**, 90, doi:10.1186/s12977-014-0090-z (2014).
145 Schulte, B. *et al.* Restriction of HIV-1 Requires the N-Terminal Region of MxB as a Capsid-Binding Motif but Not as a Nuclear Localization Signal. *Journal of virology* **89**, 8599-8610, doi:10.1128/JVI.00753-15 (2015).
146 Jin, H. K., Takada, A., Kon, Y., Haller, O. & Watanabe, T. Identification of the murine Mx2 gene: interferon-induced expression of the Mx2 protein from the feral mouse gene confers resistance to vesicular stomatitis virus. *Journal of virology* **73**, 4925-4930 (1999).
147 Noteborn, M., Arnheiter, H., Richter-Mann, L., Browning, H. & Weissmann, C. Transport of the murine Mx protein into the nucleus is dependent on a basic carboxy-terminal sequence. *Journal of interferon research* **7**, 657-669 (1987).
148 Jin, H. K. *et al.* Mouse Mx2 protein inhibits hantavirus but not influenza virus replication. *Archives of virology* **146**, 41-49 (2001).
149 Zurcher, T., Pavlovic, J. & Staeheli, P. Mouse Mx2 protein inhibits vesicular stomatitis virus but not influenza virus. *Virology* **187**, 796-800 (1992).
150 Yu, Z. *et al.* GTPase activity is not essential for the interferon-inducible MxA protein to inhibit the replication of hepatitis B virus. *Archives of virology* **153**, 1677-1684, doi:10.1007/s00705-008-0168-9 (2008).
151 Verhelst, J., Parthoens, E., Schepens, B., Fiers, W. & Saelens, X. Interferon-inducible protein Mx1 inhibits influenza virus by interfering with functional viral ribonucleoprotein complex assembly. *Journal of virology* **86**, 13445-13455, doi:10.1128/JVI.01682-12 (2012).

152 Daumke, O., Gao, S., von der Malsburg, A., Haller, O. & Kochs, G. Structure of the MxA stalk elucidates the assembly of ring-like units of an antiviral module. *Small GTPases* **1**, 62-64, doi:10.4161/sgtp.1.1.12989 (2010).
153 Haller, O., Gao, S., von der Malsburg, A., Daumke, O. & Kochs, G. Dynamin-like MxA GTPase: Structural Insights into Oligomerization and Implications for Antiviral Activity. *Journal of Biological Chemistry* **285**, 28419-28424, doi:10.1074/jbc.R110.145839 (2010).
154 Lutz, A., Dyall, J., Olivo, P. D. & Pekosz, A. Virus-inducible reporter genes as a tool for detecting and quantifying influenza A virus replication. *Journal of virological methods* **126**, 13-20, doi:10.1016/j.jviromet.2005.01.016 (2005).
155 Sakuma, T., Tonne, J. M. & Ikeda, Y. Murine leukemia virus uses TREX components for efficient nuclear export of unspliced viral transcripts. *Viruses* **6**, 1135-1148, doi:10.3390/v6031135 (2014).
156 Majerciak, V., Deng, M. & Zheng, Z. M. Requirement of UAP56, URH49, RBM15, and OTT3 in the expression of Kaposi sarcoma-associated herpesvirus ORF57. *Virology* **407**, 206-212, doi:10.1016/j.virol.2010.08.014 (2010).
157 Kane, M. *et al.* MX2 is an interferon-induced inhibitor of HIV-1 infection. *Nature* **502**, 563-566, doi:10.1038/nature12653 (2013).
158 Aebi, M. *et al.* cDNA structures and regulation of two interferon-induced human Mx proteins. *Mol Cell Biol* **9**, 5062-5072 (1989).
159 Pitossi, F. *et al.* A functional GTP-binding motif is necessary for antiviral activity of Mx proteins. *Journal of virology* **67**, 6726-6732 (1993).
160 Pfaffl, M. W. A new mathematical model for relative quantification in real-time RT-PCR. *Nucleic Acids Res* **29**, e45 (2001).
161 Chelbi-Alix, M. K. *et al.* Induction of the PML protein by interferons in normal and APL cells. *Leukemia* **9**, 2027-2033 (1995).
162 Mark, G. E., Taylor, J. M., Broni, B. & Krug, R. M. Nuclear accumulation of influenza viral RNA transcripts and the effects of cycloheximide, actinomycin D, and alpha-amanitin. *Journal of virology* **29**, 744-752 (1979).
163 Krug, R. M., Shaw, M., Broni, B., Shapiro, G. & Haller, O. Inhibition of influenza viral mRNA synthesis in cells expressing the interferon-induced Mx gene product. *Journal of virology* **56**, 201-206 (1985).
164 Engelhardt, O. G., Sirma, H., Pandolfi, P. P. & Haller, O. Mx1 GTPase accumulates in distinct nuclear domains and inhibits influenza A virus in cells that lack promyelocytic leukaemia protein nuclear bodies. *The Journal of general virology* **85**, 2315-2326, doi:10.1099/vir.0.79795-0 (2004).
165 Mitchell, P. S., Young, J. M., Emerman, M. & Malik, H. S. Evolutionary Analyses Suggest a Function of MxB Immunity Proteins Beyond Lentivirus Restriction. *PLoS Pathog* **11**, e1005304, doi:10.1371/journal.ppat.1005304 (2015).
166 Sadler, A. J. & Williams, B. R. Interferon-inducible antiviral effectors. *Nature reviews. Immunology* **8**, 559-568, doi:10.1038/nri2314 (2008).
167 Horisberger, M. A. & Gunst, M. C. Interferon-induced proteins: identification of Mx proteins in various mammalian species. *Virology* **180**, 185-190 (1991).
168 Holzinger, D. *et al.* Induction of MxA gene expression by influenza A virus requires type I or type III interferon signaling. *Journal of virology* **81**, 7776-7785, doi:10.1128/JVI.00546-06 (2007).
169 Lindenmann, J. Inheritance of Resistance to Influenza Virus in Mice. *Proceedings of the Society for Experimental Biology and Medicine. Society for Experimental Biology and Medicine* **116**, 506-509 (1964).
170 Gao, S. *et al.* Structural basis of oligomerization in the stalk region of dynamin-like MxA. *Nature* **465**, 502-506, doi:10.1038/nature08972 (2010).
171 Kochs, G., Haener, M., Aebi, U. & Haller, O. Self-assembly of human MxA GTPase into highly ordered dynamin-like oligomers. *The Journal of biological chemistry* **277**, 14172-14176, doi:10.1074/jbc.M200244200 (2002).
172 Dick, A. *et al.* Role of Nucleotide Binding and GTPase Domain Dimerization in Dynamin-like Myxovirus Resistance Protein A for GTPase Activation and Antiviral

Activity. *Journal of Biological Chemistry*, jbc.M115.650325, doi:10.1074/jbc.M115.650325 (2015).
173 Ponten, A., Sick, C., Weeber, M., Haller, O. & Kochs, G. Dominant-negative mutants of human MxA protein: domains in the carboxy-terminal moiety are important for oligomerization and antiviral activity. *Journal of virology* **71**, 2591-2599 (1997).
174 Kochs, G. GTP-bound Human MxA Protein Interacts with the Nucleocapsids of Thogoto Virus (Orthomyxoviridae). *Journal of Biological Chemistry* **274**, 4370-4376, doi:10.1074/jbc.274.7.4370 (1999).
175 Kochs, G. & Haller, O. Interferon-induced human MxA GTPase blocks nuclear import of Thogoto virus nucleocapsids. *Proc Natl Acad Sci U S A* **96**, 2082-2086 (1999).
176 Katahira, J. mRNA export and the TREX complex. *Biochimica et biophysica acta* **1819**, 507-513, doi:10.1016/j.bbagrm.2011.12.001 (2012).
177 Gotz, V. *et al.* Influenza A viruses escape from MxA restriction at the expense of efficient nuclear vRNP import. *Sci Rep* **6**, 23138, doi:10.1038/srep23138 (2016).
178 Matzinger, S. R., Carroll, T. D., Dutra, J. C., Ma, Z. M. & Miller, C. J. Myxovirus resistance gene A (MxA) expression suppresses influenza A virus replication in alpha interferon-treated primate cells. *Journal of virology* **87**, 1150-1158, doi:10.1128/JVI.02271-12 (2013).
179 Cabantous, S. *et al.* A New Protein-Protein Interaction Sensor Based on Tripartite Split-GFP Association. *Scientific Reports* **3**, doi:10.1038/srep02854 (2013).
180 Di Paolo, C., Hefti, H. P., Meli, M., Landis, H. & Pavlovic, J. Intramolecular Backfolding of the Carboxyl-terminal End of MxA Protein Is a Prerequisite for Its Oligomerization. *Journal of Biological Chemistry* **274**, 32071-32078, doi:10.1074/jbc.274.45.32071 (1999).
181 Shen, J., Zhang, L. & Zhao, R. Biochemical Characterization of the ATPase and Helicase Activity of UAP56, an Essential Pre-mRNA Splicing and mRNA Export Factor. *Journal of Biological Chemistry* **282**, 22544-22550, doi:10.1074/jbc.M702304200 (2007).
182 Weber, F., Haller, O. & Kochs, G. MxA GTPase blocks reporter gene expression of reconstituted Thogoto virus ribonucleoprotein complexes. *Journal of virology* **74**, 560-563 (2000).
183 Ruigrok, R. W. & Baudin, F. Structure of influenza virus ribonucleoprotein particles. II. Purified RNA-free influenza virus ribonucleoprotein forms structures that are indistinguishable from the intact influenza virus ribonucleoprotein particles. *The Journal of general virology* **76 (Pt 4)**, 1009-1014, doi:10.1099/0022-1317-76-4-1009 (1995).
184 Rio, D. C. Electrophoretic mobility shift assays for RNA-protein complexes. *Cold Spring Harbor protocols* **2014**, 435-440, doi:10.1101/pdb.prot080721 (2014).
185 Chen, Y. *et al.* Conformational dynamics of dynamin-like MxA revealed by single-molecule FRET. *Nat Commun* **8**, 15744, doi:10.1038/ncomms15744 (2017).
186 Dufu, K. *et al.* ATP is required for interactions between UAP56 and two conserved mRNA export proteins, Aly and CIP29, to assemble the TREX complex. *Genes & development* **24**, 2043-2053, doi:10.1101/gad.1898610 (2010).
187 Chi, B. *et al.* Aly and THO are required for assembly of the human TREX complex and association of TREX components with the spliced mRNA. *Nucleic Acids Res* **41**, 1294-1306, doi:10.1093/nar/gks1188 (2013).
188 Taniguchi, I. & Ohno, M. ATP-dependent recruitment of export factor Aly/REF onto intronless mRNAs by RNA helicase UAP56. *Mol Cell Biol* **28**, 601-608, doi:10.1128/MCB.01341-07 (2008).
189 Yamazaki, T. *et al.* The closely related RNA helicases, UAP56 and URH49, preferentially form distinct mRNA export machineries and coordinately regulate mitotic progression. *Molecular biology of the cell* **21**, 2953-2965, doi:10.1091/mbc.E09-10-0913 (2010).
190 Schumann, S., Jackson, B. R., Baquero-Perez, B. & Whitehouse, A. Kaposi's sarcoma-associated herpesvirus ORF57 protein: exploiting all stages of viral mRNA processing. *Viruses* **5**, 1901-1923, doi:10.3390/v5081901 (2013).

191 Mitchell, P. S., Emerman, M. & Malik, H. S. An evolutionary perspective on the broad antiviral specificity of MxA. *Curr Opin Microbiol* **16**, 493-499, doi:10.1016/j.mib.2013.04.005 (2013).
192 Lehner, B. *et al.* Analysis of a high-throughput yeast two-hybrid system and its use to predict the function of intracellular proteins encoded within the human MHC class III region. *Genomics* **83**, 153-167 (2004).
193 Zhao, R., Shen, J., Green, M. R., MacMorris, M. & Blumenthal, T. Crystal structure of UAP56, a DExD/H-box protein involved in pre-mRNA splicing and mRNA export. *Structure* **12**, 1373-1381, doi:10.1016/j.str.2004.06.006 (2004).
194 Morell, M., Espargaro, A., Aviles, F. X. & Ventura, S. Detection of transient protein-protein interactions by bimolecular fluorescence complementation: the Abl-SH3 case. *Proteomics* **7**, 1023-1036, doi:10.1002/pmic.200600966 (2007).
195 Netherton, C. L. *et al.* Inhibition of a large double-stranded DNA virus by MxA protein. *Journal of virology* **83**, 2310-2320, doi:10.1128/JVI.00781-08 (2009).
196 Liu, Z. *et al.* The interferon-inducible MxB protein inhibits HIV-1 infection. *Cell Host Microbe* **14**, 398-410, doi:10.1016/j.chom.2013.08.015 (2013).
197 Rennie, Martin L., McKelvie, Siri A., Bulloch, Esther M. M. & Kingston, Richard L. Transient Dimerization of Human MxA Promotes GTP Hydrolysis, Resulting in a Mechanical Power Stroke. *Structure* **22**, 1433-1445, doi:10.1016/j.str.2014.08.015 (2014).
198 Chappie, J. S. *et al.* A pseudoatomic model of the dynamin polymer identifies a hydrolysis-dependent powerstroke. *Cell* **147**, 209-222, doi:10.1016/j.cell.2011.09.003 (2011).
199 Stranden, A. M., Staeheli, P. & Pavlovic, J. Function of the Mouse Mx1 Protein Is Inhibited by Overexpression of the PB2 Protein of Influenza Virus. *Journal of virology* **197**, 642-651 (1993).
200 Thomas, M. *et al.* pUL69 of Human Cytomegalovirus Recruits the Cellular Protein Arginine Methyltransferase 6 via a Domain That Is Crucial for mRNA Export and Efficient Viral Replication. *Journal of virology* **89**, 9601-9615, doi:10.1128/jvi.01399-15 (2015).
201 Zheng, W. *et al.* Phosphorylation controls the nuclear-cytoplasmic shuttling of influenza A virus nucleoprotein. *Journal of virology*, JVI.00015-00015, doi:10.1128/jvi.00015-15 (2015).
202 Hoff, F., Greb, C., Hollmann, C., Hönig, E. & Jacob, R. The Large GTPase Mx1 Is Involved in Apical Transport in MDCK Cells. *Traffic* **15**, 983-996, doi:10.1111/tra.12186 (2014).
203 Rothman, J. H., Raymond, C. K., Gilbert, T., O'Hara, P. J. & Stevens, T. H. A putative GTP binding protein homologous to interferon-inducible Mx proteins performs an essential function in yeast protein sorting. *Cell* **61**, 1063-1074 (1990).

Personal Information

Surname	STEINER
Name	Fiona Lara
Date of Birth	2. Nov 1989
Place of origin	Freienbach (SZ)

Education and Training

June 2014-July 2018 **PhD studies at the Institute of Medical Virology, University of Zurich, Switzerland**

Supervision: PD Dr. Jovan Pavlovic

May 2014 **Master of Science in Molecular and Cellular Biology, University of Zurich, Switzerland**

Master Thesis: “Adapting the Brainbow technique to study cell shape dynamics and cell-cell matching during dorsal closure in *D. melanogaster*”

Supervision: Prof. Damian Brunner

Oct 2009-May 2013 **Bachelor of Science in Biology, University of Zurich, Switzerland**

Sept 2008 **Matura specializing in natural sciences, Kantonsschule Zürich Nord, KZN, Switzerland**

Internships

Jul 2011 – Sept 2011 **Institute of Molecular Life Sciences at the University of Zurich**

Supervision: Prof. Urs Greber

April 2011 **Department Aquatic Ecology at the Swiss Institute for Environmental Science and Technology (EAWAG)**
Supervision: Silke van den Wyngaert

Oct 2008 – Jan 2009 **Department Aquatic Ecology at the Swiss Institute for Environmental Science and Technology (EAWAG)**
Supervision: Dr. Piet Spaak

Conference contributions

Jan 2018 **7th Swiss Virology Meeting, Thun, Switzerland**
Poster presentation

Oct 2017 **Cytokines 2017, Kanazawa, Japan**
Poster presentation

Aug 2017 **Joint annual meeting Swiss Society for Microbiology, Basel, Switzerland**
Poster presentation

Microbiology and Immunology PhD program retreat, Locarno, Switzerland
Poster presentation

Feb 2017 **LS2 annual meeting, Zürich, Switzerland**
Poster presentation

Oct 2016 **Cytokines 2016, San Francisco, USA**
Poster presentation

Feb 2016 **6th Swiss Virology Meeting, Thun, Switzerland**
Poster presentation

Jan 2016 **Viruses 2016, Basel, Switzerland**
Poster presentation

Oct 2015 **Cytokines 2015, Bamberg, Germany**
Poster presentation

Part-time employment

June - Dec 2012 **Starbucks Airport Railway Shopping**

Function: Barista